International Journal of Nanomedicine

Dovepress
Taylor & Francis Group

Open Access Full Text Article

REVIEW

Chitosan-Based Wound Dressings: Property Modulation, Fabrication Strategies, and Emerging Applications in Tissue Regeneration

Mingjie Fan[1,*], Xinmu Zhang[1,*], Longfei Lin[1,*], Ruying Tang[1], Hui Li[1,2], Yuling Liu[1]

[1]State Key Laboratory for Quality Ensurance and Sustainable Use of Dao-di Herbs, Institute of Chinese Materia Medica, China Academy of Chinese Medical Sciences, Beijing, 100700, People's Republic of China; [2]Institute of Traditional Chinese Medicine Health Industry, China Academy of Chinese Medical Sciences, Nanchang, Jiangxi Province, 330006, People's Republic of China

*These authors contributed equally to this work

Correspondence: Yuling Liu; Hui Li, Email ylliu@icmm.ac.cn; lihuizys@126.com

Abstract: Chronic wounds are often difficult to heal because of multiple pathological barriers, including infection, vascular insufficiency, and immune imbalance, and therefore require highly effective dressings to promote repair. Chitosan (CS), a cationic polysaccharide derived from the deacetylation of chitin, has attracted broad attention in wound management because of its favorable biocompatibility, biodegradability, chemical modifiability, and intrinsic hemostatic and antibacterial activities. The therapeutic value of CS-based dressings does not depend solely on CS itself, but rather on their ability to target the dominant pathological barriers of different wound types through structural modification and formulation design. This review links the key pathological features of various chronic wounds with the functional requirements of CS-based dressings, and systematically summarizes how modification strategies such as catechol grafting, quaternization, carboxymethylation, and dynamic covalent crosslinking regulate the properties of CS, as well as the major fabrication platforms and formulation types, including crosslinked hydrogels, freeze-dried sponges, electrospun nanofibers, phase-inversion membranes, and solvent-cast films. Their effects on porosity, mechanical strength, moisture retention, and permeability are also analyzed. Finally, the review discusses the challenges facing CS-based dressings in standardization, scalable manufacturing, clinical translation, and regulatory evaluation, and highlights the need for greater emphasis on multifunctional smart design and the improvement of evidence quality in future research.

Keywords: chitosan, wound dressings, wound healing, hydrogel, polymer composites

Introduction

CS is a widely available and functionally versatile natural polysaccharide obtained by the partial deacetylation of chitin. Its fundamental structure consists of D-glucosamine and N-acetyl-D-glucosamine units linked via β-(1-4) glycosidic bonds.[1] The primary amino groups in the CS molecular structure are more reactive than the acetamido groups in the chitin, conferring superior biological functionality and a high capacity for chemical[1] modification. The presence of numerous amino ($-NH_2$), hydroxyl (-OH), and acetamido ($-NHCOCH_3$) groups allows CS to form covalent bonds through esterification, amination, and etherification reactions, making it a tissue adhesive and biocompatible polymer approved by the U.S. Food and Drug Administration (FDA) for tissue engineering and drug delivery.[2] As a highly promising wound dressing material, CS exhibits exceptional biocompatibility, non-toxicity, low allergenicity, and biodegradability,[3] ensuring safe contact with skin without causing adverse reactions. Furthermore, studies have revealed other beneficial biological activities, including antitumor, antibacterial, antioxidant, antidiabetic, and wound healing properties.[4] Over the past decades, CS research and application have evolved into diverse forms such as hydrogels, nanofibers, films, beads, microspheres, nanoparticles, sponges, and scaffolds, highlighting its versatility in biomedicine.[5] Its biodegradability allows it to be gradually degraded in the body into harmless amino sugars that are absorbed by human tissues.[6] The reactive functional groups on the CS backbone enable chemical modification, facilitating binding

https://doi.org/10.2147/IJN.S607257
Received: 6 March 2026
Accepted: 16 May 2026
Published: 8 June 2026

Graphical Abstract

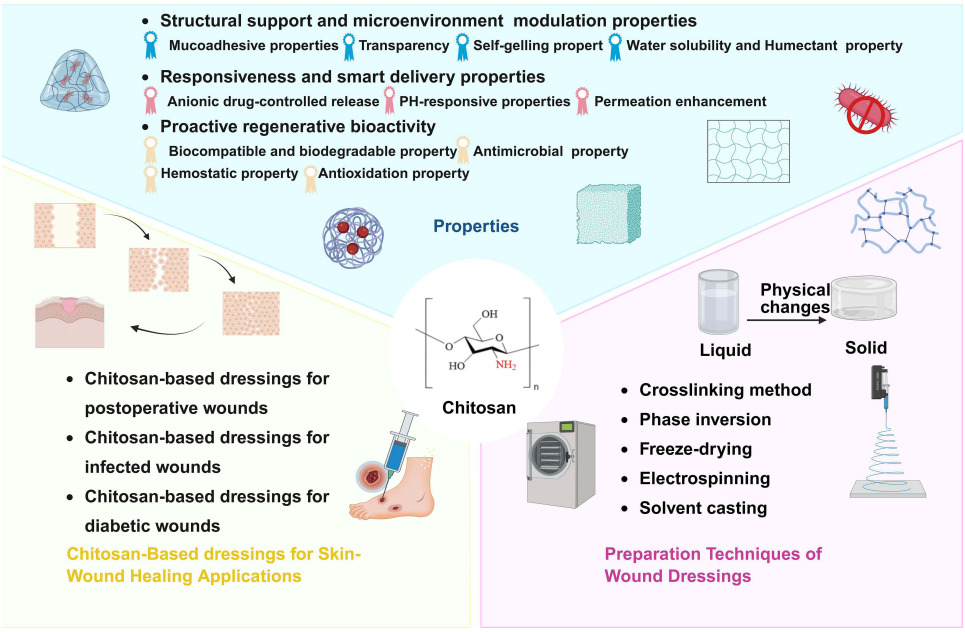

with drugs through ionic interactions, hydrogen bonding, or covalent bonds.[7] In addition, as a semi-transparent biomedical dressing, it can retain wound exudate beneath a dry scab, preventing dehydration and contamination to optimize healing conditions.[8] Therefore, CS serves as an ideal scaffold for fabricating dressings for burns, injuries, and other wound types.

The skin, the human body's largest organ, is composed of the epidermis, dermis, and subcutaneous tissue.[9] As the first line of defense against external insults, it is vital for protecting against pathogenic invasion[10] and preventing excessive water loss.[11] Therefore, when skin integrity is compromised by trauma, its protective function is lost, making timely and effective repair essential. Skin wounds are defined as the disruption of structural integrity due to external or internal factors, typically accompanied by inflammatory responses and tissue damage. Cutaneous healing is a dynamic process involving sequential stages: hemostasis, inflammation, proliferation, maturation, and remodeling.[12] Based on etiology and healing timeline, skin wounds are generally categorized as acute or chronic.[13] Acute wounds, such as lacerations, abrasions, burns, and surgical incisions, usually progress predictably through the normal healing phases and are expected to heal within 2 to 12 weeks.[14] In contrast, chronic wounds, including diabetic foot ulcers (DFUs), venous leg ulcers, and pressure ulcers,[15] are characterized by a prolonged, impaired healing process. These wounds often remain stalled in the inflammatory phase due to persistent infection,[16] impaired vascularization, or underlying systemic conditions like diabetes or immobility. According to World Health Organization data on type 2 diabetes prevalence, the global prevalence of DFUs is approximately 6.3%, and the annual number of new DFU cases worldwide has been estimated at 1.9 to 26.1 million.[17] The treatment of chronic wounds poses a significant clinical challenge and necessitates the development of advanced and effective therapeutic strategies.

Different wound types present distinct pathological barriers and therefore impose different functional requirements on wound dressings. Burn wounds are typically associated with rapid and intense inflammatory responses, disruption of the skin barrier, and a high risk of infection,[18] thus requiring dressings that combine antibacterial activity, moisture retention, pain relief, and barrier repair. Surgical wounds often involve local bleeding, exudate accumulation, wound dehiscence, and postoperative infection risk,[19] and therefore require materials with good hemostatic capacity, moderate fluid absorption, mechanical integrity, and tissue adhesiveness. Infected wounds remain in a state of high bacterial burden

and inflammatory imbalance,[20] making them more dependent on dressings with antibacterial, antibiofilm, exudate management, and microenvironment-regulating functions. Diabetic wounds, by contrast, are characterized by persistent inflammation, oxidative stress, impaired angiogenesis, and defective tissue regeneration,[21] and therefore require multi-functional dressings with anti-inflammatory, antioxidant, pro-angiogenic, and tissue-repair-promoting properties. Owing to its inherent hemostatic activity, antibacterial properties, biocompatibility, biodegradability, film- and gel-forming ability, as well as its ease of chemical modification and loading with bioactive molecules, CS is well suited to meet the therapeutic demands of these different wound types (Figure 1).

The use of wound dressings in managing chronic wounds has demonstrated considerable feasibility and therapeutic advantages. Characterized by prolonged inflammation, impaired re-epithelialization, and high risk of infection, chronic

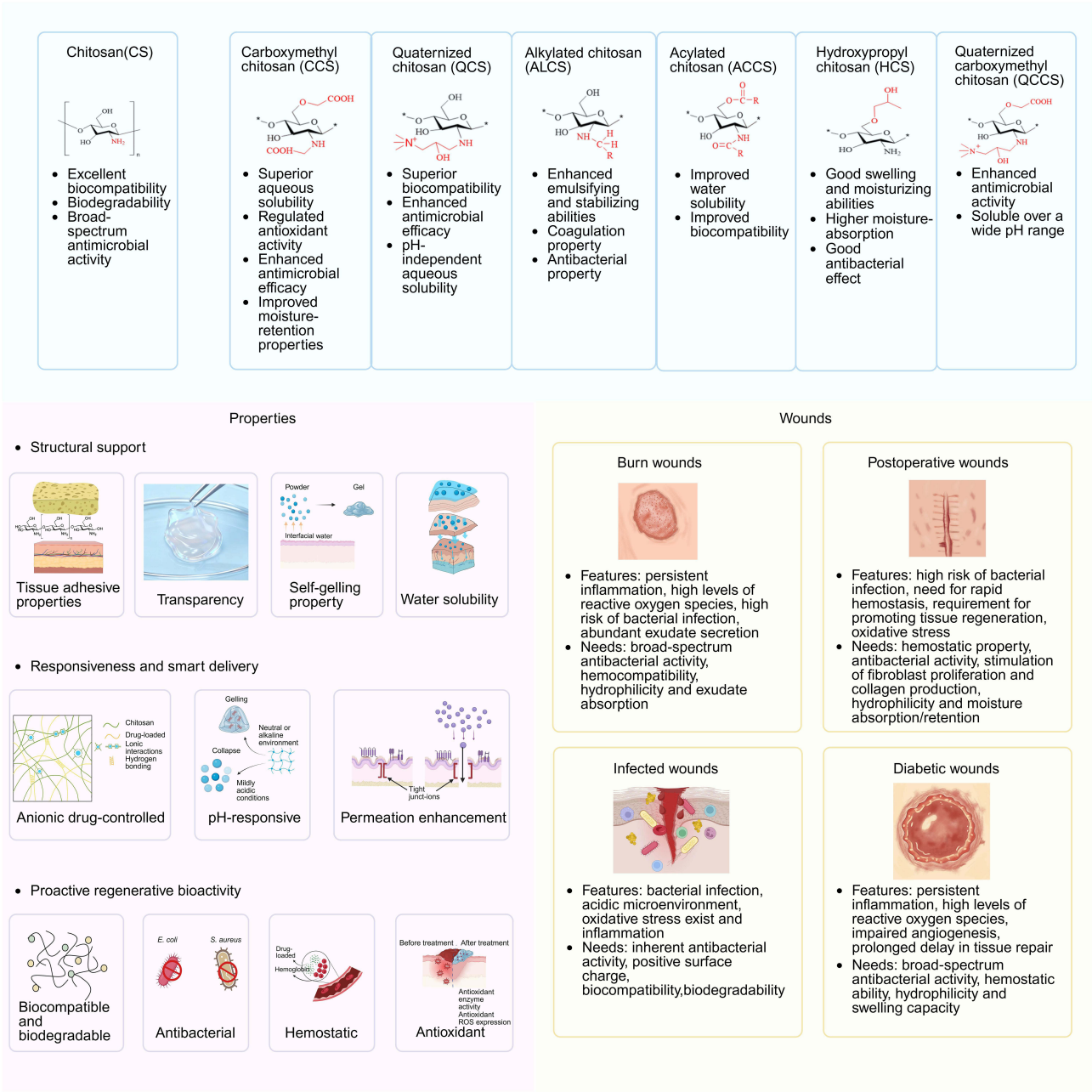

Figure 1 Schematic illustration of the relationships among CS derivatives, functional properties of CS-based dressings, and the pathological barriers and clinical needs of different wound types (Created with Biorender.com).

https://doi.org/10.2147/IJN.S607257

wounds require a moist, protected, and biologically supportive environment to facilitate healing. Advanced wound dressings—such as hydrogels, hydrocolloids, foams, growth factor-containing dressings, and bioactive materials—maintain optimal moisture balance, absorb excess exudate, and serve as physical barriers against microbial invasion. Hydrogels contain 80% to 99% water or glycerol, are non-adherent, and are suitable for dry and necrotic wounds. They can relieve pain and discomfort while promoting gas and moisture exchange, thereby helping prevent exudate accumulation. Hydrocolloids usually have an outer layer composed of a waterproof polyurethane film, which effectively prevents the entry of bacteria and debris into the wound and is suitable for wounds with minimal to moderate exudate. Foam dressings possess a breathable backing that can regulate gas exchange and moisture evaporation, thereby maintaining the optimal moisture balance required for wound healing while preventing exudate-induced maceration. In addition, these materials have a relatively long service life and can effectively retain exudate without frequent replacement, making them suitable for DFUs, postoperative wounds, pressure ulcers, and venous ulcers with moderate to heavy exudation. Growth factor-containing dressings can regulate key biological processes, enhance cell motility, and promote new tissue formation while reducing scar formation. They are suitable for chronic or complex wounds, particularly burns, surgical wounds, and diabetic ulcers.[22] However, compared with conventional gauze dressings, biopolymer-based dressings offer clear functional advantages, but their large-scale application is still constrained by cost and manufacturing complexity. For instance, the extraction and purification of CS is relatively costly, and dressings containing bioactive components often require stricter sterilization strategies that ensure sterility without compromising biological activity, such as irradiation or ethylene oxide treatment. In addition, advanced preparation techniques, including electrospinning and supercritical fluid processing, may further increase equipment investment and production costs.

Some dressings are also engineered to deliver therapeutic agents, such as antimicrobials, growth factors, and anti-inflammatory drugs, thereby further accelerating wound closure and tissue regeneration. Compared to conventional dry dressings, these modern materials can reduce pain, minimize scarring, decrease dressing change frequency, and ultimately improve patient outcomes. An ideal dressing should meet several requirements: (1) excellent biocompatibility without causing inflammation or toxicity;[23] (2) satisfactory hemostatic performance;[16] (3) effective antibacterial and antioxidant activity;[24] (4) good healing and pain-relieving effects;[25] (5) adequate exudate absorption and water vapor transmission capacity; (6) sufficient mechanical strength; (7) an appropriate microstructure for drug loading and promoting cell proliferation/differentiation; and (8) easy and atraumatic application and removal.[26] CS, owing to its inherent biocompatibility, antibacterial activity, hemostatic properties, film-forming ability, and promotion of wound healing, is regarded as a promising candidate matrix that meets multiple ideal requirements. However, to fully realize its potential and overcome limitations such as insufficient mechanical strength, limited drug-loading capacity, and uncontrolled release, researchers have employed various strategies to modify and optimize CS-based materials. To enhance the wound-healing efficacy of CS-based dressings, researchers have employed covalent and non-covalent crosslinking methods to modify CS, thereby significantly improving the mechanical properties of the resulting dressings to meet the ideal requirement of having sufficient mechanical strength to prevent breakage. Additionally, chemical modifications of CS and its blending with other polymeric materials play a crucial role in optimizing the antibacterial and hemostatic performance of CS-based wound dressings,[27] thereby meeting the ideal requirements of providing satisfactory hemostatic properties, effective antibacterial and antioxidant activities to shorten the inflammatory phase.

With the accelerating global aging population and the high prevalence of chronic diseases such as diabetes, the incidence of chronic non-healing wounds continues to rise, creating broad application prospects for wound dressings capable of modulating the wound microenvironment and promoting tissue repair. Although CS-based dressings, as biopolymer-based dressings, generally have higher direct costs than conventional materials such as traditional gauze, they can accelerate wound healing, reduce dressing change frequency, and lower the risks of infection and complications, thereby shortening the overall treatment course and reducing the burden on healthcare providers. Therefore, from a health economics perspective, they often offer better overall cost-effectiveness.

However, at present, the transition of CS-based wound dressings toward scalable production and clinical translation still faces multiple challenges, involving raw materials, fabrication processes, quality control, regulatory approval, and market acceptance. First, the cost of high-quality CS raw materials and the required additives is relatively high, which increases overall production expenses to some extent. Second, CS materials are sensitive to environmental conditions,

and fluctuations in humidity and temperature during production may affect their physicochemical properties, thereby compromising the structural integrity and performance of the final products. In addition, the medical device industry is subject to strict regulation, and related products usually require systematic testing for safety, efficacy, and stability, together with comprehensive documentation to meet compliance standards. Therefore, establishing standardized quality assurance protocols and batch-to-batch consistency control not only increases production complexity but also further raises research, development, and manufacturing costs. Meanwhile, high-quality clinical studies are still needed to verify the clinical safety and therapeutic efficacy of these innovative dressings, which often requires substantial time, funding, and interdisciplinary resources. Overall, addressing these challenges will require coordinated efforts across materials science, engineering, regulatory science, and clinical medicine in order to more effectively realize the practical medical potential of innovative CS-based wound dressings.

This review systematically summarizes the structural and functional characteristics of CS, the commonly used crosslinking strategies in dressing construction, the fabrication methods of CS-based dressings, and their applications in chronic wound management. The aim of this review is to correlate the key pathological barriers and therapeutic needs of different wound types with the properties and design strategies of CS-based dressings. In addition, it further compares the effects of different crosslinking methods, fabrication processes, and material architectures on dressing performance and application suitability, and provides a critical analysis of the current challenges faced by CS-based wound dressings in scalable production, biosafety, quality control, regulatory approval, and clinical translation. Finally, in light of current research trends and practical application needs, we propose potential future directions to provide more targeted insights and guidance for the rational design and clinical translation of next-generation high-performance, multifunctional CS-based wound dressings.

Properties

CS, a naturally derived cationic polysaccharide with tunable structure and wide availability, possesses a variety of distinctive properties that make it an ideal matrix for wound dressings. In terms of structural support, its excellent tissue adhesive property allows for intimate contact with the skin or wound surface; its transparency facilitates real-time observation and clinical monitoring; and its self-gelling property together with good water solubility enables flexible fabrication into various dressing forms such as films, hydrogels, and sponges. Furthermore, in terms of responsiveness and smart delivery, CS can achieve targeted and sustained drug release through its anionic drug-controlled binding and pH-responsive characteristics, while its permeation enhancement promotes the penetration of active agents into deeper tissues. More importantly, CS exhibits proactive regenerative bioactivity, characterized by biocompatibility and biodegradability, broad-spectrum antimicrobial activity, hemostatic capability, and antioxidant properties. The synergistic integration of these features enables CS not only to serve as an ideal physical barrier but also to actively participate in tissue repair and regeneration, establishing its central role as a multifunctional and intelligent wound dressing material. This section introduces the biological properties of CS and their roles in dressing construction and wound healing, aiming to provide guidance for the design and development of multifunctional CS-based dressings.

Structural Support and Microenvironment Modulation Properties

Tissue Adhesive Properties

Skin tissue contains functional groups such as primary amines, sulfhydryl groups, carboxyl groups, and aromatic moieties, which can interact with adhesive materials. CS is particularly attractive for adhesive dressing design because its hydroxyl and amino groups allow convenient chemical modification and functionalization. Therefore, the adhesive strength of CS-based dressings to skin tissue can be markedly enhanced by structural modification of CS. At present, catechol-containing compounds such as hydrocaffeic acid, dopamine, and 3,4-dihydroxyphenylalanine (DOPA) are commonly used to modify the CS structure. Catechol moieties can enable rapid and effective wet-tissue adhesion through π-π interactions, hydrogen bonding, and catechol-thiol-related interfacial interactions, but their phenolic hydroxyl groups can also be oxidized under alkaline conditions to form benzoquinone structures, which further enhance tissue adhesion strength by reacting with nucleophilic groups via Michael addition.[28] Ma et alcombined 3,4-dihydroxyphenylacetic acid-modified chitosan (DLC) with poly(vinyl alcohol) (PVA) to fabricate DLC/PVA hydrogel microneedles

loaded with the SAMnPor@TA/Ag-HA nanocomposite. The DLC/PVA microneedle formulation exhibited strong skin adhesion with a shear adhesive strength of 0.048 MPa on porcine skin. At room temperature, the DLC/PVA microneedles closely conformed to curved skin surfaces, thereby improving retention stability during treatment.[29] Tissue adhesion can also be enhanced through covalent crosslinking via Schiff base reactions. Dai et al designed a double-network hydrogel composed of dialdehyde cellulose (DAC), CCS, and polyacrylamide (PAM). The aldehyde groups of DAC reacted with the amino groups of CCS via Schiff base reactions to form a dynamic covalent network. This network was further reinforced by the free-radical polymerization of acrylamide (AM), generating a secondary covalent network. The synergistic interaction between DAC and CCS conferred excellent adhesive properties, with a skin adhesion strength of 2.70 kPa.[30] The intrinsic adhesive potential of CS is partly related to its cationic nature, which enables electrostatic interactions with anionic wound surface components;[31] however, the practical adhesion of CS-based dressings often depends on additional chemical modifications and formulation design. In wound dressings, improved interfacial adhesion may enhance conformal contact with the wound surface and help maintain a protective barrier. Effective tissue adhesion depends not only on interfacial bonding but also on sufficient material cohesiveness. However, under hydrated conditions, CS-based materials without sufficient crosslinking or modification often exhibit limited cohesiveness, which can restrict their final adhesive performance. Chemical modification such as trimethylation can increase the cationic charge density of CS and broaden its pH solubility range through the introduction of quaternary ammonium groups ($-N^{+}(CH_3)_3$). As a result, trimethyl CS may exhibit improved interfacial retention and wet-tissue adhesion, making it more suitable for application on moist wound surfaces.[32] Beyond charge regulation through chemical modification, physical interlocking at hydrated interfaces also plays an important role in improving the adhesion of CS-based materials. Benjamin et al employed topological entanglement by bringing a dry CS film into contact with a wet hydrogel. The film rapidly absorbs surface moisture from the hydrogel, enabling the amino and hydroxyl groups to quickly form hydrogen bonds. Simultaneously, chain segment diffusion leads to entanglement. The CS chains and the hydrogel polymer network interlock at the nanoscale, forming a physical crosslinking structure similar to "molecular hooking." This results in an adhesion energy more than three times higher than that of liquid CS.[33] Therefore, dressings designed with excellent tissue adhesive properties through the mentioned strategies can tightly adhere to the wound surface, continuously providing a moist environment while serving as a physical barrier to effectively prevent external contamination and bacterial invasion.[34]

Transparency

Certain CS-based hydrogels can exhibit high optical transparency, which may facilitate non-invasive visual inspection of the wound without frequent dressing removal, thereby minimizing wound disturbance and the risk of secondary infection. This optical property is formulation-dependent and can be influenced by factors such as the degree of deacetylation (DD) and network structure. Noriyuki et al added the acetylating agent at −10°C to prepare N-acetylated CS hydrogels, which exhibited greater transparency than commercial transparent ocular biomaterials. This high transparency, along with integrity and regenerative properties, was attributed to the nanofiber network made of α-chitin crystals.[35] This feature not only enhances clinical convenience but also satisfies aesthetic requirements for exposed areas such as the face and hands.

Self-Gelling Property

Self-gelling behavior in CS-based hydrogels generally arises from the reversible dissociation and reassembly of crosslinks within the designed hydrogel network.[36] This behavior is enabled by the abundant hydroxyl and amino groups in CS, which allow the formation of dynamic covalent and non-covalent interactions.[28] These reversible yet sufficiently stable interactions support the formation of self-gelling CS-based hydrogels. Dynamic covalent bonds can reversibly break and reform under mild conditions.[37] For example, Schiff base bonds, also known as dynamic imine bonds (-N=CH-), are formed through reactions between aldehyde groups and primary amine groups.[38] In the presence of water molecules, dynamic equilibrium can occur through the continuous breaking and reformation of these Schiff base linkages.[39] Dynamic non-covalent bonds, such as hydrogen bonds, create reversible crosslinks between different polymer chains through electrostatic interactions between hydrogen donors and various electronegative atoms serving as hydrogen acceptors.[37] In CS, various intermolecular and intramolecular hydrogen bonds are formed through interactions involving

amino groups, hydroxyl groups, and N-acetylated amino groups along the molecular chains. The hemostatic powder developed by Liu et al showed high liquid absorption capacity and can rapidly form a gel on the wound surface after hemostasis. This was achieved by combining CS derivatives (such as CCS) with other polysaccharides (such as oxidized SA). Upon contact with blood, gelation is completed within 5 seconds. Its rapid gelation was attributed to the synergistic contribution of Schiff base linkages and hydrogen-bonding interactions.[40] Zhang et al developed a multifunctional self-gelling powder composed of tannic acid (TA), CS, and polyethylene glycol (PEG). This powder can rapidly undergo in situ self-gelation upon absorbing interfacial moisture, forming a hydrogel that adheres tightly to moist tissue surfaces. The gelation mechanism is primarily driven by a liquid-liquid phase separation process, in which phase segregation promotes the formation of a physically associated network. It is dominated by strong intermolecular hydrogen bonds formed among the hydroxyl groups of TA, the ether groups of PEG, and the amino groups of CS, along with hydrophobic interactions.[41]

Water Solubility and Humectant Property

CS is widely used in moisturizing formulations due to its inherent hygroscopic nature. The water absorption capacity of CS-based materials is influenced by its molecular weight (MW) and degree of substitution (DS). When the MW decreases, its water absorption capacity increases.[42] The moisturizing properties of CS improve with increasing MW. However, CS is insoluble in water under neutral conditions, which limits its applications to some extent. In contrast, CS derivatives such as CCS exhibit excellent water solubility, allowing for broader applications. The water solubility properties and applications of CCS are determined by its structural characteristics, such as the average DS, the sites of carboxymethylation (whether on amino or hydroxyl groups), and the extent of hydroxyl substitution by carboxymethyl groups.[43] Compared to CS, CCS possesses greater water solubility, which may be advantageous for the development of more hydrophilic or moisture-retaining formulations. The water retention capacity of CCS is related to the presence of positive charges and its high MW, which help it adhere to the skin when used as a moisturizer.[44] In addition, by utilizing higher MW, the intermolecular hydrogen bonding within the polymer chains leads to more hydrated water molecules surrounding the CCS chains compared to those around CS chains, significantly enhancing CCS's water absorption and retention properties.[45] Further research on CCS is still needed to make it more suitable for applications involving skin irritation in human subjects.

Overall, the structural-support and microenvironment-modulating performance of CS-based dressings arises from the combined effects of the intrinsic chemical characteristics of CS and formulation-level design. The cationic backbone, amino and hydroxyl groups, hydrogen-bonding capability, and high chemical modifiability of CS provide the material basis for adhesion, moisture retention, and dynamic network construction. However, the final performance of the dressing depends to a greater extent on its specific configuration and fabrication strategy. For example, catechol modification, Schiff base crosslinking, and topological entanglement are mainly used to enhance wet-tissue adhesion; the degree of acetylation and nanofiber network structure influence optical transparency; dynamic covalent and non-covalent interactions determine in situ self-gelling behavior; and carboxymethylation primarily improves water solubility and humectant performance. These properties do not always improve in parallel. For instance, stronger interfacial adhesion usually requires greater material cohesion and crosslinking stability, whereas higher water solubility may compromise structural integrity. Therefore, in functional design, CS-based dressings should balance conformability, visibility, in situ gelation, and moisture retention according to the specific wound type and application scenario.

Responsiveness and Smart Delivery Properties

Anionic Drug-Controlled Release

When simple drug release mechanisms such as diffusion, erosion, membrane control, or osmosis fail to meet the desired therapeutic requirements, polyelectrolyte complex (PEC) nanoparticles,which are formed through electrostatic association between oppositely charged polymers or macromolecules, can be employed for the microencapsulation and controlled release of drugs, enzymes, proteins, and DNA.[46,47] Usually, PEC nanoparticles are prepared by complexation of two double-hydrophilic block copolymers which have opposite charges.[48] CS, as the most abundant natural cationic polysaccharide, is an excellent candidate for the preparation of PECs. Studies have shown that CS can form complexes

through electrostatic interactions with various polyelectrolytes.[49] For example, Aastha et al prepared all-natural, biodegradable PEC colloidal nanoparticles composed of CS and casein, achieving an encapsulation efficiency of up to 75% for the model drug insulin. They also investigated the role of competitive binding between casein and insulin with CS in the internal particle regions, which contributed to the controlled release of insulin.[50] Zhang et al mixed CS with 2-acrylamido-2-methylpropanesulfonic acid (AMPS) in an aqueous solution to form CS-AMPS composite nanoparticles through electrostatic interactions between the NH_3^+ groups of CS and the SO_3^{2-} groups of AMPS. These nanoparticles were used to encapsulate doxorubicin, achieving high drug loading and encapsulation efficiency. By adjusting the pH of the release medium, controlled drug release was achieved, demonstrating promising potential for applications in the field of drug delivery.[48]

pH-Responsive Properties

CS possesses remarkable pH-responsive properties due to the abundant amino ($-NH_2$) groups along its molecular chains.[51] In acidic environments, these amino groups are protonated into $-NH_3^+$, leading to electrostatic repulsion between the chains, which causes chain expansion and ultimately increases the water absorption of CS-based hydrogels. In neutral or alkaline environments, the amino groups gradually lose their protons, reducing the charge density of CS with decreased solubility, which can result in gelation or precipitation. The swelling behavior of ionic pH-sensitive hydrogels primarily depends on the degree of ionization.[52]

Formulation strategies have been explored to regulate the pH-responsive behavior of CS-based systems by adding various additives, grafting or blending with other polymers, and forming PECs with anionic polymers.[51] Wang et al synthesized aldehyde CS hydrogel via an oxidation reaction between CS and sodium periodate by adjusting the concentration, and prepared a stimulus-responsive injectable hydrogel based on the dynamic Schiff base reaction to achieve on-demand drug release.[53] Lin et al introduced a dual dynamic pH-responsive network structure by forming imine bonds (-C=N-) and acylhydrazone bonds (-C=NHNH-) through the reaction of aldehyde groups (-CHO) on oxidized konjac glucomannan chains with the amino groups ($-NH_2$) on carboxyethyl CS and the hydrazide groups ($-NHNH_2$) on poly(aspartic acid hydrazide). Under mildly acidic conditions (pH = 6.5), the dynamic crosslinked network is disrupted, accelerating hydrogel degradation. The biodegradation process occurs faster than in neutral environments (pH=7.4), enabling controlled release of bovine serum albumin under different pH conditions and demonstrating long-term sustained release behavior.[54] The inherent pH-dependent behavior of CS makes it a highly promising biomaterial for developing advanced formulations used in drug delivery, tissue engineering, and smart wound dressings.

Permeation Enhancement

CS has been investigated as a permeation-enhancing polymer in certain drug delivery systems, where permeation enhancement refers to facilitating the transport of therapeutic agents across epithelial or mucosal barriers, primarily due to its positively charged molecular structure. These positive charges enable interactions with cell membranes, resulting in a structural reorganization of the tight-junction proteins, with a consequent reversible opening of the junctions, which favors drug permeation without negatively affecting cell viability or provoking any membrane injury.[31,55] Studies have shown that the efficacy of CS in enhancing permeation largely depends on its structural characteristics, including DD and MW. CS with a high MW and a high DD exhibits a more pronounced effect on enhancing epithelial permeability.[31,56] Furthermore, the permeation-enhancing properties of CS can be further improved through appropriate chemical modifications. For example, thiolated CS derivatives not only exhibit stronger tissue adhesive interactions—attributable to disulfide bond formation with cysteine residues in mucins—but also demonstrate significantly improved permeation-enhancing effects on certain mucosal membranes,[57,58] with increases of over 30-fold.[59] This enhancement is believed to be associated with the stronger ability of thiolated CS to open tight-junctions, resulting from its interactions with thiol groups on cysteine residues present in membrane receptors and enzymes.[57]

In summary, the responsiveness and smart delivery capabilities of CS-based systems are not determined by CS alone, but rather arise from the combined effects of its intrinsic cationic nature and pH-dependent behavior after formulation-level design. CS provides reactive amino sites, charge-driven complexation ability, and pH-sensitive ionization characteristics, making it an important building block for polyelectrolyte complex nanoparticles, pH-responsive hydrogels,

and permeation-enhancing systems. Among these strategies, polyelectrolyte complex systems are more suitable for the encapsulation and release of oppositely charged biomolecules, whereas dynamic covalent cross-linked networks are more advantageous for achieving pH-triggered degradation and on-demand release. By comparison, permeation enhancement is more of a function in specific interfacial environments, particularly in drug delivery or mucosal administration systems, rather than a universal advantage of all wound dressings.

Proactive Regenerative Bioactivity

Although CS possesses various biological activities such as hemostatic, antibacterial, antioxidant, and anti-inflammatory effects, it is currently only accepted as an excipient by regulatory agencies and not as a drug for the treatment of diseases.

Biocompatible and Biodegradable Property

When the medical dressing is applied in the wound, the biocompatibility of the dressing matrix may still trigger some degree of immune rejection by the immune system. CS, as a natural polysaccharide, possesses excellent biocompatibility and biodegradability, which are key features supporting its wide application in the biomedical field.[60] Its excellent biological performance stems from its structural similarity to glycosaminoglycans (GAGs) found in the human extracellular matrix (ECM). This intrinsic characteristic minimizes immune rejection and allergic reactions, providing an ideal biomaterial foundation for formulating scaffolds and hydrogels that can effectively promote cell adhesion and proliferation. Barbara et al implanted ectopic cell-laden hydrogels of three specific cell types, along with acellular hydrogels, in athymic nude mice to investigate the biocompatibility and safety of CS-based hydrogels in a more complex in vivo environment. Throughout the in vivo experiment, no signs of infection or rejection were observed in the mice, and the hydrogels remained subcutaneously intact. Moreover, no signs of distress were observed in the animals.[61]

CS is degraded under the action of enzymes through the hydrolysis of glycosidic bonds, resulting in the formation of non-toxic small molecules such as glucosamine and various oligosaccharides, which can be completely absorbed and metabolized by the human body.[62] Furthermore, the degradation rate of CS can be finely tuned by adjusting its DD, MW, and chemical modifications (such as carboxymethylation), making it adaptable to various clinical scenarios. Ramasamy et al found that both the biodegradation and biocompatibility of CS depend on its DD. When DD ranges between 50% and 60%, its biodegradation is impaired, whereas when it exceeds 90%, CS can be used for anticancer applications.[63]

Antimicrobial Property

Bacterial infection commonly occurs during skin wound healing, and bacterial colonization at the wound site can trigger persistent inflammatory responses, including immune cell activation and the release of pro-inflammatory cytokines, thereby delaying wound healing and impairing final healing outcomes. CS has been widely reported to exhibit broad-spectrum antimicrobial activity and significant inhibitory effects against a wide range of bacteria. Several mechanisms have been proposed to explain the antibacterial activity of CS, including disruption of cell membrane permeability, interference with bacterial phospholipid and protein synthesis, and metal ion chelation. In an acidic environment, the surface -NH_2 groups of CS are protonated to form positively charged -NH^{3+} groups, which can disrupt the integrity of negatively charged microbial cell walls and increase cell membrane permeability through electrostatic interactions, leading to osmotic imbalance and leakage of intracellular contents, ultimately reducing cellular biological activity.[64] Meanwhile, DD also determines the content of free amino groups in CS: a higher DD results in more amino groups at the C_2 position of CS and, after protonation, a greater positive charge density (-NH^{3+}), thereby leading to stronger antibacterial activity.[65] Watcharaporn et al directly observed damage to the cell membranes of B. pseudomallei treated with CS using transmission electron microscopy, along with the release of intracellular contents, confirming the antimicrobial activity of CS against B. pseudomallei cells.[66] After entering the cell, CS can bind to negatively charged proteins and nucleic acids, thereby inhibiting the synthesis of proteins and mRNA. This interference with the normal physiological functions of bacterial cells ultimately suppresses their growth and reproduction.[67]

Some studies have shown that the antibacterial activity of CS is related to its MW and may increase as MW increases. High-molecular-weight CS contains more active groups and tends to form denser nanofibrous structures, which are generally associated with stronger antibacterial performance. However, excessively high MW can also enhance

intermolecular interactions and increase fiber diameter accordingly.[68] Supernak et al prepared CS films using CS powders with different MWs. Antibacterial activity studies showed that high-molecular-weight CS was a more suitable carrier for gentamicin, and the resulting CS films exhibited significant antibacterial efficacy against *Staphylococcus aureus(S. aureus)* infection.[69] Other studies have found that low-molecular-weight CS usually has higher water solubility, which helps promote its interaction with bacterial surfaces, increase membrane permeability, and cause leakage of intracellular components, thereby enhancing its antibacterial activity.[70] Li et al used non-thermal plasma (NTP) treatment to reduce the MW of CS, thereby adjusting the polymer chain length to improve its solubility and membrane interactions, which significantly enhanced its broad-spectrum antibacterial activity against both Gram-positive and Gram-negative bacteria.[71] The literature reported that the MW range of CS with strong antibacterial activity was about 42.5~155 kDa.[72]

The antibacterial activity of CS results from the combined effects of multiple interactions between its molecules and the microbial cell wall/cell membrane, and the efficiency of these interactions is closely related to the molecular conformation and formulation state of CS. Soluble CS, referring to chitosan in its dissolved or well-dispersed form under acidic conditions, usually exists in a dissociated and extended state in solution, with its active groups more fully exposed, which facilitates contact with bacterial surfaces and promotes antibacterial activity; however, its performance is also more susceptible to environmental factors. In contrast, solid or semi-solid CS systems, such as fibers, films, hydrogels, microspheres, and nanoparticles, mainly interact with the external medium through surface contact. Their reactive surface area, interfacial contact mode, and accessibility of active sites therefore differ from those of soluble CS, resulting in different antibacterial efficiencies.[73]

In addition, the antibacterial activity of CS is also influenced by the concentration of metal ions. The -NH_2 and -OH groups in CS possess certain metal-binding capabilities, and the formation of metal complexes can enhance the overall antibacterial performance of CS-based dressings. CS can selectively bind to metal ions and essential nutrients within bacteria, thereby inhibiting the production of bacterial toxins and suppressing microbial growth and development.[74] Antibacterial activity remains a central and enduring focus in wound healing research. Although CS itself possesses favorable antibacterial properties, future CS-based wound dressings will continue to capitalize on its inherent antibacterial mechanisms while integrating multiple strategies, such as CS modification and the incorporation of other antibacterial agents, to achieve improved therapeutic outcomes.

Hemostatic Property

The initial development of CS-based dressings was aimed at hemostasis. In 2002, the HemCon hemostatic bandage was approved by the U.S. Food and Drug Administration (FDA) and was soon deployed for battlefield hemorrhage control.[75] The hemostatic mechanism of CS includes promoting platelet adhesion and aggregation, inducing red blood cell aggregation, and inhibiting fibrinolysis. During the hemostatic process, an appropriate balance between the positive charges of CS and the negative charges of proteins within blood cells is crucial. CS can enhance the expression of GPIIb/IIIa on the platelet membrane, thereby promoting platelet adhesion to the vascular wall and platelet aggregation.[76] Shujun et al prepared a cryogel using CS, citric acid and silver nanoparticles, which achieved rapid hemostasis by absorbing large amounts of blood and promoting blood cell adhesion.[77] Sun et al combined ALCS with diatom biosilica (DB) to develop a safe and effective hemostatic composite sponge (AC-DB sponge). The strong interfacial interactions between the AC-DB sponge and blood induced the activation, deformation, and aggregation of red blood cells and platelets, thereby triggering the intrinsic coagulation pathway and significantly accelerating the blood-clotting process.[78] In addition, CS stimulates the coagulation cascade to condense blood. Research has shown that the positive charges on the surface of CS electrostatically attract the negatively charged phosphatidylcholine and phosphatidylethanolamine on the surfaces of red blood cells and platelets, accelerating the aggregation of these cells around the wound site.[79] Meanwhile, CS with different MWs and DD has been reported to exhibit different effects on red blood cell aggregation and platelet adhesion.[80] In some studies, low-molecular-weight CS showed a greater ability to activate the coagulation system and promote hemostasis. This may be related to its tendency to self-aggregate in blood and form a three-dimensional network capable of trapping red blood cells and facilitating their aggregation, thereby contributing to rapid hemostasis.[81] Moreover, CS can promote platelet aggregation and inhibit fibrinolysis by altering the microstructure of hemoglobin and increasing blood viscosity.[82] Zhenhua et al found that the NH_3^+ groups on the protonated CS molecular

chains are the key functional groups responsible for promoting coagulation. Their team developed protonated CS that accelerates the coagulation cascade by recruiting coagulation factors and assembling plasma proteins, thereby activating platelets and enhancing the secretion of procoagulant substances from platelets.[83] CS can also facilitate coagulation through its fluid absorption capacity. Liu et al developed a multifunctional hemostatic powder composed of doubly crosslinked poly([2-(methacryloyloxy) ethyl]trimethylammonium chloride-co-acrylic acid) (pMATC-co-AA) and N-[(2-hydroxy-3-trimethylammonium)propyl] CS chloride (HTCC), which were associated through electrostatic interactions and hydrogen bonding. The resulting powder showed excellent absorbency, with water and blood absorption capacities of 94.5 and 9.1 times its own weight, respectively. This high absorbency, attributed to electrostatic repulsion within the network, enabled rapid fluid uptake at the bleeding site and promoted the local concentration of blood cells and platelets, thereby contributing to hemostasis.[84]

Although CS itself possesses certain hemostatic properties, the hemostatic performance of single-component CS materials remains limited. To further enhance their hemostatic efficacy, researchers have combined CS with other hemostatic medical materials or advanced fabrication strategies to develop a variety of CS-based composite hemostatic dressings, including composite hemostatic films, sponges, hydrogels, particles, and other composite hemostatic materials. Through the synergistic action of multiple mechanisms, these composite systems can achieve more rapid and effective hemostasis.[85] For example, the Celox™ patch (MedTrade Products Ltd., Crewe, UK) is a hemostatic dressing composed of CS particles and flake-like components, which provides a large surface area for contact with blood. Upon contact with blood, the CS particles absorb fluid and swell to form a viscous granular gel that becomes widely distributed within the wound, forming a firm sealing structure that helps achieve rapid hemostasis.[86]

Antioxidation Property

At present, antioxidative properties have become an indispensable function of wound dressings. Studies have shown that appropriate levels of reactive oxygen species (ROS) play important roles in lymphocyte recruitment, regulation of vasoconstriction, and antimicrobial defense.[87,88] However, excessive ROS can disrupt the balance between oxidants and reductants, thereby causing tissue damage, aggravating infection, and delaying wound healing.[89–92] CS has been reported to exhibit antioxidant activity, which may help mitigate excessive oxidative stress in wounds. This effect is mainly attributed to the amino (-NH2) and hydroxyl (-OH) groups present along its polymer chains. These functional groups may donate electrons or hydrogen atoms to neutralize certain ROS, such as superoxide anions, hydroxyl radicals, and hydrogen peroxide, thereby contributing to the attenuation of excessive oxidative stress under pathological conditions.[93] Since amino groups can stabilize oxidized structures, the free radical scavenging ability of CS, defined as the neutralization of reactive radical species through electron or hydrogen donation, is negatively correlated with its degree of acetylation.[94] Studies have found that CS possesses strong metal ion chelating ability and can scavenge free radicals or chelate metal ions by donating hydrogen atoms or lone pair electrons.[95,96] In particular, it can inhibit the catalytic activity of metal ions such as Fe^{2+}/Fe^{3+}.[97,98] These metal ions are key factors in efficient antioxidant systems and serve as major catalysts in biological oxidation processes,[99,100] as they are involved in the oxidation of cellular macromolecules such as lipids and DNA.[101–103] Giftania et al found that CS can protect cardiac cell damage through antioxidative stress pathways by reducing ROS and enhancing the expression of nuclear factor erythroid 2-related factor 2 (Nrf2), as well as increasing the levels of antioxidant enzymes such as SOD and GPX. Furthermore, it exerts anti-apoptotic effects by upregulating BCL-2 expression and downregulating Caspase-3 expression.[104] In addition, γ-irradiation has the ability to alter the chemical and physical properties of certain polymeric materials.[105] Its capacity to break polymer chains makes it useful for enhancing the solubility of solvents[106,107] and stabilizing solutes.[108] When applied to CS, γ-irradiation may alter MW and expose more reactive functional groups, which has been associated with enhanced radical-scavenging activity in some studies. Siddhartha et al compared the antioxidant activity of irradiated and non-irradiated CS and found that γ-irradiation at a dose rate of 20 kGy/h significantly altered the structure of CS and reduced its MW. Additionally, the CS exhibited active amino functional groups, and the degree of degradation was sufficient to enhance its antioxidant activity.[109] Nevertheless, from the perspective of wound healing, antioxidant design should aim to rebalance redox homeostasis rather than completely suppress ROS, because excessive ROS scavenging may interfere with beneficial early healing events.

The favorable biocompatibility and biodegradability of CS provide a fundamental basis for its biomedical applications, but its actual safety profile is still influenced by multiple factors, including purity, DD, MW, and composite components. Antibacterial activity is one of the most representative advantages of CS, yet its magnitude depends strongly on the protonation state, MW, formulation type, and whether additional antibacterial agents are incorporated. Hemostatic performance is related not only to charge-mediated interactions with blood cells, but also to fluid absorption, local clot concentration, and material architecture, particularly in sponges, particles, and self-gelling systems. Antioxidant activity may help alleviate excessive oxidative stress, but its real value lies in restoring redox homeostasis rather than indiscriminately scavenging ROS. Therefore, the therapeutic efficacy of CS-based dressings is usually not determined by a single mechanism of CS alone, but rather by the synergistic integration of multiple functions matched to the pathological barriers of specific wound types.

Preparation Techniques of Wound Dressings

To meet the requirements of different types of wounds, various preparation techniques can be employed to fabricate distinct forms of CS-based dressings, which directly influence their mechanical properties, physicochemical characteristics, and biological functions. Among the commonly used methods, crosslinking enables the formation of stable hydrogel networks; phase inversion typically produces asymmetric membranes or porous structures, achieving a balance between moisture retention and breathability; freeze-drying generates lightweight and highly porous sponges with excellent fluid absorption and oxygen permeability; electrospinning allows the fabrication of nanofibrous mats that mimic the ECM, promoting cell adhesion and proliferation; and solvent casting is suitable for producing uniform, transparent films with controllable thickness and smooth surfaces, ideal for superficial wound treatment. In this section, we discuss the performance advantages and wound-healing applications of CS-based dressings prepared by these different preparation techniques, as presented in Table 1.

Crosslinking Method

The commonly used crosslinking strategies for hydrogel preparation can be broadly classified into physical crosslinking and chemical crosslinking. Physical crosslinking involves the formation of a three-dimensional network through non-covalent interactions such as hydrogen bonding and electrostatic interactions. Representative techniques include freeze-thaw cycles, ionic crosslinking, and similar processes. These methods offer advantages such as low cytotoxicity, good biodegradability, and reversibility, making them attractive for biomedical applications. However, due to the relatively weak interactions, physically crosslinked hydrogels often suffer from poor mechanical properties, limited structural stability, and fast degradation, which restrict their use in treating complex or high-stress wound environments. Chemical crosslinking, on the other hand, creates stable polymeric networks by forming covalent bonds between polymer chains. Common approaches include initiator-induced, photo-induced, and radiation-induced crosslinking. These techniques significantly improve the mechanical strength, stability, and durability of hydrogels, making them more suitable for long-term wound dressings or load-bearing applications. However, a major concern with chemical crosslinking is the residual crosslinking agents or byproducts, which may introduce cytotoxicity. Therefore, to ensure clinical safety, it is essential to select biocompatible or degradable crosslinkers and to implement efficient purification steps to remove any potentially harmful residues. In summary, each crosslinking method presents a trade-off among biocompatibility, mechanical performance, and biodegradability, and the selection of an appropriate strategy should be tailored to the specific clinical application.

Chen et al developed a catechol-modified CS-silver nanoparticle/esterified SA composite hydrogel (C/S/A/P/P) with integrated photothermal and antimicrobial properties for the treatment of infected and burn wounds. In this study, 3,4-dihydroxybenzaldehyde (DBA) was reacted with HCS via a Schiff-base reaction to introduce catechol groups, enhancing the hydrogel's adhesiveness and reducing capability, while 3-aminophenylboronic acid was grafted onto sodium alginate (SA) to improve its self-healing ability. The composite network, reinforced through the physical crosslinking of PVA and polyvinylpyrrolidone (PVP), exhibited significantly enhanced mechanical strength and moisture-retention capacity.[143] Hwang et al successfully developed a double-network (DN) hydrogel by combining thermosensitive methylcellulose (MC) with a pH-responsive adhesive conjugate of CS and gallic acid (CS-GA), synthesized via an EDC/NHS coupling

Table 1 Summary of Preparation Techniques for CS-Based Wound Dressings

Dressing Types	Preparation Technique	Advantage	Key Parameters	Reference
Hydrogel	Physical and chemical crosslinking	1) Improved mechanical strength 2) Faster gelation 3) Enhanced structural stability 4) Good cytocompatibility	1) Compressive strength increased from 0.65 kPa to 2.72 kPa 2) Gelation time shortened from 182.7 s to 35.8 s 3) Swelling ratio decreased (1155% → 706%); gel fraction increased (55.5% → 82.3%); pore size reduced (33.0 μm → 7.7 μm) 4) Cell viability >80% in cell counting kit-8 assay; few dead cells in live/dead staining	[110]
	Grafting and crosslinking	1) Strong tissue adhesion under wet conditions 2) Self-healing property 3) In vivo degradability 4) Excellent biocompatibility and hemocompatibility	1) Shear adhesion strength is 31.40 ± 5.09 kilopascal. Burst pressure is 132.04 ± 9.66 millimeter mercury column 2) >95% G' recovery after high strain (1000%); fragment reintegration within 30 min 3) Complete degradation by day 10 post-implantation 4) Cell viability is above 80% for L929 and human umbilical vein endothelial cells. Hemolysis ratio is below 5%	[111]
	Schiff base reaction and physical blending self-assembly	1) Favorable physical properties for wound dressing 2) Shear-thinning property 3) Reversible sol-gel transition	1) Water losing rate of 26.08 ± 1.05% at 24 hours, water sorption percentage of 57.77 ± 0.82%, and gelation time of 17 minutes at 0.3% cinnamaldehyde 2) Viscosity decreases from ~1000 Pa·s to ~10 Pa·s over shear rate 0.01–10 rad/s 3) Gel-to-sol transition at ~35% strain	[112]
	Ionic crosslinking and physical crosslinking	1) Excellent mechanical strength 2) Strong tissue adhesion 3) Sustained release profile	1) Compressive strength of 1.03 MPa and a 3.5-fold increase in storage modulus compared to the pristine matrix 2) Lap-shear strength of approximately 8.26 kPa 3) Cumulative release: ~40% at 1 h, ~63.67% at 72 h	[113]
	One-pot synthesis, chemical graft modification, dynamic covalent cross-linking assembly, physical blending loading	1) Good degradability 2) Injectable and self-healing hydrogel	1) Hydrogel storage modulus 5645 Pa loss modulus 1620 Pa 2) Viscosity decreases with shear rate (0.1–500 s^{-1}); G' = 5645 Pa, G" = 1620 Pa; self-healing within seconds after 500% strain	[114]
	Freeze-drying method and thermal initiation polymerization method	1) Controllable mild photothermal heating effect 2) Excellent mechanical and adhesive properties 3) Good biocompatibility and cell promotion	1) Stable temperature of about 45 °C under 808 nm near-infrared irradiation with power density of 0.5 W cm^{-2} 2) Elongation at break of hydrogel up to 262% tensile strength up to 62 kPa adhesion strength about 1.06 kPa 3) Cell viability higher than 85% significantly enhanced cell migration effect within 24 hours	[115]
	Schiff base reaction and in-situ gelation	1) Injectable and shear-thinning 2) High wet adhesion strength 3) Enhanced rheological stability 4) Improved porous microstructure 5) Adhesion stability	1) Shear rate range 0.1–100 rad/s (rheology); forms continuous filament ~0.5 mm diameter 2) Lap-shear on porcine skin: COS hydrogel reinforced with Laponite (COSL)0.75 = 42.3 kPa; peak adhesion 520.2 kPa at 24 h (vs. 267.7 kPa without Laponite at 36 h). Tensile on bovine bone: 349.4 kPa 3) Frequency sweep 0.1–10 Hz, strain 1%, 25 °C; base hydrogel without Laponite (COS) G' ~ 1200 Pa, COSL0.75 G' ~ 2800 Pa 4) COS shows disconnected flattened pores; COSL0.75 shows uniform interconnected 3D porous architecture 5) Visual demonstration lifting 900 g weight after bonding porcine skin for 12 h; air-bonded then submerged, pre-wetted bone, and direct underwater bonding; all stable after 7 days	[116]
	Crosslinking	1) Enhanced mechanical strength 2) Tissue adhesion 3) Biocompatibility	1) G' of dual-network hydrogel = 1219 Pa, 4.3× higher than single-network (281 Pa) 2) Adhesion strength = 45 kPa (vs 20 kPa for single-network) 3) Cell viability >99%	[40]

(*Continued*)

https://doi.org/10.2147/IJN.S607257

https://doi.org/10.2147/IJN.S607257

Table 1 (Continued).

Dressing Types	Preparation Technique	Advantage	Key Parameters	Reference
	One-step method based on HCS and TBA	1) Injectable and shear-thinning 2) High water content and swelling ability 3) Biocompatibility	1) Viscosity drops to 10^0 Pa·s at high shear rate 2) Water content ~90%; swelling ratio increases over time; moisture retention at 37 °C for 48 h 3) Hemolysis rate <5%; cell viability >90% for human umbilical vein endothelial cells, rat adrenal pheochromocytoma cells, mouse macrophage cell line after 5 days	[117]
	One-step electrodeposition	1) Excellent mechanical property 2) Sustained silver ion release 3) Good water content and thickness control	1) Tensile strength (2.18 MPa), elongation at break (133%) 2) Silver concentration after 5 days (344.27 ± 5.55 ppm), metallic silver (65.2%), silver ions (43.8%) 3) Thickness: pure CS hydrogel 0.31 mm, CS-Ag-montmorillonite (MMT) 0.44 mm; water content: CS 86.7%, CS-Ag-MMT ~80%	[118]
	Two-tube syringe-based co-injection and in situ cross-linking	1) Rapid gelation 2) Shear-thinning and injectability 3) High water content and swelling ratio 4) Excellent biocompatibility	1) Gelation time ≤ 30 seconds 2) Shear rate range 0.1–100 rad/s; viscosity decreases continuously 3) Water content >94%; equilibrium swelling ratio 20–23 in phosphate buffered saline at 37 °C 4) Cell viability > 90%; hemolysis rate < 4%	[119]
	Dual-layer fabrication via thermal polymerization and Fe^{3+}-mediated coordination bonding	1) Temperature-responsive contraction 2) High mechanical strength and fatigue resistance 3) Good hemocompatibility	1) 43% area shrinkage, >25 kPa contractile stress 2) Tensile strength increases with Fe^{3+}; quaternary ammonium chitosan/poly(N-isopropylacrylamide) janus hydrogel (QPJ-1) after 20 cycles to 200% strain retains 96.4±2.4% stress; mechanical hysteresis 68.7±11.7% 3) Hemolysis rate: QPJ-1 3.95% (<5% safe threshold), QPJ-0 5.32% (borderline); blood clotting index of QPJ-1 significantly lower than gauze and blank	[120]
	Dynamic Fe^{3+}/Mn^{2+}-phenolic coordination	1) Excellent biocompatibility 2) Shear-thinning and injectability 3) Tunable swelling ratio	1) L929 fibroblast viability exceeds 95% 2) Viscosity drops from 820.2 to 2.6 Pa·s as shear rate increases from 0.1 to 100 s^{-1} 3) Equilibrium swelling ratio: quaternary ammonium chitosan-tannic acid/layered double hydroxide-poly(sulfonatoaniline) hydrogel – version1 385.8%, poly(sulfonatoaniline) 2286.6%, poly(sulfonatoaniline) 3211.8%	[121]
	Dynamic cross-linking	1) Rapid gelation 2) Excellent mechanical properties 3) Provides a moist wound environment 4) Sustained release 5) Good blood compatibility and cytocompatibility	1) Gelation time < 10s 2) Stretchability up to 550%; compressive stress 0.6842 MPa at 90% strain; compressive modulus 0.2561 MPa 3) Water content ~94% 4) 52.6% at 12 h, 76.7% at 24 h, 97.9% at 72 h 5) Hemolysis ratio <1%, cell viability >90%	[122]
	Spray-coating technique	1) Excellent spray ability and mechanical properties 2) Rheological stability 3) Good biocompatibility	1) Film formation time < 2 minutes; tensile strength = 12.4 MPa; elongation at break = 715%; swelling ratio = 107–215% 2) Frequency sweep 1–10 rad/s, strain 1%; strain sweep 0.1–100% at 10 rad/s 3) Cell viability > 90% at working concentration	[123]
	Schiff base reaction	1) Excellent silver ion release efficiency 2) Sprayable and mechanically adaptable 3) Good biocompatibility	1) Silver ion release efficiency of 66% 2) In situ gelation time less than 2 minutes; tensile strength of 12.4 megapascals; elongation at break of 715%; swelling ratio from 107% to 215% 3) Cell viability above 90%	[124]
	Schiff base reaction	1) High mechanical strength 2) Strong self-adhesion 3) Sustained drug release 4) Excellent biocompatibility	1) Tensile strength > 400 kPa, stretchability > 1400%, toughness > 2900 kilojoules per cubic meter 2) Adhesive strength to skin is 2.7 kPa 3) Cumulative release of genitopirocide over 36 hours 4) Cell viability > 90% in mouse fibroblast cells	[30]

	Photothermal therapy (PTT) and nitric oxide (NO) gas therapy	1) Enhanced mechanical strength 2) Good injectability and conformability 3) Photothermal stability	1) Strain sweep (0.1–100%, 10 rad/s): gel hydrogel loaded with hollow copper sulfide and sodium nitroprusside shows higher G' and G" than Gel; frequency sweep (0.1–100 rad/s, 1% strain): G' > G" for both 2) Demonstrated on pig skin: no adhesion to tissue or detachment 3) 5 cycles of 10 min ON/10 min OFF at 0.39 W/cm^2; no significant difference in heating curves	[125]
	Schiff base reaction	1) Excellent injectability, self-healing, and pH-responsive degradation 2) Controlled release 3) Excellent biocompatibility and low hemolysis	1) Gelation time of 90 seconds; storage modulus (G') > loss modulus (G") up to 1000% strain; degradation faster at pH 5.0–6.5 than at pH 7.4 2) Total protein release of 42.44% at 8 hours (pH 7.4) vs 53.05% (pH 5.5); sustained release over 90 hours 3) Cell viability of 111.8% for L929 cells after 3 days; hemolysis rate <4% at 5 mg/mL	[126]
	Electrical stimulation and electrospinning	1) Strong bio adhesion 2) Good mechanical properties 3) Rheological stability	1) Adhesion strength ~ 3.0 kPa on fresh porcine skin 2) Tensile strength > 10 kPa, elongation at break 423%, compressive pressure > 700 Newtons at 80% strain 3) Frequency sweep 0.1–100 rad/s, strain 0.1%; G' > G" for chitosan/graphene oxide hydrogels	[127]
	A one-step mixing method	1) Good mechanical properties 2) High swelling and water content 3) Sustained and low-concentration release 4. Excellent cytocompatibility	1) Storage modulus greater than loss modulus (viscoelastic solid), compression modulus >25 kPa at 60% strain, fatigue resistance over 20 compression cycles 2) Swelling ratio 250–300%, water content over 80% 3) Tannic acid release <30 micrograms per milliliter, copper ion release <0.15 micrograms per milliliter, lasting up to 7 days 4) Cell viability >100%	[128]
	Solvent displacement strategy	1) Excellent mechanical properties 2) Low-temperature resistance 3) High critical strain in rheology 4) Good biocompatibility	1) Tensile strength 1.01 Megapascal, fracture strain 510%, and elastic modulus 53.8 kPa 2) Gelatin-chitosan oligosaccharides-emodin eutectogel has no crystallization peak; hydrogel shows freezing peak near 0 °C 3) Strain sweep (1–1000%, 1 Hz): G' > G" up to 410% strain; G" surpasses G' at >1000% strain 4) Cell viability of L929 cells greater than 90% at 24 hours and 48 hours	[129]
Sponge	Combining humidity-controlled electrospinningwith freeze-drying stabilization	1) High porosity and water absorption 2) High compression resilience 3) High hemocompatibility	1) Porosity of 99.8%, volume density of 2.8 mg/cm^3, and water absorption ratio of 539% 2) 100 cycles at 10 mm/min; resilience 87.9% after 100 cycles; height recovery 93% after single compression 3) Hemolysis rate <5% for all samples	[130]
	Freeze-drying	1) Excellent mechanical properties and fatigue resistance 2) Highly-interconnected superporous structure 3) Biocompatibility	1) Maximum stress retention 95% after 100 compression cycles at 85% strain, compressive pressure after liquid absorption 123.72 kPa for water and 32.76 kPa for blood 2) Pore diameter 1052.0 ± 208.9 μm; porosity 88.42 ± 6.18% 3) Cell viability of 3T3 fibroblasts above 90%	[131]
Membrane	Electrospinning	1) Sustained drug release 2) Enhanced mechanical properties 3) Improved thermal stability 4) Good biocompatibility	1) Rapid release within 30 min followed by slow release and complete release at about 120 min 2) Tensile strength: pectin polysaccharides/chitosan/polyvinyl alcohol (PP/CS/PVA) 11.35 ±0.42 MPa; PP/CS/PVA@15% hydroxypropyl-β-cyclodextrin/dihydromyricetin inclusion complex (HDIC); elongation at break: PP/CS/PVA 7.38±1.37%; PP/CS/PVA@15%HDIC higher 3) Thermogravimetry/derivative thermogravimetry: initial weight loss (25–120 °C) 6.4–8.2%; main degradation at 200–400 °C; HDIC increases decomposition temperature; PP/CS/PVA@10% and @15% HDIC show higher residue at 800 °C 4) Cell viability higher than 98% hemolysis rate lower than 2%	[132]

(*Continued*)

https://doi.org/10.2147/IJN.S607257

https://doi.org/10.2147/IJN.S607257

Table 1 (Continued).

Dressing Types	Preparation Technique	Advantage	Key Parameters	Reference
	Emulsion spinning technology	1) Improved mechanical flexibility 2) Favorable biodegradability 3) Improved spinnability and fiber uniformity 4) Sustained drug release 5) Excellent hydrophilicity and water retention	1) Elastic modulus 25.21±3.38 MPa elongation at break 23.05±2.35% 2) Degradation rate up to 81.4±1.11% at 10 days 3) Fiber diameter 116.5±35.8 nm polydispersity index close to 0 4) Sustained release for 168 h 5) Water contact angle reduced swelling rate up to 846.02±5.32%	[133]
Flim	In-situ oxidative polymerization followed by solution casting	1) Have tunable electrical conductivity 2) Mechanical property modulation by glycerol plasticizer 3) High swelling ratio and water vapor transmission	1) Electrical conductivity from 10^{-2} to 10^{-3} S/m 2) Ultimate tensile strength (UTS) 5.33 MPa, elongation 39.1%; adding 10% glycerol: UTS 5.54 MPa, elongation 75.8%; >10% glycerol decreases UTS 3) Swelling ratio after 60 min: chitosan 105%; water vapor transmission rate: 1400–1640 $g \cdot m^{-2} \cdot day^{-1}$	[134]
Nanomaterial	A one-step hydrothermal method	1) Long-term colloidal stability 2) Small and uniform particle size 3) Good biocompatibility	1) Stable without precipitation after 2 months 2) Transmission electron microscope average diameter 5.51 nm; high-resolution transmission electron microscopy lattice fringe 0.21 nm; dynamic light scattering hydrodynamic diameter 9.949 nm 3) Cell viability above 80%, hemolysis rate below 5%, no acute toxicity in mice	[135]
	Electrospinning	1) High mechanical strength and stability 2) Controlled biphasic drug release 3) Suitable porosity for wound healing 4) Excellent cytocompatibility	1) Tensile strength of 7.44 MPa and minimal weight loss after degradation 2) Approximately 38% drug released within 60 min 3) Porosity between 58.3 ± 3.3% and 85.7 ± 2.6% 4) Cell viability over 95% on human umbilical vein endothelial cells within two days	[136]
	Electrospinning	1) Suitable water management performance 2) Good mechanical and thermal properties 3) Outstanding biocompatibility	1) Water absorption rate 80.85±2.70% 94.23±3.45% water vapor transmission rate 0.19 ±0.02 $g \cdot m^{-1} \cdot 24h^{-1}$ 2) Ultimate tensile strength 5.08±0.15 MPa to 9.76±0.52 MPa initial thermal decomposition temperature over 110.0°C 3) Cell viability over 80% hemolysis rate less than 5%	[137]
	Electrospinning	1) Ultra-high water absorption capacity 2) Excellent water vapor transmission performance 3) Satisfactory mechanical property 4) Good biocompatibility	1) Water absorption rate reaches 2770.70±122% per time 2) Water vapor transmission rate is 4585.99±65 $g \cdot m^{-2} \cdot day^{-1}$ 3) Tensile stress of tri-layer dressing is 149.18±32 kPa 4) Cell viability of all dressing groups is above 80% and the highest is 120.89±2.98%	[138]
Microneedle	Vacuum-assisted mold filling UV photo crosslinking	1) Moderate swelling 2) Good structural integrity 3) Excellent biocompatibility	1) Swelling ratio measured in phosphate buffered saline (PBS) at 37 °C; equilibrium reached after 2 h 2) Digital and stereomicroscope images show no cracks or deformation 3) Cell viability exceeds 230% of initial value after 3 days hemolysis rate below 0.5%	[139]
	Electro-assembly	1) pH-responsive drug release 2) Voltage-responsive drug release 3) Good cytocompatibility, blood compatibility and low hemolysis rate	1) Release in PBS pH 5.4, 7.4, 10.4 at 37 °C; significantly higher release at pH 5.4 2) Direct current voltages applied: +2 V, 0 V, −2 V; release in PBS pH 7.4 at 37 °C; positive voltage increases release, negative decreases 3) Cell viability exceeds 80%, and hemolysis rate is 0.28%	[140]
Bandage	Drug encapsulation; freeze-drying molding; ionic crosslinking	1) Stable ionic conductivity and mechanical property 2) Sustained drug release 3) Stable degradation profile	1) Ionic conductivity 140 mS/cm, hydrated elastic modulus 0.43±0.18 MPa, chitosan molecular weight 310–375 kDa, degree of deacetylation 85% 2) Cumulative 4AP release from crosslinked chitosan and halloysite nanotubes/4-Aminopyridine: 6–8% over 21 days (≈2.2 μg per scaffold); non-crosslinked chitosan and 4-Aminopyridine released ≈20% with burst within 24 h 3) Remaining scaffold after 21 days ≈ 80–90%	[141]
Scaffold	A blending and freeze1-drying technique	1) Good colloidal stability 2) High swelling capacity 3) Sustained drug release 4) Biodegradability	1) Zeta potential of 34.5 ± 3.83 mV 2) Swelling ratio of 43.6% 3) 75% cumulative release at day 7 4) 80.5% mass loss of QnChS scaffold at day 14	[142]

reaction The formation of the MC hydrogel relied on physical crosslinking driven by hydrogen bonding and hydrophobic interactions at physiological temperatures. Meanwhile, the CS-GA component underwent spontaneous self-crosslinking under neutral pH through Schiff base and Michael addition reactions, enabling chemical crosslinking without the need for additional crosslinking agents. This resulted in a stable dual-crosslinked network under physiological conditions. The synergistic interaction between covalent and non-covalent bonds significantly enhanced the hydrogel's compressive strength and structural integrity. Moreover, the incorporation of CS-GA facilitated the formation of a compact microporous structure, which is beneficial for absorbing blood and wound exudates. In addition to maintaining thermosensitive properties, the hydrogel exhibited excellent cytocompatibility, notable hemostatic performance, and strong adhesion to various organ tissues. These features underscore its great potential as an effective hemostatic tissue adhesive[110] (Figure 2A). Guo et al utilized TA as a dynamic and physical crosslinker to fabricate a QCS/TA hydrogel by crosslinking QCS through ionic and hydrogen bonding interactions. Owing to the rapid and reversible formation of these interactions between QCS and TA, the hydrogel exhibits excellent shear-thinning properties, allowing it to be injected or formed in situ to conform precisely to irregular wound surfaces. The QCS/TA hydrogel demonstrates tunable gelation time, good injectability, strong tissue adhesion, self-healing capability, as well as remarkable antibacterial activity and free radical scavenging ability. In full-thickness skin wound models, the hydrogel significantly accelerated wound healing and enhanced collagen (CO) deposition. Therefore, the QCS/TA hydrogel shows great potential as an emergency biomedical material for rapid hemostasis and wound repair, offering promising applications in the biomedical field.[144] Gong et al developed a self-supplying hydrogen sulfide (H_2S) CS-hyaluronic acid composite hydrogel system. In this design, CCS

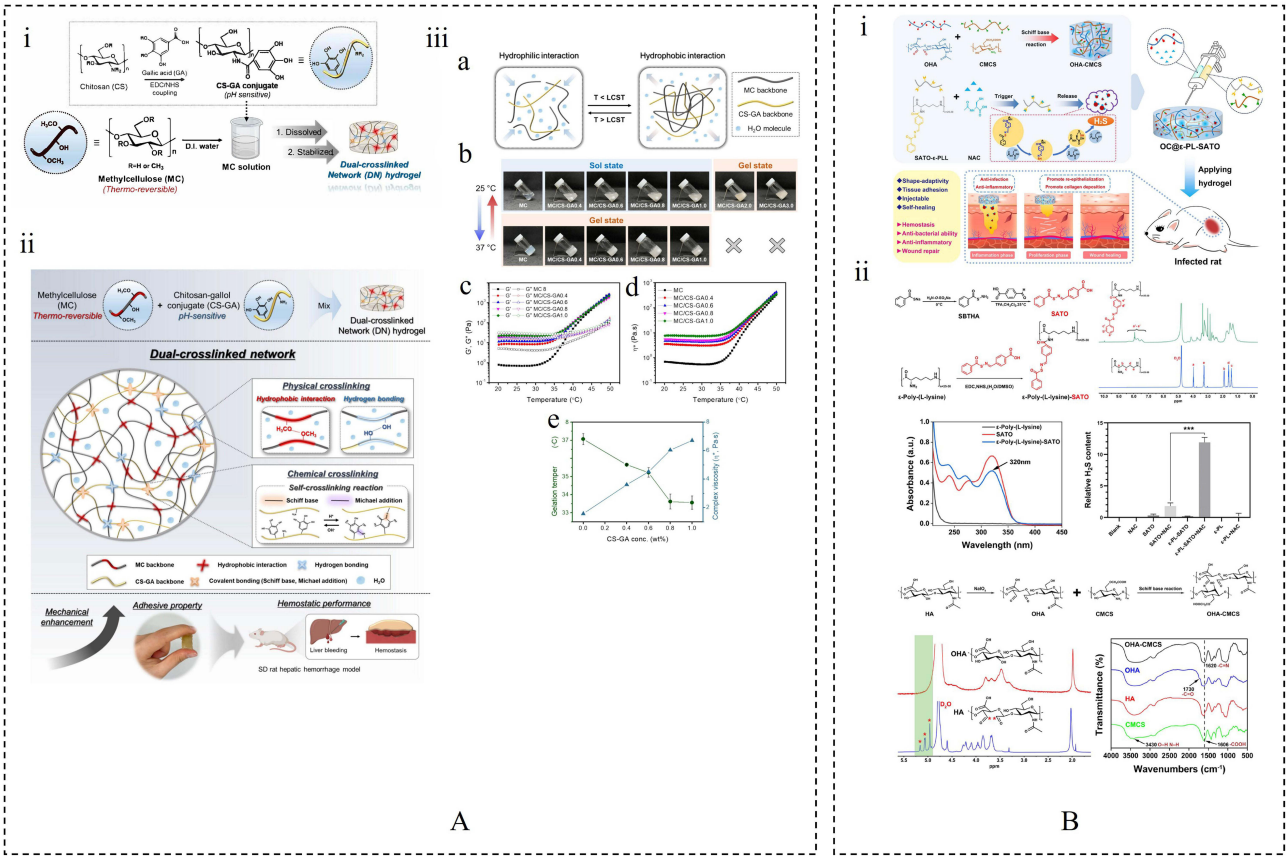

Figure 2 (**A**) (i) Schematic illustration of the preparation of the CS-gallol (CS-GA) conjugate and the fabrication of the dual-crosslinked network hydrogel of MC and CS-GA. (ii) Schematic illustration of a dual-crosslinked network hydrogel composed of MC and CS-GA. (iii) (a) Schematic depiction of the lower critical solution temperature sol-gel transition of MC/CS-GA. (b) Photographs showing the vial-tilting test conducted on the MC and MC/CS-GA systems. (c) Changes in the storage moduli and loss moduli of the MC and MC/CS-GA systems during dynamic temperature sweep measurements. (d) Variation in the complex viscosities (η^*) of the MC and MC/CS-GA systems during the temperature sweep tests.(e) Relationship between the gelation temperature (n=3) and complex viscosity.[110] Copyright 2024, Elsevier. (**B**) (i) Schematic illustration of OC@ε-PL-SATO hydrogel preparation and application for infected wound care in rat. (ii) Synthesis scheme of ε-PL-CE.[119] ***p < 0.001. Copyright 2025, Elsevier.

https://doi.org/10.2147/IJN.S607257

and the H_2S donor ε-polylysine-S-aroylthiooxime (ε-PL-SATO) were loaded into component A, while oxidized hyaluronic acid (OHA) and the initiator N-acetylcysteine were loaded into component B. Upon mixing the two components, a Schiff base reaction rapidly formed a hydrogel within 30 seconds. This hydrogel was capable of sustained H_2S release during the inflammatory phase of wound healing, promoting M2 macrophage polarization and exerting anti-inflammatory effects. Additionally, by leveraging the excellent biocompatibility, hemostatic ability, and tissue regeneration properties of natural polysaccharides, along with the broad-spectrum antibacterial activity of CCS and ε-PL-SATO, the hydrogel demonstrated enhanced anti-inflammatory efficacy and wound healing potential[119] (Figure 2B). Currently, chemical, physical, and dual crosslinking strategies are commonly employed to fabricate hydrogels in order to achieve sufficient mechanical strength. When a hydrogel comes into contact with a wound, it can absorb exudate, promote autolysis of necrotic tissue, maintain a moist wound environment, and relieve pain. Therefore, hydrogel dressings are more suitable for exuding wounds and dry necrotic wounds.[51]

Phase Inversion

Phase inversion is a commonly used film-forming technique that transforms a polymer from a liquid to a solid state through physical changes. This process typically involves either the evaporation of the solvent from a homogeneous polymer solution or the introduction of a non-solvent to induce phase separation, resulting in the formation of a solid polymer-rich phase and a liquid polymer-poor phase. Common phase inversion methods include solvent evaporation precipitation, controlled evaporation precipitation, and immersion precipitation, all of which fall under the category of phase inversion techniques. Based on the mechanisms of phase separation induction, phase inversion can generally be induced through four main approaches: (1) lowering the temperature of the polymer solution; (2) immersing it in a non-solvent; (3) exposing it to a non-solvent vapor environment; or (4) directly evaporating the solvent under ambient air or elevated temperatures.[145] The rate of phase inversion, as well as the structure and properties of the resulting membrane, are influenced by various factors, such as the solubility of the solvent in the non-solvent, the insolubility of the polymer in the non-solvent, and the temperature of the non-solvent.[146] Therefore, careful control of these parameters is crucial for fabricating polymer membranes with desired microstructures and functional properties.

Bajpai et al developed CS/microcrystalline cellulose (MCC) composite films using a novel technique known as vapor-induced phase inversion(VIPI). In this process, a CS suspension is prepared in an aqueous medium and exposed to ammonia vapor. The ammonia vapor rapidly induces the precipitation of CS, transforming the suspension from a liquid to a solid phase and forming the composite film. Within the resulting film, MCC is uniformly distributed throughout the CS matrix, acting as a diffusion barrier in the membrane structure. This uniform dispersion of MCC effectively regulates the film's water absorption, moisture permeability, and drug release properties[147] (Figure 3A). Shahrzad et al fabricated a composite wound dressing with controlled drug release capability using the phase inversion method, featuring an asymmetrical poly(ε-caprolactone) (PCL) membrane. The dressing consists of two integrated layers: a bottom layer of asymmetrical PCL membrane and a top layer composed of a drug-loaded CS-silica matrix. In vitro studies demonstrated that the composite dressing achieved a cumulative drug release rate of approximately 70%, providing a porous substrate that supports skin cell growth and facilitates tissue regeneration. Moreover, drug release analysis revealed that the PCL layer significantly reduced the initial burst release of lidocaine hydrochloride and enabled sustained delivery of the drug from the CS-silica-lidocaine layer to the wound site. The PCL membrane not only serves as a supportive scaffold for dermal cells but also contributes to prolonged analgesic effects, thereby promoting wound healing[148] (Figure 3B and C). Joana C et al prepared CS and PVA films using a combination of solvent casting and phase inversion methods. The CS solution was added to the PVA solution, mixed thoroughly, and then cast into glass Petri dishes to form films. After drying, the samples were immersed in a coagulation bath containing sodium hydroxide and sodium sulfate to induce acid-base neutralization and promote the precipitation of the mixture from the solution to form solid films, which simultaneously detached from the Petri dishes. The resulting CS/PVA blended films exhibited significant antibacterial properties conferred by CS, showing strong inhibitory effects against *S. aureus* and Pseudomonas aeruginosa, while the PVA enhanced the flexibility and hydrophilicity of the films[49] (Figure 3D).

Phase inversion is currently the most commonly used method for preparing porous polymer membranes. CS-based membrane dressings typically feature a porous and highly permeable structure, which not only enables effective

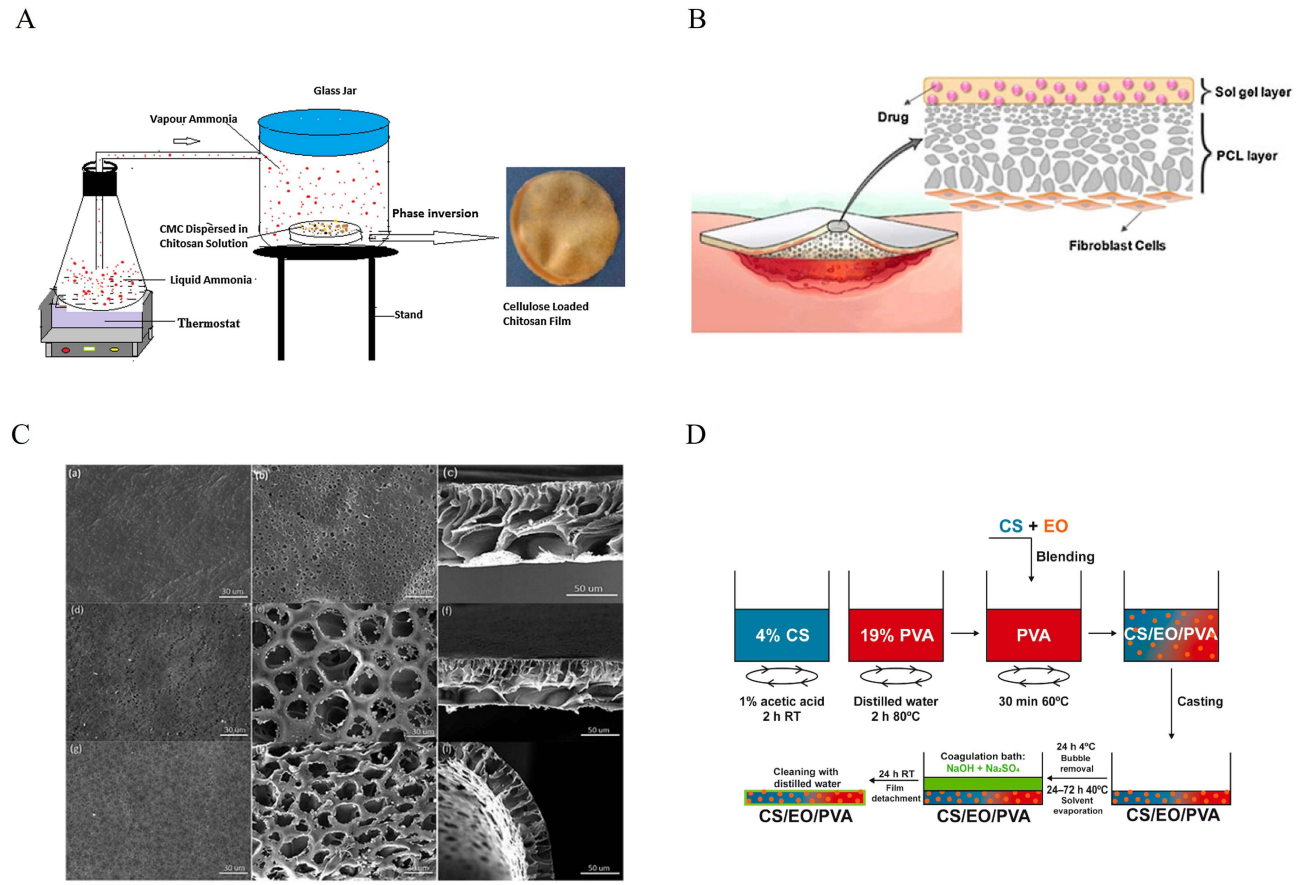

Figure 3 (**A**) In-lab built apparatus for the VIPI approach.[147] Copyright 2015, Cellulose. (**B**) Schematic of the two-layered wound dressing; (**C**) The scanning electron microscopy (SEM) micrographs of the membranes (a, d and g) bottom surface (b, e and h) and cross-sectional (c, f and i) area of the PCL, PCL-polyethylene glycol $(PEG)_{400}$ and PCL-PEG_{1500} membranes, respectively.[148] Copyright 2017, John Wiley & Sons, Ltd. (**D**) Preparation of EO-loaded CS/PVA blended films.[49] Copyright 2021, Elsevier Ltd.

absorption of wound exudates but also provides excellent drug-loading capacity and supports cell proliferation. Meanwhile, the structure serves as a barrier against external harmful factors and helps regulate gas exchange.[149] Therefore, this type of dressing is particularly well-suited for managing wounds with exudate.

Freeze-Drying

Freeze-drying, also known as lyophilization, is a highly effective technique for fabricating three-dimensional porous dressings. In this method, a precursor solution composed of a solvent and dispersed solute particles is initially frozen within a mold at low temperatures, resulting in the formation of solidified solvent crystals. Under reduced pressure and low-temperature vacuum conditions, these crystals undergo direct sublimation, transforming the liquid-gas interface into a solid-gas interface. This phase transition effectively minimizes capillary forces by eliminating liquid-vapor surface tension, thereby preserving the structural integrity and dimensional stability of the material during the drying process. Consequently, this technique yields porous scaffolds with well-defined architecture, making it particularly suitable for biomedical dressing applications.[150,151]

Lin et al developed a hemostatic dressing (CS1N1-1‰CO) with rapid and efficient hemostatic performance, antibacterial activity, and biocompatibility by integrating halloysite nanotubes (HNTs), CS, and collagen through directional freeze-drying and asymmetric structural design. In their method, a mixed suspension of HNTs and CS was poured into a mold and subjected to directional freezing using liquid nitrogen as the cooling source to establish a bottom-up temperature gradient. This thermal gradient guided the formation of ice crystals along a specific direction, during which HNTs and CS were physically excluded and concentrated at the interfaces between the growing ice crystals, achieving solid-liquid phase separation. Subsequent freeze-drying removed the ice crystals via sublimation, leaving

https://doi.org/10.2147/IJN.S607257

behind an axially aligned porous structure. The resulting sponge exhibited a high porosity and highly oriented architecture, which significantly increased the surface area, facilitating the adhesion and aggregation of red blood cells. Meanwhile, the interconnected porous network promoted oxygen and nutrient exchange, providing a favorable physiological microenvironment for cell survival. This not only helped maintain a moist wound environment but also supported cell proliferation and accelerated wound healing[152] (Figure 4A). Hu et al developed a multifunctional electrospun fiber sponge (EFS) for chronic wound healing by combining humidity-controlled electrospinning with freeze-drying stabilization. The humidity-induced phase separation triggered spontaneous curling and stacking of polylactic acid (PLA) electrospun fibers, resulting in a unique fluffy and voluminous architecture. Subsequent freeze-drying further enhanced the structural stability and compressive resilience of the EFS. The drug-loaded variant (CC@EFS), incorporating curcumin and ciprofloxacin hydrochloride, exhibited high porosity, which provided ample interfacial area for efficient drug release. The distinctive fluffy morphology also contributed to improved hemostatic performance both in vitro and in vivo. CC@EFS effectively accelerated epithelialization, stimulated CO deposition, and promoted angiogenesis by eradicating pathogenic bacteria and suppressing inflammatory responses[130] (Figure 4B). Jiang et al developed a superporous CS sponge (spCS) by precisely controlling the pre-freeze-drying temperature at 0 °C. At this temperature, the polymer chains of CS exhibit optimal mobility, enabling a controllable secondary polymer network reorganization and compaction during the freeze-drying process. This leads to the formation of spCS with a unique structural architecture characterized by highly interconnected macroporous networks. Upon blood absorption, the spCS rapidly recovers its original shape and maintains sufficient compressive pressure on the wound surface, thereby forming a robust physical barrier that significantly enhances hemostatic efficiency. Moreover, in non-compressible organ

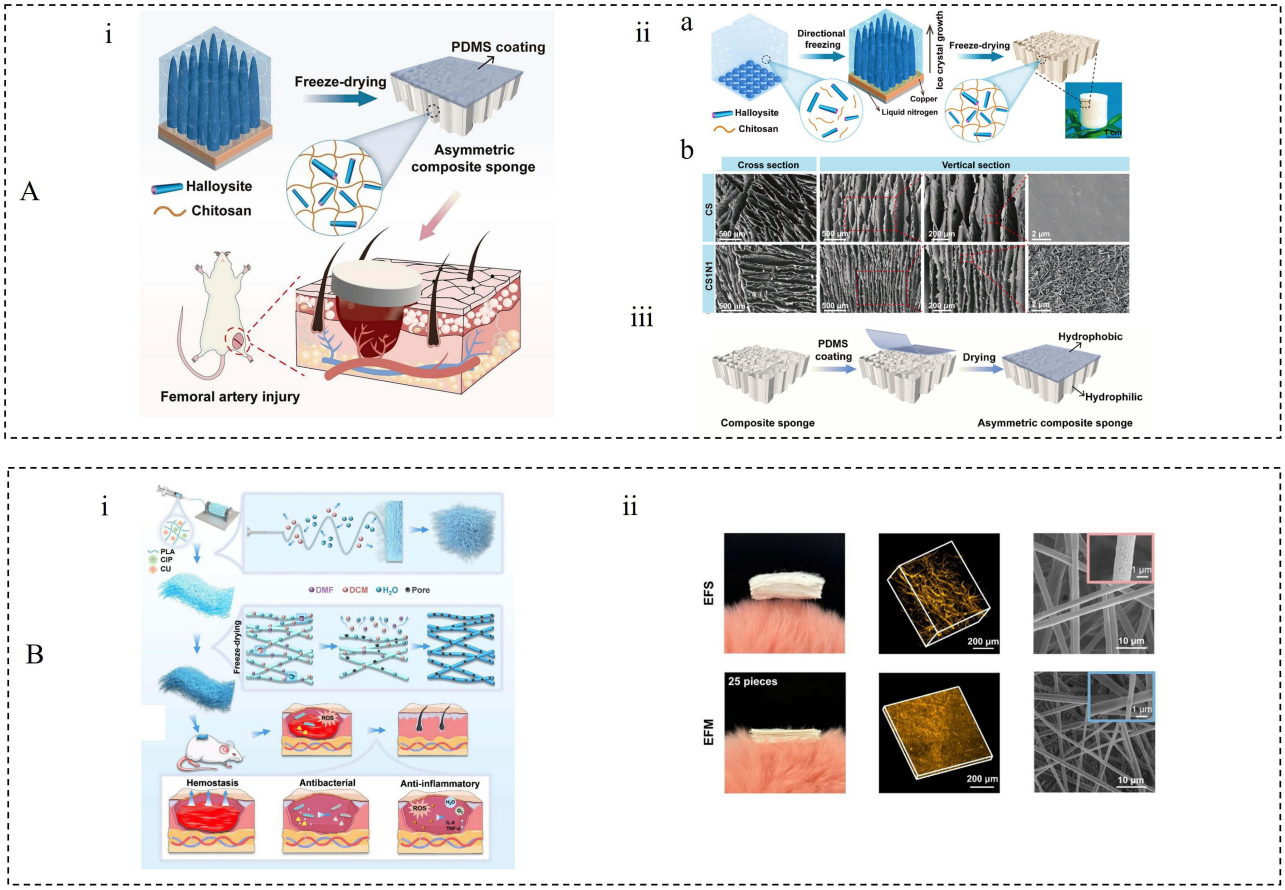

Figure 4 (A) (i) Schematic illustration of an asymmetric halloysite/CS/CO sponge with hydrophobic coating. (ii) (a) Schematic illustration of HNTs/CS composite sponge prepared by directional freeze-drying method. (b) SEM images of pure CS and CS_1N_1. (iii) The preparation of asymmetric composite sponge.[152] Copyright 2023, Elsevier. (**B**) (i) Schematic illustration of the preparation and application of multifunctional EFS. (ii) Morphology and structure of EFS.[130] Copyright 2025, Wiley-VCH GmbH.

 https://doi.org/10.2147/IJN.S607257

hemorrhage models, the spCS demonstrates superior performance compared to conventional dressings in terms of hemostasis, cellular infiltration, vascular regeneration, and in situ tissue remodeling, highlighting its promising potential for advanced clinical wound management.[131]

Freeze-drying is one of the most commonly used techniques for preparing sponge dressings.[153] The resulting dressings possess a highly porous structure, enabling efficient absorption of wound exudate, which makes them particularly suitable for managing heavily exuding wounds.[154] However, sponge dressings alone have low intrinsic water content and are thus insufficient in maintaining a moist wound environment. As a result, their effectiveness in treating dry and necrotic wounds is limited.[155]

Electrospinning

Electrospinning is a technique that utilizes a high-voltage electric field to draw charged polymer solutions into fine jets, producing fibers with diameters ranging from the nanometer to micrometer scale.[156] Compared with traditional solution or melt spinning methods, electrospinning can yield fibers that are 100 to 10,000 times thinner.[157,158] This technology combines the advantages of electrospraying and conventional dry spinning,[159] allowing the formation of solid fibers directly from solution without the need for chemical coagulation or high temperatures. Due to the polycationic nature and strong intramolecular interactions of CS, it can be challenging to form an electrospinning solution with optimal charge density and viscosity, which in turn affects jet stability and the formation of uniform fibers.[132] To improve the spinnability of CS, the ability of a polymer solution to form stable fibers during electrospinning, co-spinning agents such as polyethylene oxide, PVA, PLA, and polycaprolactone are often introduced during the electrospinning process.[160] Among these, PVA is widely used due to its excellent biocompatibility and hydrophilicity. In addition, PVA offers tunable mechanical properties, making it suitable for various wound dressing applications.[161] Guo et al prepared a hydroxypropyl-β-cyclodextrin/dihydromyricetin inclusion complex (HDIC) to enhance the solubility and stability of dihydromyricetin. Subsequently, HDIC was incorporated into a mixed electrospinning solution composed of pectic polysaccharide (PP), CS, and PVA, leading to the development of a novel PP/CS/PVA@HDIC electrospun membrane for wound dressing applications. The resulting PP/CS/PVA membrane exhibited randomly oriented fibers with an average diameter ranging from 200 to 400 nm, resembling the collagen fibers found in natural skin. These membranes demonstrated excellent biocompatibility, hemocompatibility, surface hydrophilicity, and wettability, while enabling sustained release of dihydromyricetin. Notably, the membranes showed significant antibacterial, anti-inflammatory, and free radical scavenging activities.[132] Liu et al encapsulated mupirocin (MP) and cerium oxide nanoparticles (CeNPs) into a PVA/CS polymer and fabricated nanofiber membranes via electrospinning, with an average fiber diameter of 200–300 nm. The CeNPs, approximately 40–50 nm in size, were uniformly distributed on the smooth surface of the nanofibers. The resulting fibers exhibited small pore sizes and high porosity, and their well-interconnected porous structure facilitated the sustained release of both MP and CeNPs, making them suitable for wound dressing applications. The dressing enabled controlled release of MP and demonstrated rapid and long-lasting antibacterial activity against both methicillin-sensitive and methicillin-resistant *S. aureus* (MRSA) strains. Meanwhile, the embedded CeNPs effectively scavenged ROS maintaining redox homeostasis at the wound site, accelerating healing, and promoting skin regeneration[162] (Figure 5A and B). Zhao et al developed an antioxidant nanofiber scaffold based on an ascorbyl palmitate (AP)/2-hydroxypropyl-β-cyclodextrin (HP-β-CD) inclusion complex (AP/CD-IC) using electrospinning technology First, AP was encapsulated in HP-β-CD to enhance its solubility and chemical stability. The resulting AP/CD-IC was then combined with PVA and quaternary ammonium CS, and processed via electrospinning to fabricate PVA/QCS-IC nanofibers with both antioxidant and antibacterial properties. These nanofibers not only enable the controlled release of drugs within the fiber matrix but also maintain the stability and bioavailability of the active compounds, thereby enhancing therapeutic efficacy. This design offers valuable insights for the future development of HP-β-CD-based electrospun nanofibers in the treatment of chronic diabetic wounds and provides new perspectives for applying poorly soluble compounds in skin wound healing[163] (Figure 5C and D). Electrospinning has been regarded as a simple and efficient method for fabricating nanofiber-based membranes.[164,165] Nanofibers possess unique advantages, such as nanoscale topography that mimics cellular signaling, a high specific surface area conducive to biomolecule adsorption, and a structural composition highly similar to the natural ECM. These features make them promising candidates for advanced wound dressings. Notably, nanofiber dressings not only structurally resemble natural skin but also exhibit excellent absorption and breathability, effectively preventing issues such as wound dehydration or

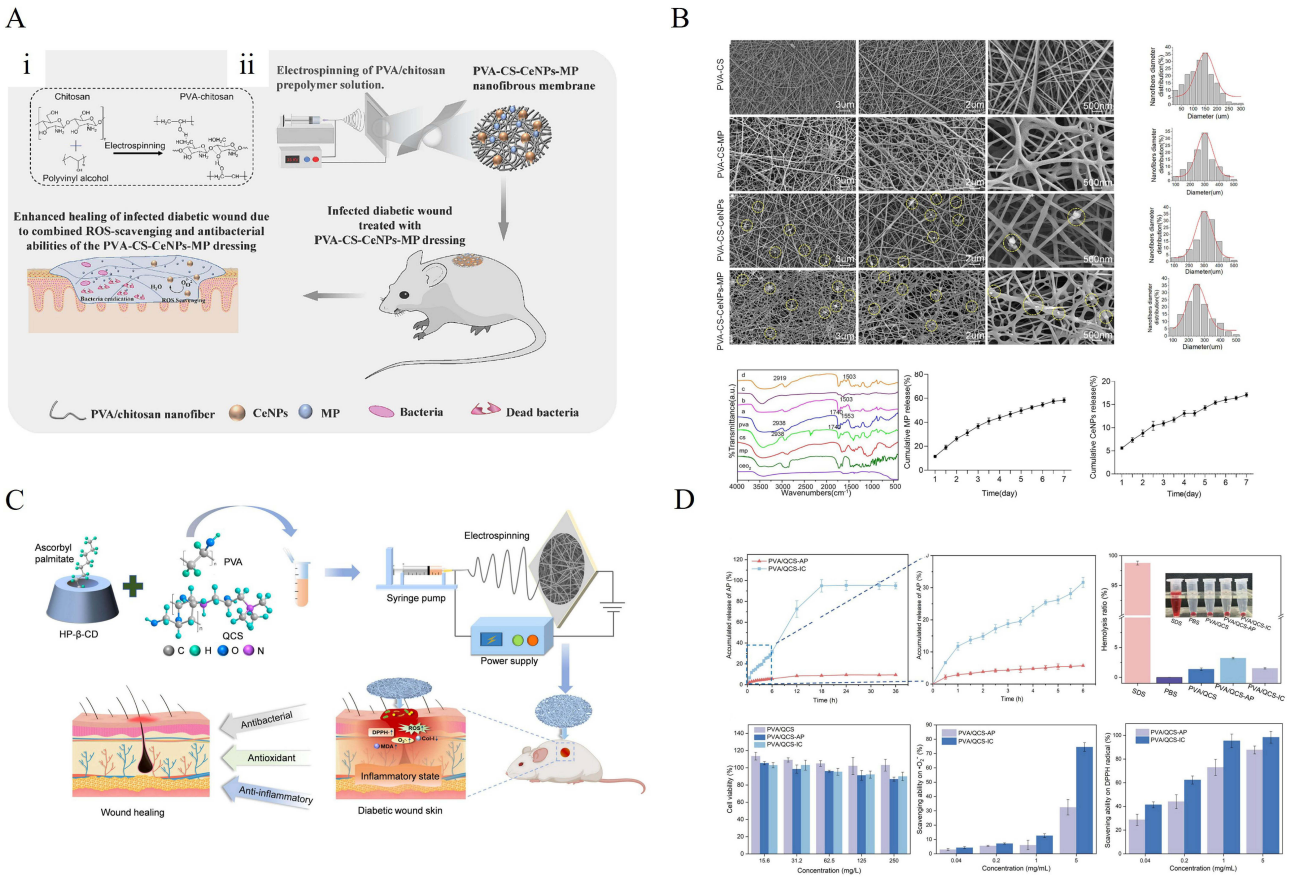

Figure 5 (**A**) (i) Schematic representation of the chemical crosslinking of PVA-CS electrospun nanofibers. (ii) Schematic illustration of the CeNPs-MP dressing promoting healing in an infected diabetic wound. (**B**) Characterization of PVA-CS-based nanofibers.[162] Copyright 2023, Elsevier. (**C**) Schematic illustration of the fabrication process and diabetic wound healing effect of PVA/quaternary ammonium CS-inclusion complex (QCS-IC) nanofibers. (**D**) Biocompatibility, drug release, and antioxidant evaluation of nanofibers.[163] Copyright 2024, The Author(s).

fluid accumulation. Their micron-scale pore structure plays a vital role in promoting fibroblast migration, proliferation, and tissue infiltration. In addition, it supports neovascularization and nutrient exchange, thereby accelerating wound healing and reducing the risk of scarring. Furthermore, the alignment of nanofibers significantly influences cell morphology. By mimicking the distinct layers and orderly arrangement of natural skin, well-aligned nanofibers can create a more favorable environment for cell growth, further enhancing the healing process.[166]

Solvent Casting

Solvent casting is a widely employed technique in which a polymer and a plasticizer are dissolved in a volatile solvent, while the active pharmaceutical ingredient may be either dissolved or dispersed within the resulting solution. The homogeneous mixture is then poured into a mold and left undisturbed to allow solvent evaporation.[167] This process involves sequential steps of polymer and plasticizer dissolution, coating of the polymeric solution onto a substrate, and controlled solvent removal, which collectively induce molecular orientation of polymer chains and intercalation of plasticizer molecules.[168] Consequently, a continuous and uniform film is formed. Owing to its simplicity, reproducibility, and relatively low production cost, solvent casting is regarded as a reliable and versatile method for the fabrication of polymeric films in pharmaceutical and biomedical applications.[169] Murilo et al successfully fabricated multilayer silk fibroin/CS/SA films using the solvent casting technique. In this multilayer configuration, the ALG layer—designed to be in direct contact with the wound—provides absorbency and promotes tissue regeneration; the intermediate CS layer exhibits antibacterial activity and serves as a carrier for therapeutic agents; while the outer silk fibroin layer acts as a protective barrier against the external environment, offering mechanical strength and structural support to the dressing.[170]

Jose M et al successfully prepared a functional biopolymer film using the solvent casting method. The film was composed of xylan, CS, and a deep eutectic solvent (DES). DES served not only as a dissolution medium for the biopolymers but also acted as a plasticizer and compatibilizer between xylan and CS. The results showed that the film with a xylan-to-CS mass ratio of 50:50 exhibited the best overall properties, featuring good structural uniformity, excellent thermal stability (up to 150 °C), and suitable mechanical performance (tensile strength up to 8.2 MPa and elongation at break up to 110%). Moreover, the film demonstrated good biocompatibility with human keratinocytes (HaCaT cell line) (cell viability ≥ 80%), outstanding UV-protection capability (transmittance ≤ 38% in the 200–400 nm range), and significant antibacterial activity against MRSA[171] (Figure 6). Seda et al prepared CS-based films containing different concentrations of Hypericum perforatum oil (0.25–1.5% v/v) using the solvent casting method. The resulting composite films exhibited notable antibacterial activity against *S. aureus* and *Escherichia coli (E. coli)*. Moreover, the CS films showed no cytotoxicity toward NIH3T3 fibroblast cells and provided a favorable surface for cell adhesion and proliferation.[172] The solvent casting method is a robust process that is well suited for large-scale industrial production. By adjusting processing parameters such as MW, the properties of the resulting films can be finely tuned, enabling the fabrication of films with high optical transparency and controllable porosity.[173] Fatima et al investigated the influence of CS MW and the type of casting acid on the properties of both unplasticized CS films and MSO-plasticized CS films prepared by solvent casting. Water absorption assessments revealed that only high-molecular-mass CS films could be considered suitable as absorbent dressings. Furthermore, the incorporation of MSO resulted in films that were markedly thicker and exhibited higher water permeability compared with the unplasticized counterparts. In addition, MSO significantly enhanced the antibacterial activity of the CS-based films against *S. aureus* and *E. coli*.[174]

Overall, preparation techniques do more than simply shape wound dressings; they fundamentally determine their macro- and microstructures, physical properties, and clinical applicability. Different methods not only impart distinct morphological features to the materials, but also significantly influence their mechanical strength, porosity, moisture-management capacity, drug-loading and release behavior, bioactivity retention, and manufacturing complexity. From a processing perspective, solvent casting and freeze-drying offer good reproducibility and scalability, whereas electrospinning, although dependent on high-voltage equipment and precise process control, provides the most advantageous

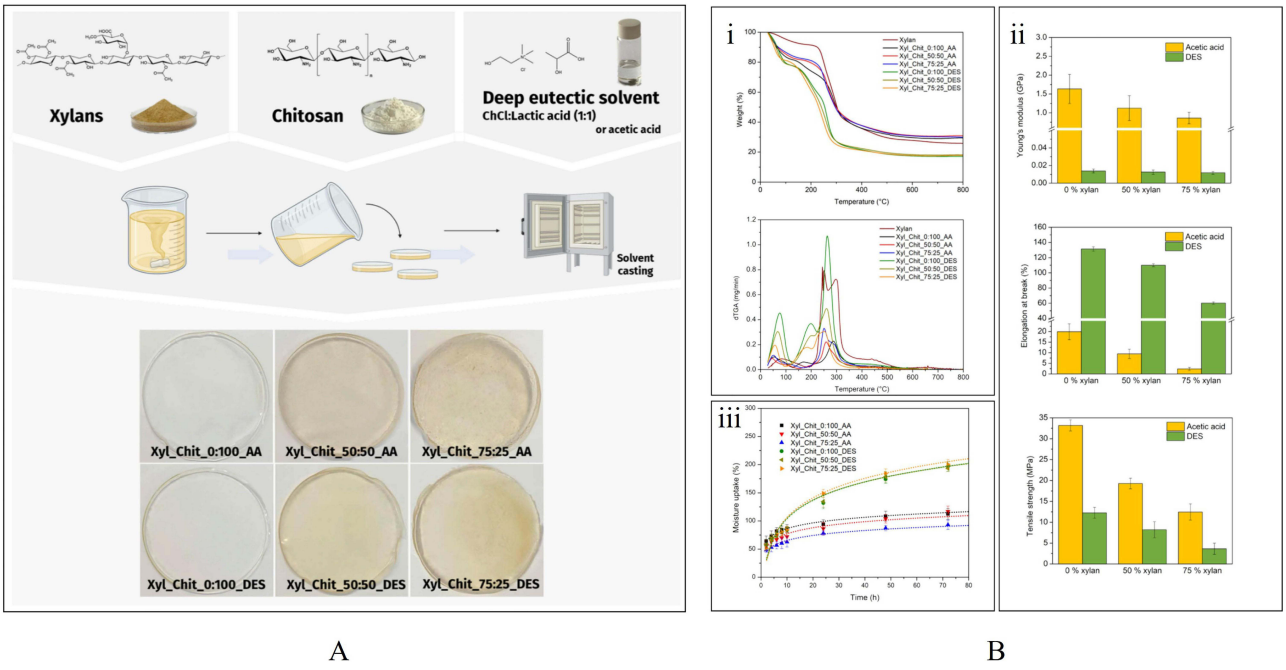

Figure 6 (**A**) Schematic representation of the preparation procedure and digital photographs of the xylan-CS based films. (**B**) (i) The thermogravimetric analysis profile and the corresponding derivatives, (ii) Young's modulus, elongation at break and tensile strength, and (iii) moisture uptake capacity of the prepared films.[171] Copyright 2025, The Authors.

https://doi.org/10.2147/IJN.S607257

nanoscale biomimetic architecture. Chemical crosslinking can markedly improve material strength and stability, but it requires strict purification procedures to eliminate residual crosslinking agents that may be harmful to the human body. In terms of performance–application matching, crosslinked hydrogels are more suitable for irregular wounds, drug delivery, and the hydration and autolytic debridement of dry necrotic wounds; phase-inversion membranes are appropriate for wounds requiring barrier protection and moderate exudate management; freeze-dried sponges, owing to their high porosity and rapid fluid absorption, are better suited for heavily exuding or bleeding wounds; electrospun nanofibrous scaffolds, with their high specific surface area and structural mimicry of the natural ECM, are more suitable for chronic wounds and tissue regeneration; and solvent-cast films, because of their transparency, uniformity, and ease of scale-up, are better suited for the protection and non-invasive observation of superficial wounds. Therefore, the fabrication strategy for CS-based dressings should be selected according to the pathological characteristics of the target wound, the required core functions, and practical considerations such as cost, scalability, and clinical application value, with comprehensive trade-offs among process complexity, structural features, functional performance, and translational feasibility.

CS-Based Dressings for Skin-Wound Healing Applications

This section reviews the therapeutic applications of CS-based dressings in the management of diverse wound types, including burns, surgical incisions, infected wounds, and diabetic ulcers, as presented in Table 2. We also briefly discuss the underlying mechanisms by which these dressings promote wound healing. Although a comprehensive account of all biomedical applications is beyond this review scope, the highlighted studies emphasize their critical and multifaceted roles in facilitating the healing process in a broad spectrum of wound environments.

CS-Based Dressings for Burn Wounds

Burn injuries are among the most common and destructive types of trauma encountered in daily life, typically caused by heat sources such as hot liquids, steam, high-temperature gases, flames, or molten metal, which damage the skin and underlying tissues or organs.[185] Superficial burns tend to heal quickly with minimal scarring. Burn wounds can be categorized as first-degree, second-degree, and third-degree burns with accordance to depth. First-degree burns damage the superficial layer of the epidermis. Superficial second-degree burns injure the epidermis and dermis. However, deep second-degree burns involve the deep dermis with residual skin appendages. In regard of third-degree burns, the full-thickness skin is destroyed up to the subcutaneous, muscular, and skeletal levels.[186,187] Burn wounds often trigger a rapid inflammatory response at the injury site, which not only degrades necrotic tissue but also activates pro-proliferative signaling pathways.[188,189] Nevertheless, severely burned skin is prone to persistent inflammation, which promotes tissue catabolism and impedes healing.[190] In addition, damage-induced destruction of cellular tissues severely compromises the skin's barrier function, significantly increasing the risk of secondary infections, and in severe cases, may lead to sepsis or systemic infections.[191,192] Clinically, conventional treatments such as skin grafting are effective for early burn wound care, improving prognosis in patients with severe burns by reducing hospitalization time and mortality.[193] However, burn wound healing and treatment still face numerous challenges, including tissue destruction, severe pain, delayed wound healing, fluid loss, and bacterial infections. Therefore, choosing appropriate burn dressing materials is crucial.[194] A major drawback of traditional dressings is their tendency to adhere to necrotic tissue on the wound surface, often causing secondary injury and increased pain upon removal.[195,196] Novel CS-based dressings offer several advantages, including high fluid absorption and retention capacity, strong antibacterial and anti-inflammatory effects, reduced adhesion, hemostatic activity, and the ability to inhibit excessive fibroblast proliferation.[197]

Radwan-Pragłowska et al designed a bilayer composite nanofibrous scaffold consisting of a poly lactic acid (PLA) nanofiber layer and a porous ACCS layer, further incorporated with bioactive nanoparticles (ZnO, Fe_3O_4, and Au). This scaffold was developed for deep burn wound repair, with its nanofibrous architecture effectively mimicking the three-dimensional ECM network while maintaining mechanical strength comparable to that of natural skin. The ACCS layer provides excellent biodegradability, biocompatibility, and inherent hemostatic and antibacterial properties, whereas the nanoparticle-doped PLA layer imparts electrical conductivity, enabling the electrostimulation-induced proliferation and activation of fibroblasts. Experimental results demonstrated that the hybrid scaffold significantly enhanced cell adhesion and proliferation and promoted the secretion of basic fibroblast growth factor. Among the different modifications, the

Table 2 Summary of Some CS Dressings Used for Wound Healing

Target Wound	Chitosan Type/Drug Loaded	Model Type	Mechanism	Functional Outcome	Clinical Readiness	Refs.
Infected wound	CS/ Insulin growth factor-1	In vitro: L929 mouse fibroblasts and human umbilical vein endothelial cell model In vivo: infected full-thickness skin defect mice model	1) Positively charged amino groups and catechol groups disrupt bacterial membranes 2) Catechol groups scavenge free radicals 3) Imine bonds break in acidic infected wounds, releasing IGF1 4) HIF-1α/VEGF/CD31/α-SMA↑ TNF-α/IL-6↓ 5) Dynamic Schiff base bonds enable self-healing; sprayable for irregular wounds	Self-healing, pH-responsive Antibacterial & antioxidant Enhances angiogenesis, cell migration Anti-inflammatory	Preclinical stage	[20]
	CCS/Polydopamine-encapsulated polydopamine-encapsulated poly (thiophene-3-acetic acid)	In vitro: L929 mouse fibroblasts cell model In vivo: mouse infected full-thickness skin wound model; mouse liver hemorrhage model	1) The Schiff base and Fe^{3+} coordination bond can be repaired automatically after the hydrogel network is disrupted 2) Conductivity to enhance endogenous electrical signals 3) Photothermal antibacterial treatment kills bacteria by using the extremely strong penetrating power of near-infrared light 4) Significantly reduce the production of free radicals at the wound site to accelerate wound closure	Self-healing Photothermal antibacterial effect Antioxidant Hemostasis	Preclinical stage	[175]
	CS/LVN	In vitro: mouse fibroblasts and mouse monocyte-macrophages cell models In vivo: rat full-thickness infected wound model; rat tail amputation bleeding model	1) ↓ PI3K/Akt and NF-κB pathways and promotes M2 macrophage polarization 2) TNF-α, IL-1β↓, IL-10, TGF-β↑ 3) Enhances angiogenesis and collagen deposition	Provides a moist environment Enhances angiogenesis, cell migration Encourages CO deposition	Preclinical stage	[119]
	CS/Montmorillonite	In vitro: mouse fibroblast model; rat red blood cell hemolysis model In vivo: rat infected wound model; rat liver hemorrhage model	1) Silver ion slow-release antibacterial 2) chitosan positive charge antibacterial 3) Montmorillonite reinforced structure	Promotes wound healing, reduces bacterial infection Rapid hemostasis, reduces blood loss	Preclinical stage	[118]
	CS/Honey	In vitro: human immortalized keratinocytes cell model	1) Cationic NH_3^+ groups disrupt bacterial cell wall 2) Chitosan/collagen: free NH_2 groups attract cell adhesion 3) Honey: may reduce cell viability at high conc. due to reduced free NH_2 groups	Antibacterial activity Promotes wound healing (cell migration and proliferation) Absorbs exudate Maintains a moist environment	Only in vitro data are available, low clinical readiness	[176]
	CS/Ciprofloxacin hydrochloride	In vitro: human foreskin fibroblasts cell model In vivo: bacteria-infected full-thickness skin wound rat model	1) pH-responsive chitosan swelling/protonation 2) Voltage-responsive electrostatic repulsion and local pH change 3) Ciprofloxacin inhibits bacterial DNA gyrase/topoisomerase II 4) Positive charge promotes coagulation 5) Restores endogenous electric field to regulate cell behavior	Controlled drug release Good cytocompatibility, hemocompatibility, hemostatic effect Accelerates infected wound healing	Preclinical stage	[140]
	CS/Bletilla striata polysaccharide	In vitro: L929 mouse fibroblasts cell model In vivo: rat tail amputation model; liver trauma model; full-thickness skin defect model	1) Same dual-network structure provides adhesion and self-healing 2) Photothermal effect kills bacteria locally and reduces inflammation 3) Absorbs exudate, maintain moist environment, physical barrier	Broad-spectrum antibacterial Antioxidant Hemostatic Accelerates wound healing	Preclinical stage	[177]

(*Continued*)

https://doi.org/10.2147/IJN.S607257

https://doi.org/10.2147/IJN.S607257

Table 2 (Continued).

Target Wound	Chitosan Type/Drug Loaded	Model Type	Mechanism	Functional Outcome	Clinical Readiness	Refs.
	CS/Tigecycline	In vitro: Human umbilical vein endothelial cell model	1) Tigecycline inhibits bacterial protein synthesis 2) Chitosan disrupts bacterial membranes 3) Multilayer structures regulate diffusion	Antibacterial Controlled release Promotes cell proliferation	Preclinical stage	[136]
	CS/TA	In vitro: human umbilical vein endothelial and L929 mouse fibroblast cell models In vivo: rat liver bleeding hemostasis model; rat back infected wound model	1) Chitosan: cationic disruption of bacterial membranes 2) Tannic acid: polyphenolic hydroxyls for ROS scavenging 3) Hydrogen bonding/electrostatic adhesion 4) Dynamic crosslinking for self-healing	Tissue adhesion Self-healing Extensibility Antibacterial Antioxidant	Preclinical stage	[178]
	CS/Emodin	In vitro: L929 mouse fibroblasts cell model In vivo: mice infected full-thickness skin wound model	1) Deep eutectic solvents forms hydrogen bonds with gelatin to enhance toughness 2) Schiff base reaction helps disperse emodin 3) Chitosan oligosaccharides, emodin and betaine work together to kill bacteria 4) The dressing promotes cell migration, angiogenesis and collagen deposition	Multi-antibacterial activity Promotes cell proliferation and migration Accelerates infected wound healing Promotes angiogenesis and collagen regeneration	Preclinical stage	[129]
	CS/HCuS, SNP	In vitro: cell model In vivo: mouse model with MRSA-infected skin wounds	1) Synergistic killing (heat/-OH/NO) 2) Anti-inflammatory repair (NO/Cu^{2+})	Eliminates MRSA Promotes wound healing Reduces inflammation, Enhances tissue repair	Preclinical stage	[125]
	Carboxylated CS/no drug	In vitro: LO2 human normal liver cells, A549 human non-small cell lung cancer cells and L929 mouse fibroblasts models In vivo: full-thickness non-infected wounds and *S. aureus*-infected mouse model	1) H_2O_2 releases Ag^+ to break bacterial membranes 2) NIR light heats Au core, killing more bacteria, speeding Ag^+ release, and helping blood vessel growth	Kill bacteria, reduce inflammation, promotes vessel growth Speed wound healing Ag^+ and photothermal therapy work together to boost effects	Preclinical stage	[123]
	CS/grafted gallic acid and thioctic acid	In vitro: L929 fibroblast cells, Human umbilical vein endothelial cells, RAW264.7 macrophages models In vivo: rat liver perforation hemostasis model; rat dorsal full-thickness infected wound model	1) Chitosan NH^{3+} disrupts bacterial membranes 2) Gallic acid blocks bacterial metabolism and ROS scavenging 3) Disulfide bonds enable UV polymerization without photoinitiators 4) Pyrogallol captures radicals for crosslinking 5) Adhesion via H-bond and π-π stacking	Rapid hemostasis Antibacterial Accelerates infected wound healing ROS scavenging, anti-inflammatory Enhances collagen deposition	Preclinical stage	[111]
Diabetic wound	CS/SA	In vitro: human umbilical vein endothelial cells and mouse fibroblast NIH3T3 cells model In vivo: diabetic mice model; diabetic bama pigs model	1) Poly(deca-4,6-diynedioic acid) degrades into succinic acid 2) IL-1β, TLR-4, NFκB↓; VEGF, Angpt2, FGF2, Col-1↑	ROS scavenging Anti-inflammation Promotes cell migration and angiogenesis	Preclinical stage	[21]
	CS/Caffeic acid	In vitro: human umbilical vein endothelial cell model In vivo: mouse liver bleeding model	1) Adenine promotes cell proliferation 2) Caffeic acid provides antioxidant effects 3) Chitosan and its phenolic hydroxyl groups synergistically act as antibacterial agents 4) Schiff base crosslinking with POSS enhancement confers self-healing and mechanical properties	Promotes cell proliferation, migration, and viability Antibacterial activity Antioxidant Accelerates wound closure, reduces bacterial load, suppresses inflammation, promotes angiogenesis	Preclinical stage	[40]

	HCS/TBA	In vitro: rat adrenal pheochromocytoma cells, human umbilical vein endothelial cells and mouse macrophage cell models In vivo: diabetic SD rats model with infected full-thickness wounds	1) ↑VEGFA/ERK pathway 2) Regulates macrophage M0→M1→M2 transition 3) Distributes exogenous electrical stimulation via conductive hydrogel to enhance cell signaling	Antimicrobial, ROS scavenging Promotes angiogenesis, neurogenesis, macrophage M2 polarization, and chronic wound healing	Preclinical stage	[117]
	CS/Quercetin nanoparticles	In vitro: human adipose-derived mesenchymal stromal cell model In vivo: diabetic wistar rat with full-thickness excisional skin defection model	1) TNF-α/IL-1β↓, VEGF↑ 2) Increases bFGF and collagen	Accelerates wound closure Increases neo-epitheliallength and dermal thickness Enhances collagen deposition Promotes angiogenesis	Preclinical stage	[142]
	CS/Curcumin	In vitro: L929mouse fibroblast cell model In vivo: diabetic male Wistar rat model	1) IGF-1, TGF-β1, VEGF↑, IL-6, MPO↓ 2) Sustains Fickian diffusion release 3) PI3K/Akt & NF-κB pathway modulation	Increases wound closure, collagen, angiogenesis and epidermal/dermal thickness Reduces inflammation	Preclinical stage	[179]
	CS,CCS/Phloretin	In vitro: L929 mouse fibroblast cell, human umbilical vein endothelial cells, mouse macrophage cell and Mouse brain microvascular endothelial cell model In vivo: diabetic rat with MRSA-infected full-thickness skin wound; rat liver hemorrhage model	1) pH response releases silver and phloretin 2) Platelet-rich plasma growth factors help blood vessels grow and cells multiply 3) Dynamic bonds allow self-repair and injection	Promotes diabetic wound healing Kills MRSA and *E. coli* Reduces inflammation;Enhances cell migration and angiogenesis Improves re-epithelialization and collagen deposition Controls bleeding	Preclinical stage	[126]
	CCS/Cinnamaldehyde	In vitro: L929 mouse fibroblast cell model In vivo: diabetic rat full-thickness skin wound model	1) Schiff base crosslinking and hydrogen bonding form the hydrogel 2) CA disrupts bacterial membrane 3) ↓NF-κB pathway, TNF-α↓, IL-10↑ 4) ↑VEGF-A and CD31 5) Promotes M2 macrophage polarization	Antibacterial Anti-inflammatory Promotes cell proliferation/ migration, re-epithelialization, collagen deposition, angiogenesis Regulates macrophage polarization	Preclinical stage	[112]
	CS/Thymol	In vitro: NIH-3T3Mouse embryonic fibroblast cell model	1) Cationic chitosan nanoparticles and PDA-rGO attract to negatively charged bacterial membranes → disrupt the membrane 2) Thymol damage bacterial enzymes and membranes, neutralize free radicals 3) Dopamine's catechol groups form hydrogen and covalent bonds with tissues 4) Reduced graphene oxide enables electrical signal transmission	Antibacterial activity Antioxidant activity Improves cell migration Possesses hemostatic properties	Only in vitro data are available, low clinical readiness	[113]
	CS/DFO@Mn-ZIF-8, UCMSC-exo	In vitro: human umbilical vein endothelial cells, L929 mouse fibroblast cells and mouse macrophage cell models In vivo: high-fat diet-induced diabetic mice model	1) Glucose/ROS responsive degradation 2) Mn-ZIF-8 remove excess ROS and release Zn^{2+} ions to kill bacteria 3) Desferrioxamine stabilizes HIF-1α to promote new blood vessel formation 4) Exosomes regulate Immune and tissue regeneration signaling	Synergistic antibacterial activity, excessive ROS scavenging, anti-inflammation Promotes angiogenesis Enhances cell proliferation and migration, accelerates re-epithelialization and collagen deposition	Preclinical stage	[114]

(*Continued*)

https://doi.org/10.2147/IJN.S607257

https://doi.org/10.2147/IJN.S607257

Table 2 (Continued).

Target Wound	Chitosan Type/Drug Loaded	Model Type	Mechanism	Functional Outcome	Clinical Readiness	Refs.
	CS/Copper-dihydromyricetin nanoparticles	In vitro: human umbilical vein endothelial cells and mouse monocyte/macrophage cell models In vivo: type 1 diabetic mice with dorsal full-thickness wounds and *S. aureus* infection	1) DMY released first, promotes M2 macrophage polarization via NF-κB inhibition and scavenges ROS 2) Cu^{2+} released later, achieves >80% killing against *S. aureus* and *P. aeruginosa* and disrupts biofilms 3) Stimulates endothelial cell migration and tube formation 4) Provides hemostatic function and accelerates diabetic wound closure	Anti-inflammation and antioxidant Antibacterial Pro-angiogenic Hemostasis & healing	Preclinical stage	[180]
Burn injuries	CCS/NSHD	In vitro: human umbilical vein endothelial cells, L929 mouse fibroblast cells and mouse macrophage cell models In vivo: mice infected third-degree burn wound model	1) H_2S release activates multiple pro-healing pathways: AMPK, RAS-MAPK-AP1, ERK1/2-p38, Nrf2-HO-1 2) Thiolated dopamine and H_2S scavenge ROS 3) Chitosan in hydrogel disrupts bacterial membranes 4) Promotes glycolysis and ATP production in endothelial cells 5) Enhances fibroblast migration via RAS-MEK-AP1 signaling	Accelerates burn wound healing Reduces bacterial infection (broad-spectrum antibacterial) Scavenges ROS, relieves oxidative stress Promotes angiogenesis and cell migration/proliferation Reprograms M1 macrophages to M2 phenotype, reducing inflammation	Preclinical stage	[18]
	CS/Astragalus polysaccharide	In vitro: L929 mouse fibroblast cell model In vivo: rat infected burn wound model	1) Hydrophilic-hydrophobic gradient creates capillary-driven unidirectional fluid transport 2) $CoCl_2$ hydrates to change color; chitosan and Co^{2+} provide antibacterial effects; APS promotes cell proliferation, anti-inflammation, and collagen synthesis	Antibacterial Promotes L929 cell proliferation, migration, adhesion Accelerates wound closure, increases collagen deposition, reduces inflammation	Preclinical stage	[138]
	CS/borneol, Gallic Acid(GA)	In vitro: L929 mouse fibroblast cells and human umbilical vein endothelial cell models In vivo: deep burn wound mouse model	1) Dynamic crosslinks: self-healing and improved strength 2) Acidic environment burst release of borneol and Zn^{2+} 3) Borneol activates TRPM8 for pain relief 4) GA and Zn^{2+} provide antibacterial and antioxidant functions 5) GA and borneol provide anti-inflammatory effects 6) Zn^{2+} and CD31 promote angiogenesis	Pain relief, antibacterial, anti-inflammatory, antioxidant, pro-angiogenic Self-healing, shape-adaptable, injectable, adhesive, and pH-responsive drug release	Preclinical stage	[181]
Postoperative wounds	N,O-carboxymethyl chitosan/ε-poly-L-lysine	In vitro: human umbilical vein endothelial cells and mouse embryonic fibroblasts models In vivo: New Zealand rabbits (liver trauma, ear artery bleeding, muscle implantation models), SD rats (sidewall defect-cecum abrasion model)	1) Physical separation of wounds 2) High water absorption concentrates blood cells to form clots 3) Inhibition of fibroblast adhesion and proliferation 4) ε-poly-L-lysine disrupts bacterial membranes via electrostatic interaction	Prevention and treatment of postoperative adhesion rapid hemostasis, broad-spectrum antibacterial Promotion of tissue repair, biodegradable Good biocompatibility	Preclinical stage	[182]

	Quaternized chitosan/ protamine	In vitro: human gingival fibroblasts model In vivo: Rat liver hemorrhage model, rat tail amputation model, rat palatal defect model, rat subcutaneous injection model	1) Dynamic non-covalent crosslinking (hydrogen and ionic bonds) 2) Protamine's positive charge electrostatically disrupts bacterial membranes 3) Tannic acid catechol groups provide wet adhesion and antioxidant activity 4) Quaternized chitosan enhances antibacterial and hemostatic effects 5) Reduces inflammation, promotes collagen deposition and angiogenesis	Promoting postoperative periodontal wound healing Broad-spectrum non-antibiotic antibacterial Antioxidant ROS scavenging, rapid hemostasis Strong tissue adhesion, self-healing	Preclinical stage	[183]
	CS/Zinc oxide and manganese dioxide nanoparticles	In vitro: mouse embryonic fibroblasts model	1) Release of Zn^{2+} and Mn^{4+} ions disrupts bacterial membrane 2) Chitosan provides biocompatibility 3) Kaolinite enhances stability 4) Nanoparticles generate reactive oxygen species scavenging	Antibacterial Antioxidant Promotes cell viability Biodegradable	Only in vitro data are available, low clinical readiness	[19]
Cachectic wounds (cancer cachexia)	CCS/Trichosanthes polysaccharide	In vitro: mouse macrophages, human umbilical vein endothelial cells, mouse myoblasts, bone marrow-derived macrophages and mouse splenic/peripheral blood lymphocytes cell models In vivo: mice full-thickness skin defect model; cachexia mouse model with dorsal skin defect; mouse hypertrophic scar model	1) Down-regulates En-1 and scar-related genes 2) Inhibits TGF-β-induced En-1 and fibronectin 3) Modulates macrophage polarization and promotes T/NK cell proliferation 4) Reduces inflammation in wounds	Accelerates wound healing in cancer cachexia Reduces scar formation Promotes angiogenesis, collagen, and epithelial repair Self-healing, injectable, and biocompatible Antibacterial against Gram-negative bacteria Modulates local immunity	Preclinical stage	[184]
Full-thickness skin wounds	CS/polypyrrole, ulvan, and glycerol	In vitro: human keratinocyte cells and mouse fibroblast cell models In vivo: mouse full-thickness wound model	1) Formation via electrostatic and hydrogen bonding interactionsConductivity mimics endogenous electric fields 2) Activates Ca^{2+} influx and MAPK/ERK and PI3K/Akt pathways to enhance cell proliferation 3) Polypyrrole induces bacterial membrane disruption and oxidative stress 4) Ulvan and chitosan provide hydrophilicity, swelling, and radical scavenging	Antibacterial against *S.aureus, E. coli*, and P aeruginosa Antioxidant protection against H_2O_2 induced oxidative stress Promotion of fibroblast proliferation under electrical stimulation Acceleration of wound closure	Preclinical stage	[134]
	CS/4-aminopyridine	In vitro: human dermal fibroblasts model In vivo: rat full-thickness excisional wound model	1) 4AP blocks potassium channels, possibly enhancing cellular excitability and metabolism 2) ES promotes migration, proliferation, and ECM synthesis 3) Together, 4AP potentiates ES effects via mitochondrial support, shifting wound from proliferation to remodeling phase with less scar	Increases fibroblast metabolism Accelerates wound closure Protects mitochondrial function Reduces inflammation Optimize ECM remodeling (collagen I/III ratio) Promotes angiogenesis Promotes hair follicle regrowth Upregulates neurotrophic factor expression	Preclinical stage	[141]

https://doi.org/10.2147/IJN.S607257

gold nanoparticle-functionalized scaffold exhibited the most pronounced cell proliferation and bioactivity. Overall, the PLA/ACCS-nanoparticle composite scaffold shows great potential in promoting angiogenesis, tissue remodeling, and the healing of deep burn wounds, offering a promising strategy for the development of advanced CS-based bioactive wound dressings.[198] Zhang et al constructed a bioactive hydrogel-based synthetic skin (HBSS) by forming a hydrogel matrix through Schiff-base crosslinking between aldehyde-modified hyaluronic acid and CCS, into which dopamine nanoparticles loaded with N-(benzoyl mercapto) benzamide (NSHD) were encapsulated. The HBSS creates an artificial barrier over burn wounds, effectively preventing bacterial infection and removing excess exudate, thereby providing a moist environment conducive to tissue regeneration. The high ROS levels and acidic conditions in the wound microenvironment induce hydrogel degradation and the release of the hydrogen sulfide (H_2S) precursor NSHD, achieving in situ H_2S delivery. The released H_2S not only alleviates oxidative stress at the wound site but also activates multiple pro-healing signaling pathways, including AMPK, RAS-MAPK-AP1, MAPK-ERK1/2-p38, and Nrf2-HO-1, thereby markedly suppressing excessive inflammation, promoting the proliferation and migration of skin cells, and enhancing angiogenesis in the wound tissue. Consequently, in murine skin injury models, HBSS significantly accelerates wound healing, reduces bacterial infection and scar formation, and offers a promising new strategy for clinical burn treatment[18](Figure 7A). Zhu et al developed CS/ALG-based nanospheres encapsulating Esculentoside A (EsA), a traditional Chinese medicine with potent anti-inflammatory activity This system was capable of inhibiting M1 macrophage polarization while enhancing the proportion of M2 macrophages. It achieved sustained drug release and long-lasting anti-inflammatory effects while reducing cytotoxicity. The prolonged release of EsA from the nanoparticles not only extended the duration of therapeutic action but also accelerated wound healing, promoted better epithelialization, enhanced angiogenesis, and facilitated collagen synthesis and remodeling. The synergistic combination of EsA, nanoparticles, and scaffolds offers a promising strategy for the treatment of burn injuries[199] (Figure 7B).

CS-Based Dressings for Postoperative Wounds

Postoperative wounds face multiple challenges during postoperative recovery, particularly complications such as infection, bleeding, and tissue adhesion, which can significantly affect patients' quality of life and even pose life-threatening risks.[200–202] It has been reported that patients with surgical site infections (SSI) have a mortality rate twice that of uninfected individuals;[203] intraoperative or postoperative bleeding occurs in approximately 10–35% of cases.[204] Severe hemorrhage can induce hypotension, organ dysfunction, or even death. In cases involving irregular wound shapes, non-compressible internal organs, or ruptured high-pressure vessels, conventional hemostatic approaches often prove ineffective.[205] Meanwhile, although some natural polysaccharide-based anti-adhesion materials have shown promising performance in open surgeries, their use in minimally invasive procedures remains limited due to poor handling and insufficient tissue adherence. Therefore, the development of multifunctional wound dressings that exhibit good biocompatibility, hemostatic capacity, antibacterial activity, and anti-adhesion properties—particularly those suitable for complex wound conditions—is crucial for improving surgical safety and postoperative healing outcomes. Postoperative wounds following cesarean section are frequently associated with complications such as bacterial infection, ulceration, and tissue dehydration. Wang et al developed a CS-based nCu/ZnO hydrogel wound dressing with promising wound healing potential. This hydrogel exhibits excellent tissue adhesion and water retention properties, while also serving as a physical barrier to protect the wound site. In vivo experiments demonstrated that, compared to the CS-ZnO and control groups, the CS-nCu/ZnO-treated group showed significantly increased leukocyte infiltration and enhanced collagen deposition, with complete wound closure observed within 16 days. These findings suggest that the CS-nCu/ZnO hydrogel holds considerable promise as a wound repair material for post-cesarean section applications.[206] Wang et al systematically evaluated the efficacy of CS-based dressings in the management of surgical bleeding wounds. Compared with conventional gauze, the CS dressing demonstrated a high specific surface area, excellent biocompatibility, and superior blood absorption capacity. It significantly promoted platelet aggregation and enhanced coagulation function, as indicated by the reduced prothrombin time and activated partial thromboplastin time (APTT). Moreover, the CS dressing exhibited sustained antibacterial activity for up to 8 days postoperatively and facilitated the proliferation of probiotic microbiota, thereby strengthening cutaneous immune responses and promoting wound healing.[207] Geng et al engineered an injectable, biocompatible hydrogel composed of naturally derived Cirsium setosum extracts, a traditional medicinal herb, and

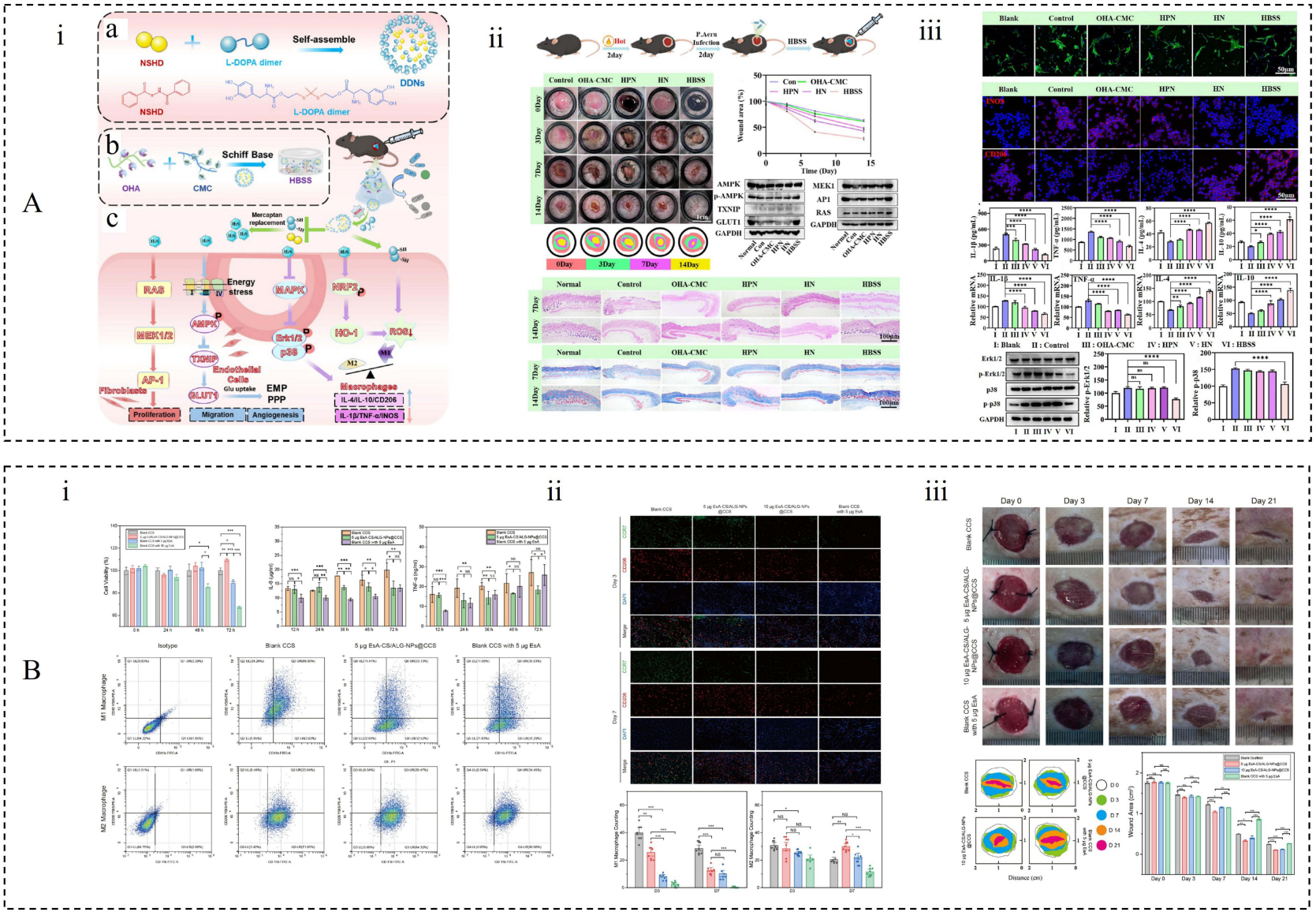

Figure 7 (**A**) (i) (a) Synthetic Process of dopamine dimer to form nanoscale assemblies (DDNs) through the Self-Assembly of NSHD and L-DOPA Dimers; (b) Schematic Illustration of the Integration Process of DDNs into the Hydrogel Network through Spontaneous Schiff Base-Ligation Enabled Hydrogel Formation; (c) Mechanism of HBSS for Promoting Skin burn wound (SBW) Healing (ii) SBW treatment efficacy of HBSS in vivo. (iii) HBSS-mediated macrophage reprogramming in vivo.[18] *p < 0.05, **p < 0.01, ***p < 0.001, and ****p < 0.0001. Copyright 2025, American Chemical Society. (**B**) (i) Cytotoxicity and anti-inflammatory effects of EsA-CS/ALG-NPs@CCS in vitro. (ii) Evaluation of M1 and M2 macrophages in burn wounds in early and middle stages. (iii) EsA-CS/ALG-NPs@CCS expedited burn wound healing.[199] *p < 0.05, **p < 0.01, ***p < 0.001. Copyright 2023, American Chemical Society.

CCS. The hydrogel exhibited robust hemostatic efficacy in a liver hemorrhage model and demonstrated potent antibacterial activity against *S. aureus* and *E. coli*-induced infections in clinically relevant models, highlighting its potential as a multifunctional biomaterial for the management of hemorrhage and infection in surgical applications.[208]

CS-Based Dressings for Infected Wounds

Once the integrity of the skin is compromised and a wound is formed, the body initiates a complex cascade of physiological processes to regenerate the damaged or lost tissue.[209] However, the wound healing process can be significantly influenced by various factors, including wound size and depth, microbial infection, advanced age, and underlying health conditions. Among these, infection is particularly prevalent due to the nutrient-rich microenvironment of the wound, which favors microbial colonization and proliferation.[205] If not promptly and effectively managed, wound infections can lead to severe consequences such as purulence, tissue necrosis,[210,211] osteomyelitis, sepsis, and even mortality.[212] Cutaneous wound infections caused by pathogenic microorganisms not only impede the orderly progression of tissue repair but also pose a substantial risk to patient health and clinical outcomes.[213] Yang et al designed and developed a CS-based composite hydrogel with antibacterial, adhesive, and self-healing properties for the treatment of infected wounds. Initially, Fe^{3+} was chelated with TA to form self-assembled nanoparticles (TFe NPs) exhibiting efficient photothermal activity. These nanoparticles were then incorporated into a hydrogel matrix crosslinked from acrylamide (AM), 3-acrylamidophenylboronic acid (AAPBA), and CS. Benefiting from the high photothermal conversion efficiency of TFe NPs, the hydrogel was able to effectively eliminate both Gram-positive (*S. aureus*) and Gram-negative (*E. coli*) bacteria and inhibit biofilm formation by *S. aureus*. In addition, the TFe NPs endowed the hydrogel with excellent antioxidant activity, anti-inflammatory properties, and the ability to promote cell proliferation, thereby facilitating skin tissue regeneration[38] (Figure 8A). Insulin-like growth factor-1 (IGF1) is a bioactive factor that can effectively promote tissue regeneration and angiogenesis.[214,215] Tan et al synthesized caffeic acid-modified CS via an amidation reaction and prepared oxidized dextran (ODex) using sodium periodate as an oxidizing agent. A sprayable CS-based hydrogel (HCS/CCS/ODex-IGF1) was subsequently developed by crosslinking HCS and CCS with ODex through dynamic imine (Schiff base) bonds, while simultaneously loading insulin-like growth factor 1 (IGF1). The amino groups of HCS and CCS react with the aldehyde groups of ODex to form a pH-responsive dynamic network, enabling the controlled release of IGF1 in the mildly acidic wound microenvironment to facilitate skin tissue repair. The hydrogel exhibited excellent cytocompatibility and hemocompatibility, and effectively promoted cell proliferation and migration. Moreover, it significantly enhanced angiogenesis and tissue regeneration by upregulating the expression of pro-angiogenic and anti-inflammatory factors, while downregulating pro-inflammatory cytokines such as TNF-α and IL-6, thereby accelerating the wound healing process[20] (Figure 8B). CS modified with quaternary ammonium polymers demonstrated good biocompatibility, better water solubility and enhanced antimicrobial activity.[216,217] Besides, PEG, a synthetic polymer, has also been widely used for its biosafety and hydrophilic properties.[218,219] Qiao et al developed a dual dynamic-bond cross-linked hydrogel based on oxidized sodium alginate (OSD) and CCS. In this system, the catechol hydroxyl groups of dopamine, the carboxyl groups of CCS, and the Fe^{3+} coordination bonds synergistically form a stable and self-healable triple dynamic network. The incorporation of poly(thiophene-3-acetic acid) (PA) further endowed the hydrogel with excellent antibacterial activity and suitable electrical conductivity. In an infected full-thickness skin wound model in mice, the conductive and photothermal OSD/CCS/Fe/PA_3 hydrogel exhibited superior wound closure compared with the commercial Tegaderm™ film and OSD/CCS hydrogel. Moreover, the regenerated vasculature, hair follicles, and epidermal thickness were more similar to those of normal skin, accompanied by reduced inflammatory responses. Immunofluorescence staining for TNF-α and vascular endothelial growth factor (VEGF) revealed that this multifunctional hydrogel could effectively suppress inflammation and promote angiogenesis during the wound healing process[175] (Figure 8C).

CS-Based Dressings for Diabetic Wounds

According to the 10th edition of the IDF Diabetes Atlas, over 1 in 10 adults globally were living with diabetes in 2021.[220] Among these individuals, 15–25% are estimated to develop diabetic ulcers or chronic wounds.[221,222] Diabetic wounds represent a serious and difficult-to-treat complication due to the elevated glucose content in the interstitial fluid, which

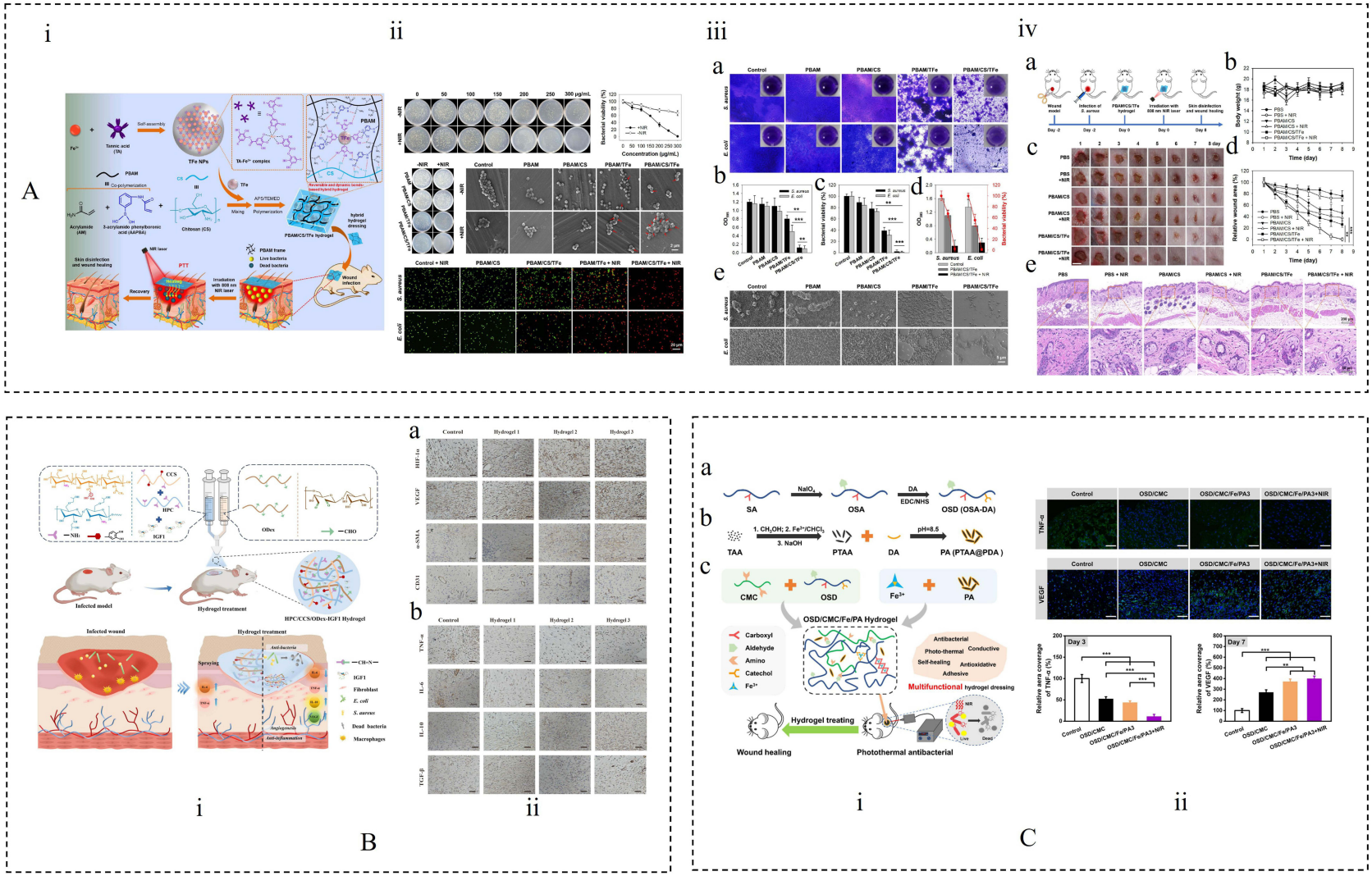

Figure 8 (**A**) (i) Schematic Diagram for the Preparation and in vivo Antibacterial Application of the PBAM/CS/TFe Hybrid Hydrogel Dressing. (ii) Antibacterial activities of PBAM/CS/TFe hydrogels. (iii) (a) Microscopy images of crystal violet-stained biofilms of *S. aureus* and *E. coli* with different treatments. (b) Absorbances of crystal violet-stained *S. aureus* and *E. coli* biofilms. (c) Viabilities of *S. aureus* and *E. coli* in their biofilms after different treatments. (d) Antibiofilm performance of PBAM/CS/TFe hydrogels of NIR laser. (e) SEM images of *S. aureus* and *E. coli* biofilms after various treatments. (iv) (a) Illustration of in vivo antibacterial assays. (b) Body-weight changes in mice with different treatments. (c) Photographs of the *S. aureus*-infected wounds on mice with different treatments. (d) Changes of wound area over time. (e) H&E staining images of wound slices.[38] $^{**}p < 0.05$, $^{***}p < 0.005$. Copyright 2025, American Chemical Society. (**B**) (i) Diagram of the sprayable CS-based hydrogels loaded with IGF1 for promoting wound healing. (ii) (a) Immunohistochemical (IHC) staining images of HIF-1α, VEGF, CD31 and α-SMA. (b) IHC staining images of TNF-α, IL-6, IL-10 and TGF-β.[20] Copyright 2024, Elsevier Ltd. (**C**) (i) (a) Preparation scheme of oxidized sodium ALG -grafted dopamine (OSD) and (b) polydopamine-coating PA; (c) Preparation and application of OSD/CCS/Fe^{3+}/PA (OSD/CCS/Fe/PA) hydrogels. (ii) Immunofluorescently labeled wound tissue with TNF α and VEGF.[175] $^{**}P < 0.01$, $^{***}P < 0.001$. Copyright 2023, The Authors.

https://doi.org/10.2147/IJN.S607257

disrupts ECM remodeling and creates a favorable environment for bacterial proliferation.[205] These wounds are characterized by persistent inflammation, which leads to excessive production of ROS and heightened oxidative stress,[223] thereby disrupting key healing processes such as angiogenesis (the formation of new blood vessels from existing ones), collagen deposition, and tissue regeneration.[224,225] Effective treatment thus requires coordinated regulation of both the dysregulated inflammatory microenvironment and the subsequent tissue repair phases. To address this, Cheng et al developed a bilayer wound dressing based on CS and a polydiyne material, poly(deca-4,6-diynedioic acid) (PDDA). The alternating diyne structure of PDDA enables it to gradually scavenge ROS, conferring the dressing with sustained antioxidative capability within the wound microenvironment. The main degradation product of PDDA upon interaction with ROS is succinic acid (SA), a bioactive metabolite known to promote tissue repair and regeneration. The structural layer of the dressing is composed of CS, a natural polysaccharide with well-documented hemostatic and antibacterial properties. The resulting PDDA-CS bilayer dressing (PCD) exhibits favorable hydrophilicity and porosity, which further support its hemostatic performance. In vivo studies in diabetic mouse and porcine models showed that PCD significantly accelerated wound healing, suggesting promising preclinical potential for further translational evaluation.[21] Puerarin (PUE), a flavonoid compound extracted from the traditional Chinese medicine Pueraria lobata, has demonstrated excellent cardioprotective, neuroprotective, and blood glucose-regulating effects in diabetic patients.[226–228] Zeng et al developed an injectable and self-healing CS-puerarin (C@P) hydrogel with a nanofibrous architecture, which promoted diabetic wound healing by suppressing excessive inflammation and modulating macrophage activation. In diabetic wounds, aberrantly elevated levels of miR-29a and miR-29b1 are closely associated with sustained M1 macrophage activation and increased expression of pro-inflammatory cytokines such as IL-1β and TNF-α, thereby creating a chronic inflammatory microenvironment that is unfavorable for tissue repair. The C@P hydrogel was able to correct the abnormal expression of miR-29ab1, inhibit persistent M1-type inflammatory responses, and improve angiogenesis and collagen deposition, ultimately promoting diabetic wound repair.[229] Nic D. Leipzig et al developed a multifunctional CS-based oxygen-delivering antibiotic hydrogel dressing for the treatment of chronic infected wounds in diabetes The dressing is composed of a perfluorocarbon-functionalized methacrylated CS (MACF) hydrogel, which enables oxygen delivery, and the antimicrobial agent polyhexamethylene biguanide (PHMB). By incorporating MACF into the hydrogel, the dressing not only supplies additional oxygen to enhance the antimicrobial response and accelerate the healing process but also allows for the controlled release of PHMB, effectively reducing the risk of infection and promoting wound repair while avoiding tissue necrosis associated with prolonged PHMB use. Furthermore, switching to a pure MACF dressing after infection control can further improve re-epithelialization and overall wound healing outcomes.[230]

Overall, the therapeutic application of CS-based dressings is highly dependent on wound type. For burn and postoperative wounds, the main therapeutic priorities are rapid barrier restoration, inflammation control, exudate management, and the provision of hemostatic and antibacterial protection; accordingly, CS is more often engineered into highly absorbent, tissue-adhesive hydrogels or biomimetic extracellular matrix-like scaffolds. In contrast, chronic and complex wounds such as infected wounds and diabetic wounds remain in a hostile microenvironment characterized by persistent biofilms, elevated oxidative stress, inflammatory imbalance, and impaired tissue regeneration, and thus the role of CS shifts from passive protection to active regulation. In infected wounds, it is commonly combined with photothermal nanoparticles, metal-ion chelation, or other synergistic antibacterial mechanisms to enhance bacterial clearance and antibiofilm activity. In diabetic wounds, it is more frequently integrated with ROS-scavenging components, oxygen-delivery systems, or immunomodulatory molecules to simultaneously improve oxidative stress, chronic inflammation, angiogenesis, and tissue regeneration. These comparisons indicate that CS-based wound care is evolving from traditional single-function covering materials into multifunctional platforms tailored to specific pathological mechanisms, in which CS serves as a highly adaptable matrix for integrating structural support, responsive delivery, and bioactive modulation to enable more precise wound intervention.

Future Trends and Challenges in CS-Based Dressings

In recent years, CS-based wound dressings in the form of hydrogels, films, foams, and nanoparticles have been widely applied in the medical field. These dressings play multiple roles in promoting wound healing, including antibacterial activity, absorption of wound exudate, promotion of angiogenesis, controlled drug release, and provision of mechanical

support for tissue regeneration. However, it must be emphasized that the selection of an appropriate wound dressing requires careful consideration of factors such as wound size, depth, exudate level, and overall clinical condition in order to achieve the best therapeutic outcome. The treatment of chronic wounds is more complex because of the presence of necrotic tissue, bacterial biofilms, and vascularization problems, thus requiring the development of advanced wound dressings with tailored properties to meet the specific needs of different wound types. The rapid development of bioresponsive materials is driving a paradigm shift in wound dressings from passive protection toward active sensing and precise intervention, leading to the establishment of intelligent systems with the capabilities of "recognition, response, and intervention".[231,232] Accordingly, the development of smart responsive dressings capable of adapting to the dynamic changes that occur throughout the different stages of wound healing has become a central focus in contemporary wound management research. Owing to its excellent structural and functional properties, safe origin, and tunable responsiveness, CS has become an ideal candidate for the development of various smart responsive dressings.[233–235] Through chemical modification or composite construction, CS-based dressings can be engineered to respond to multiple endogenous signals, such as pH, enzymes, and ROS, as well as exogenous signals, including temperature and electromagnetic fields. This responsiveness helps identify wound status and enables targeted intervention.[236] Dang et al successfully developed a multifunctional conductive hydrogel (CPPFe@TA) based on carboxymethyl cellulose and a TA/Fe^{3+} complex (TA@Fe^{3+}). This hydrogel exhibited near-infrared (NIR) photothermal responsiveness and showed significant photothermal antibacterial activity under NIR irradiation, while also demonstrating potential for health monitoring and wound healing promotion. In a mouse full-thickness skin defect model, CPPFe@TA markedly accelerated wound repair; after 14 days of treatment, the wound healing rate in the CPPFe@TA3 hydrogel + NIR treatment group reached 95.49%, which was significantly higher than that of the commercial dressing group. In addition, this advancement opened up new possibilities for the development of environmentally friendly strain and temperature sensors.[237] Electronic skin (e-skin) patches based on conductive hydrogels represent an emerging category of smart wound dressings, offering innovative solutions for chronic wound repair and real-time monitoring. Dang et al developed a multifunctional biomass-derived conductive hydrogel e-skin patch prepared through the supramolecular self-assembly of three environmentally friendly polymers: carboxymethyl cellulose (CMC), CCS, and PVA. By incorporating amino-functionalized multi-walled carbon nanotubes (MWCNTs-NH2) to enhance conductivity and combining them with the thermoresponsive properties of NIPAM, the patch was able to achieve precise temperature regulation while simultaneously exhibiting multiple therapeutic functions, including accelerated wound healing and strong antibacterial activity, with a wound healing rate of up to 98% within 14 days. In addition, this e-skin patch demonstrated excellent real-time monitoring capability, enabling dynamic tracking of wound micromotion, inflammation-associated temperature elevation, and other physiological signals, thus highlighting its considerable potential in precise wound management and intelligent healthcare applications.[238] Dang et al proposed a fully natural, injectable multifunctional biobased hydrogel bioadhesive composed of CCS, sericin (SS), and natural moisturizing factor (NMF), enabling the synergistic integration of skin bioelectronic functions and regenerative wound healing. This hydrogel bioadhesive exhibited high sensitivity to temperature, stress-strain changes, and bioelectrical signals, allowing effective monitoring of body motion and providing temperature warnings. Notably, its tunable mechanical modulus enabled close matching with the mechanical properties of skin tissue at the wound site, thereby offering a more suitable microenvironment for tissue repair. In vivo, the material achieved nearly complete wound healing within 14 days and significantly reduced the levels of pro-inflammatory factors. As a flexible and durable interfacial material, this hydrogel bioadhesive could sense human motion and physiological signals while partially mimicking the sensory functions of skin, highlighting its potential for intelligent wound management and skin bioelectronics.[239] The team led by Fumlya Iida recently developed a gelatin-based "electronic skin" hydrogel characterized by low cost, excellent stretchability, and piezoresistive strain responsiveness. This material can monitor environmental temperature and humidity in real time, and its electrical and mechanical properties can be tuned via composition adjustments to meet specific application needs. The hydrogel supports over 860,000 transmembrane conductive pathways and can recognize at least six different types of multimodal stimuli, including human touch, mechanical damage, multi-point pressure, and localized heating.[240] Introducing this technology into wound management holds promise for developing next-generation smart dressings capable of continuous wound environment monitoring and early warning, thereby avoiding frequent dressing changes

that may disrupt healing. When combined with antimicrobial agents or integrated with CS-based materials, such dressings are expected to offer multifunctional therapeutic, monitoring, and feedback capabilities, especially suitable for personalized management of chronic hard-to-heal wounds such as DFUs and pressure sores, driving wound repair toward precise, dynamic, and individualized intelligent treatment.

The rapid development of smart responsive materials and advanced manufacturing technologies, especially 4D printing, which integrates 3D printing with intelligent materials science, has shown broad prospects for personalized wound care. Unlike conventional static structures, 4D printing introduces smart materials that can respond to external stimuli such as pH, temperature, humidity, light, and magnetic fields, enabling constructs to undergo predictable dynamic deformation and functional transformation over time. This gives dressings greater adaptability and controllability in complex wound environments. CS-based hydrogels, owing to their tunable pH responsiveness, exhibit unique advantages within 4D printing material systems. By combining CS-based materials with 3D/4D printing technologies, dressings can be precisely designed to match specific wound characteristics. Through layer-by-layer deposition based on digital models, the final structure and function can be accurately controlled.[241] This high degree of personalization is particularly valuable in wound care, because patients may differ substantially in wound morphology, exudate level, and pathological condition, and customized dressings therefore have the potential to improve therapeutic outcomes and reduce infection risk. Chen et al developed a nanoclay-reinforced 3D-printed CS hydrogel in which the hydrogen bonding and electrostatic interactions between halloysite nanotubes (HNTs) and CS optimized the rheological properties of the CS/HNTs ink, allowing it to meet the hydrodynamic requirements of extrusion printing while exhibiting excellent self-supporting capability. As a result, complex structures with high printing fidelity could be achieved. The incorporation of HNTs also improved the mechanical strength and hemostatic potential of the hydrogel. Furthermore, after loading the active drug levofloxacin (Lev), the 3D-printed hydrogel showed significant in vitro antibacterial activity. Owing to its favorable drug-delivery performance, printability, enhanced hemostatic properties, and mechanical strength, the CS/HNTs/Lev hydrogel effectively promoted the healing of infected wounds in vivo.[242] At the same time, the integration of artificial intelligence with materials modeling technologies has made it possible to achieve intelligent wound classification and typing through AI algorithms. By combining clinical data with patient-specific information, these approaches may optimize treatment selection and enable more accurate prediction of the structural design, drug release profiles, and response behavior of 4D-printed dressings, thereby supporting more precise customization. Overall, these trends suggest that interdisciplinary integration and technological innovation will continue to drive the development of next-generation smart wound dressings and may accelerate the translation of novel biomaterials from laboratory research to clinical application.

At the frontier of innovation, CS-based dressings can be further enhanced by incorporating regenerative therapeutic components such as stem cells, exosomes, and gene-based agents. These "bioactive" dressings provide not only passive support but also active therapeutic signaling to promote tissue regeneration. The mild gelation conditions of CS are favorable for the encapsulation and preservation of viable cells and exosomes, while ROS- or pH-responsive microenvironments help enable the controlled release of these bioactive cargos. Huang et al constructed an intrinsically immunomodulatory hydrogel composed of oxidized hyaluronic acid (OHA), sulfated chitosan (SCS), and CMC, and loaded VEGF plasmids into M0 macrophage-derived exosomes (Ep) via electroporation. This hydrogel not only exhibited excellent ROS-scavenging capability but also induced macrophage polarization, thereby modulating the inflammatory microenvironment and promoting wound healing. The released Ep could be internalized by cells and express VEGF in vivo, while the combination of M2 polarization, VEGF generation and release, and the high affinity of SCS for VEGF endowed the system with strong pro-angiogenic activity, highlighting its great potential for diabetic wound therapy.[243] In addition, the intrinsic cationic nature of CS facilitates the delivery of siRNA, miRNA, and other genetic materials, thereby improving transfection efficiency and regulating inflammation- or fibrosis-related pathways. Multifunctional systems integrating stem cells, exosomes, and miRNAs are therefore expected to exert synergistic effects on angiogenesis, immunomodulation, and tissue remodeling. Meanwhile, living algae, as natural photosynthetic organisms, have shown unique potential in the treatment of complex wounds. Under light or laser stimulation, living algae can continuously generate oxygen, thereby improving the local hypoxic condition of the wound. At the same time, the ROS they produce may assist in eliminating bacteria in infected regions through photodynamic action. In addition, living algae can utilize the elevated glucose levels present in the diabetic wound microenvironment and, through genetic engineering,

may be further designed to release pro-angiogenic factors such as VEGF, thereby synergistically promoting neovascularization and tissue repair.[244] When integrated with innovative dressing platforms and other functional healing components, living algae may become an important element of next-generation smart bioactive dressings. However, their successful clinical translation will still require rigorous evaluation frameworks to systematically verify biosafety, stability, and the controllability of release behavior.

Although CS-based smart dressings have shown many advantages in wound repair, their clinical translation is still limited by multiple challenges. First, CS materials are relatively sensitive to environmental conditions, and fluctuations in humidity and temperature during production and storage may alter their physicochemical properties and network structure, resulting in insufficient batch-to-batch stability and affecting reproducibility and controllability. Second, these smart responsive systems usually rely on specific trigger signals in the wound microenvironment, such as pH, enzymes, and ROS. However, pathological wounds often exhibit pronounced spatiotemporal heterogeneity, which may lead to delayed responsiveness, inaccurate release behavior, or unstable therapeutic outcomes. Therefore, it is necessary to develop intelligent biomaterials that can maintain long-term structural integrity and functional stability while adapting to complex wound environments, and to promote standardized production to ensure consistent quality and application safety. In addition, sterilization compatibility remains a major barrier to translation. Conventional sterilization methods, such as gamma irradiation and autoclaving, may induce polymer chain scission or alter network architecture, thereby affecting the mechanical performance and structural stability of the materials. Ethylene oxide sterilization, although suitable for heat-sensitive materials, still raises concerns regarding potential toxic residues, making the development of mild and low-damage sterilization strategies particularly important. Meanwhile, the medical device field is subject to strict regulatory requirements, and related products typically require systematic evaluation of safety, efficacy, and stability, together with the establishment of standardized quality-control systems. While these measures improve clinical reliability, they also increase the cost and complexity of development, manufacturing, and regulatory approval. Notably, most current studies still remain at the animal-experiment stage, with limited systematic human safety evaluation and long-term follow-up data, which further constrains clinical adoption. Overall, only through systematic advances in mechanistic understanding, material standardization, sterilization compatibility, and high-quality clinical evaluation can the clinical potential of CS-based smart dressings be more fully realized.

Future progress in CS-based smart dressings should prioritize improving the precision of stimulus responsiveness, enhancing biological integration, and accelerating clinical translation. In intelligent design, the incorporation of dynamic covalent regulation, mechanically adaptive architectures, and multimodal triggering systems will be particularly important. These strategies may enable more precise spatiotemporal intervention and closed-loop diagnostic-therapeutic feedback, thereby better addressing the spatial heterogeneity and signal fluctuation commonly present in pathological wound microenvironments. From the perspective of functional construction, future dressings should further integrate antibacterial activity, pro-angiogenic capability, immunomodulation, and tissue-inductive functions into a single platform in order to meet the dynamic therapeutic demands of complex wounds at different healing stages. In terms of material sourcing and manufacturing, a transition toward more sustainable practices should also be promoted, including the preferential use of renewable raw materials and the adoption of green solvents and low-environmental-burden processes in chemical synthesis.[22] With regard to sterilization, it may be valuable to move beyond the traditional "fabricate first, terminally sterilize later" paradigm and instead develop aseptic processing systems in which raw material purification, hydrogel preparation, 3D/4D printing, and final packaging are all conducted under high-cleanliness GMP conditions, thereby minimizing damage to material structure, mechanical performance, and bioactivity caused by terminal sterilization. At the translational level, there remains an urgent need to establish multilayered evaluation frameworks covering efficacy, safety, stability, and long-term follow-up, together with more rigorous human studies to improve evidence quality and clinical acceptability. In addition, interdisciplinary collaboration will be essential for integrating smart sensing, data analysis, and telemedicine modules, thereby promoting the evolution of CS-based dressings from therapeutic materials toward platforms for precise, dynamic, and individualized wound management. With continued progress, CS-based smart dressings are expected to develop into multifunctional solutions that are both clinically feasible and industrially scalable, providing more reliable technical support for precision wound management.

Conclusion

CS-based wound dressings have shown significant clinical potential in the treatment of various complex wounds, including burns, postoperative incisions, infected wounds, and DFUs, owing to their excellent biocompatibility, biodegradability, and intrinsic multifunctional bioactivity. However, the core value of CS-based wound dressings does not lie simply in the properties of CS itself, but rather in the fact that its favorable biocompatibility, biodegradability, cationic nature, and chemical modifiability can be combined with different fabrication strategies and functional components to enable customized designs tailored to the pathological barriers of different wound types. This review systematically summarized representative preparation strategies, including phase inversion, electrospinning, vacuum freeze-drying, and emulsion crosslinking. These methods endow the dressings with favorable mechanical properties and biomimetic porous structures that effectively mimic the native ECM, thereby providing an ideal microenvironment for cell adhesion, migration, and proliferation and enabling the coordinated tuning of physicochemical and functional properties to meet the diverse demands of different wound types.

From the perspective of modification strategies, catechol grafting, quaternization, carboxymethylation, and dynamic covalent network construction are currently among the most consistent and repeatedly reported routes for functional enhancement. Catechol modification and dynamic covalent crosslinking, such as Schiff base formation, most consistently improve tissue adhesion, self-healing behavior, and in situ gelation capability. Carboxymethylation and quaternization are more advantageous for enhancing water solubility, pH adaptability, and certain aspects of antibacterial performance. In addition, compositing with hyaluronic acid, alginate, cellulose, PVA, and metal or photothermal nanocomponents can further improve mechanical properties, microenvironmental responsiveness, and multifunctional bioactivity. In terms of fabrication platforms, crosslinked hydrogels and freeze-dried sponges are currently the most mature and extensively studied systems: crosslinked hydrogels are particularly advantageous for irregular wound adaptation, drug delivery, and microenvironment regulation, whereas freeze-dried sponges are more suitable for highly exuding or bleeding wounds. By contrast, electrospun nanofibers offer unique advantages in mimicking ECM architecture and promoting tissue regeneration, although their process control, batch-to-batch consistency, and translational maturity for industrial application still require further improvement.

From a functional design perspective, CS-based dressings can achieve multi-mechanistic therapeutic effects through structural regulation and functional modification. Their hemostatic and antibacterial properties are particularly beneficial for burns and postoperative wounds, whereas self-healing, antioxidant, and anti-inflammatory activities play crucial roles in the treatment of infected wounds and diabetic chronic wounds. However, the complex interactions among multiple therapeutic components remain a major challenge. Combinations of bioactive agents may produce antagonistic effects, and co-loading may compromise drug efficacy or lead to uncontrolled release. In addition, achieving temporally staged release that matches the different phases of wound healing remains technically difficult. To address the prolonged healing cycle and multifactorial pathophysiology of chronic wounds, future research should focus more on multifunctional synergistic hydrogel systems. Integrating antibacterial, anti-inflammatory, antioxidant, and pro-angiogenic components into a single dressing could enable comprehensive multi-targeted therapy. Continued investigation into synergistic or antagonistic interactions among different bioactive agents remains essential. Advanced techniques such as layer-by-layer assembly, microencapsulation, and dynamic covalent crosslinking may help achieve stable co-loading and sustained bioactivity. Moreover, stimuli-responsive release systems based on pH, ROS, or enzymatic triggers may allow phase-specific delivery of therapeutic factors during the inflammatory, proliferative, and remodeling stages. The integration of high-throughput screening with AI-assisted modeling may further optimize drug concentration ratios, release kinetics, and therapeutic windows, thereby enhancing efficacy while minimizing side effects.

Although extensive in vitro and in vivo studies have supported the therapeutic efficacy of CS-based systems in wound repair, their clinical translation remains limited. Large-scale, systematic clinical trials are urgently needed to verify their safety and efficacy across different wound types and patient populations. Major challenges still include process standardization and scale-up, long-term stability and safety assurance, the development of more pathologically relevant animal models, and the design of robust randomized controlled clinical trials. In addition, balancing therapeutic performance with cost-effectiveness and manufacturability remains a critical bottleneck in commercialization.

In summary, CS-based hydrogel dressings, with their tunable functional properties and diverse fabrication strategies, exhibit considerable promise in wound healing. Future progress will depend on the deep integration of materials science, biomedical engineering, and artificial intelligence to achieve intelligent, personalized, and efficient wound management, ultimately improving patient prognosis and quality of life.

Abbreviations

CS, Chitosan; FDA, Food and Drug Administration; DFUs, Diabetic Foot Ulcers; CCS, Carboxymethyl chitosan; QCS, Quaternized chitosan; ACCS, Acylated chitosan; HCS, Hydroxypropyl chitosan; TA, Tannic acid; PEG, Polyethylene glycol; MW, Molecular weight; DS, Degree of substitution; PEC, Polyelectrolyte complex; AMPS, 2-acrylamido-2-methylpropanesulfonic acid; DD, Degree of deacetylation; DB, Diatom biosilica; ROS, Reactive oxygen species; Nrf2, Nuclear factorn-like 2; ECM, Extracellular matrix; PVA, Polyvinyl alcohol; MC, Methylcellulose; CS-GA, Chitosan and gallic acid; CO, Collagen; H_2S, Hydrogen sulfide; ε-PL-SATO, ε-polylysine-S-aroylthiooxime; HA, Oxidized hyaluronic acid; MCC, Microcrystalline cellulose; VIPI, Phase inversion; PCL, Poly(ε-caprolactone); SEM, Scanning electron microscopy; HNTs, Halloysite nanotubes; EFS, Electrospun fiber sponge; PLA, Polylactic acid; spCS, Superporous chitosan sponge; HDIC, Hydroxypropyl-β-cyclodextrin/dihydromyricetin inclusion complex; PP, Pectic polysaccharide; MP, Mupirocin; CeNPs, Cerium oxide nanoparticles; MRSA, Methicillin-resistant staphylococcus aureus; HP-β-CD, 2-hydroxypropyl-β-cyclodextrin; AP/CD-IC, Ascorbyl palmitate /2-hydroxypropyl-β-cyclodextrin inclusion complex; QCS-IC, Quaternary ammonium chitosan-inclusion complex; DES, Deep eutectic solvent; TBA, Trihydroxybenzaldehyde; NIR, Near-infrared; PTT, Photothermal therapy; NO, Nitric oxide; HBSS, Hydrogel-based synthetic skin; NSHD, N-(benzoyl mercapto) benzamide; EsA, Esculentoside A; DDNs, Dopamine dimer to form nanoscale assemblies; SBW, Skin burn wound; TFe NPs, Fe^{3+} was chelated with TA to form self-assembled nanoparticles; AM, Acrylamide; IGF1, Insulin growth factor-1; ODex, Oxidized dextran; OSD, Oxidized sodium alginate; IHC, Immunohistochemical; PDDA, Poly(deca-4,6-diynedioic acid); SA, Succinic acid; PCD, Poly(deca-4,6-diynedioic acid)–chitosan bilayer dressing; PUE, Puerarin; MACF, Methacrylated cjitosan; PHMB, Polyhexamethylene biguanide; CE, Cirsium setosum extracts; Lev, Levofloxacin; MMT, Montmorillonite; NIPAM, N-isopropylacrylamide; ZIF-8, Zeolitic imidazolate framework-8; HCuS, Hollow copper sulfide nanoparticles; SNP, Sodium nitroprusside; PA, Proanthocyanidins; AgNPs, Silver nanoparticles; PENG, Piezoelectric nanogenerator; VEGF, Vascular endothelial growth factor.

Data Sharing Statement

No data was used for the research described in the article.

Acknowledgments

This work was financially supported by the Beijing Natural Science Foundation (7262207); the Scientific and technological innovation project of China Academy of Chinese Medical Sciences (CI2026A04303,CI2024E003); and the Fundamental Research Funds for the Central Public Welfare Research Institutes (ZZ13-YQ-041, ZXKT21013).

Author Contributions

All authors made a significant contribution to the work reported, whether that is in the conception, study design, execution, acquisition of data, analysis and interpretation, or in all these areas; took part in drafting, revising or critically reviewing the article; gave final approval of the version to be published; have agreed on the journal to which the article has been submitted; and agree to be accountable for all aspects of the work.

Disclosure

The authors acknowledged that the work described in this manuscript has no known conflicting financial or personal interests.

References

1. Bhardwaj D, Chawla V, Nandwani V, Thakur Y, Singh Y, Agrawal G. A multifunctional electrospun nanofiber/hydrogel-based pro-healing bilayer dressing as a next generation biomaterial for skin wound care. *J Mater Chem B*. 2025;13(37):11821–11834. doi:10.1039/D5TB00800J
2. Mohammed M, Syeda J, Wasan K, Wasan E. An overview of chitosan nanoparticles and its application in non-parenteral drug delivery. *Pharmaceutics*. 2017;9(4):53. doi:10.3390/pharmaceutics9040053
3. Kumar MNVR, Muzzarelli RAA, Muzzarelli C, Sashiwa H, Domb AJ. Chitosan chemistry and pharmaceutical perspectives. *Chem Rev*. 2004;104(12):6017–6084. doi:10.1021/cr030441b
4. Shariatinia Z. Pharmaceutical applications of chitosan. *Adv Colloid Interface Sci*. 2019;263:131–194. doi:10.1016/j.cis.2018.11.008
5. Zargar V, Asghari M, Dashti A. A review on chitin and chitosan polymers: structure, chemistry, solubility, derivatives, and applications. *ChemBioEng Rev*. 2015;2(3):204–226. doi:10.1002/cben.201400025
6. Abourehab MAS, Pramanik S, Abdelgawad MA, et al. Recent advances of chitosan formulations in biomedical applications. *IJMS*. 2022;23(18):10975. doi:10.3390/ijms231810975
7. Islam MDS, Haque P, Rashid TU, et al. Core–shell drug carrier from folate conjugated chitosan obtained from prawn shell for targeted doxorubicin delivery. *J Mater Sci*. 2017;28(4):55. doi:10.1007/s10856-017-5859-x
8. Dai T, Tanaka M, Huang YY, Hamblin MR. Chitosan preparations for wounds and burns: antimicrobial and wound-healing effects. *Exp Rev Anti-Infective Ther*. 2011;9(7):857–879. doi:10.1586/eri.11.59
9. Ambekar RS, Kandasubramanian B. Advancements in nanofibers for wound dressing: a review. *Eur Polym J*. 2019;117:304–336. doi:10.1016/j.eurpolymj.2019.05.020
10. Proksch E, Brandner JM, Jensen J. The skin: an indispensable barrier. *Exper Dermatol*. 2008;17(12):1063–1072. doi:10.1111/j.1600-0625.2008.00786.x
11. Madison KC. Barrier function of the skin: "La Raison d'Être" of the epidermis. *J Invest Dermatol*. 2003;121(2):231–241. doi:10.1046/j.1523-1747.2003.12359.x
12. Liu H, Wang C, Li C, et al. A functional chitosan-based hydrogel as a wound dressing and drug delivery system in the treatment of wound healing. *RSC Adv*. 2018;8(14):7533–7549. doi:10.1039/C7RA13510F
13. Liang Y, He J, Guo B. Functional hydrogels as wound dressing to enhance wound healing. *ACS Nano*. 2021;15(8):12687–12722. doi:10.1021/acsnano.1c04206
14. Schultz GS, Wysocki A. Interactions between extracellular matrix and growth factors in wound healing. *Wound Repair Regen*. 2009;17(2):153–162. doi:10.1111/j.1524-475X.2009.00466.x
15. Varaprasad K, Jayaramudu T, Kanikireddy V, Toro C, Sadiku ER. Alginate-based composite materials for wound dressing application:A mini review. *Carbohydr Polym*. 2020;236:116025. doi:10.1016/j.carbpol.2020.116025
16. Guo H, Bai M, Zhu Y, et al. Pro-healing zwitterionic skin sensor enables multi-indicator distinction and continuous real-time monitoring. *Adv Funct Mater*. 2021;31(50):2106406. doi:10.1002/adfm.202106406
17. Piran N, Farhadian M, Soltanian AR, Borzouei S. Diabetic foot ulcers risk prediction in patients with type 2 diabetes using classifier based on associations rule mining. *Sci Rep*. 2024;14(1):635. doi:10.1038/s41598-023-47576-w
18. Zhang H, Zhou W, Wang H, et al. Hydrogel-based bioactive synthetic skin stimulates regenerative gas signaling and eliminates interfacial pathogens to promote burn wound healing. *ACS Nano*. 2025;19(15):15002–15017. doi:10.1021/acsnano.5c01134
19. Cheng X, Yao J, Fan W, Zhen L. Facile fabrication and biological investigations of metal oxides intercalated in kaolinite clay-based dressing material to improve wound healing ability in nursing care after post-operative period. *Heliyon*. 2024;10(3):e25289. doi:10.1016/j.heliyon.2024.e25289
20. Tan Y, Xu C, Liu Y, Bai Y, Li X, Wang X. Sprayable and self-healing chitosan-based hydrogels for promoting healing of infected wound via anti-bacteria, anti-inflammation and angiogenesis. *Carbohydr Polym*. 2024;337:122147. doi:10.1016/j.carbpol.2024.122147
21. Cheng L, Zhuang Z, Yin M, et al. A microenvironment-modulating dressing with proliferative degradants for the healing of diabetic wounds. *Nat Commun*. 2024;15(1):9786. doi:10.1038/s41467-024-54075-7
22. Gupta MN, Rangaraju A, Ambre P. Sustainable dressings for wound healing. *Biotechnol Sustain Mater*. 2025;2(1):1. doi:10.1186/s44316-024-00023-w
23. Muxika A, Etxabide A, Uranga J, Guerrero P, De La Caba K. Chitosan as a bioactive polymer: processing, properties and applications. *Int J Biol Macromol*. 2017;105:1358–1368. doi:10.1016/j.ijbiomac.2017.07.087
24. Khubiev OM, Egorov AR, Kirichuk AA, Khrustalev VN, Tskhovrebov AG, Kritchenkov AS. Chitosan-based antibacterial films for biomedical and food applications. *IJMS*. 2023;24(13):10738. doi:10.3390/ijms241310738
25. Wang W, Xue C, Mao X. Chitosan: structural modification, biological activity and application. *Int J Biol Macromol*. 2020;164:4532–4546. doi:10.1016/j.ijbiomac.2020.09.042
26. Ji M, Li J, Wang Y, et al. Advances in chitosan-based wound dressings: modifications, fabrications, applications and prospects. *Carbohydr Polym*. 2022;297:120058. doi:10.1016/j.carbpol.2022.120058
27. Zhang S, Li J, Li J, et al. Application status and technical analysis of chitosan-based medical dressings: a review. *RSC Adv*. 2020;10(56):34308–34322. doi:10.1039/D0RA05692H
28. Zhang X, Liang Y, Huang S, Guo B. Chitosan-based self-healing hydrogel dressing for wound healing. *Adv Colloid Interface Sci*. 2024;332:103267. doi:10.1016/j.cis.2024.103267
29. Ma W, Zhang H, Liu J, et al. Catechol-functionalized Chitosan/Polyvinyl alcohol hydrogel microneedles integrating multimodal antibacterial nanocomposites for enhanced wound healing. *Mater Des*. 2026;264:115811. doi:10.1016/j.matdes.2026.115811
30. Dai L, Geng Y, Ding X, et al. Highly stretchable, self-adhesive, and biocompatible cellulose/chitosan based double network hydrogel for wound dressing. *Carbohydr Polym*. 2025;366:123869. doi:10.1016/j.carbpol.2025.123869
31. Bernkop-Schnürch A, Dünnhaupt S. Chitosan-based drug delivery systems. *Eur J Pharm Biopharm*. 2012;81(3):463–469. doi:10.1016/j.ejpb.2012.04.007
32. Kulkarni AD, Patel HM, Surana SJ, Vanjari YH, Belgamwar VS, Pardeshi CV. N,N,N-Trimethyl chitosan: an advanced polymer with myriad of opportunities in nanomedicine. *Carbohydr Polym*. 2017;157:875–902. doi:10.1016/j.carbpol.2016.10.041

33. Freedman BR, Cintron Cruz JA, Kwon P, et al. Instant tough adhesion of polymer networks. *Proc Natl Acad Sci USA*. 2024;121(9): e2304643121. doi:10.1073/pnas.2304643121
34. Pinnaratip R, Bhuiyan MSA, Meyers K, Rajachar RM, Lee BP. Multifunctional biomedical adhesives. *Adv Healthcare Mate*. 2019;8 (11):1801568. doi:10.1002/adhm.201801568
35. Isobe N, Tsudome M, Kusumi R, et al. Moldable crystalline α-chitin hydrogel with toughness and transparency toward ocular applications. *ACS Appl Polym Mater*. 2020;2(4):1656–1663. doi:10.1021/acsapm.0c00087
36. Maiz-Fernández S, Pérez-álvarez L, Ruiz-Rubio L, Vilas-Vilela JL, Lanceros-Mendez S. Polysaccharide-based in situ self-healing hydrogels for tissue engineering applications. *Polymers*. 2020;12(10):2261. doi:10.3390/polym12102261
37. Taylor DL, In Het Panhuis M. Self-healing hydrogels. *Adv Mater*. 2016;28(41):9060–9093. doi:10.1002/adma.201601613
38. Yang K, Zhou X, Li Z, et al. Ultrastretchable, self-healable, and tissue-adhesive hydrogel dressings involving nanoscale tannic acid/ferric ion complexes for combating bacterial infection and promoting wound healing. *ACS Appl Mater Interfaces*. 2022;14(38):43010–43025. doi:10.1021/acsami.2c13283
39. Ding X, Fan L, Wang L, Zhou M, Wang Y, Zhao Y. Designing self-healing hydrogels for biomedical applications. *Mater Horiz*. 2023;10 (10):3929–3947. doi:10.1039/D3MH00891F
40. Liu X, Wang Y, Zhang W, et al. Caffeic acid and adenine modified chitosan dual-network hydrogel with antioxidant and pro-proliferative properties for diabetic wound healing. *Carbohydr Polym*. 2025;369:124290. doi:10.1016/j.carbpol.2025.124290
41. Zhang J, Fu C, Tian T, et al. In situ ultrafast self-gelling coacervate powder with antibacterial, antioxidant, and robust wet adhesion properties for hemostasis and wound healing. *Adv Funct Mater*. 2025;35(36):2502577. doi:10.1002/adfm.202502577
42. Aranaz I, Acosta N, Civera C, et al. Cosmetics and cosmeceutical applications of chitin, chitosan and their derivatives. *Polymers*. 2018;10 (2):213. doi:10.3390/polym10020213
43. Zhou X, Yang J, Qu G. Study on synthesis and properties of modified starch binder for foundry. *J Mater Process Technol*. 2007;183(2–3):407–411. doi:10.1016/j.jmatprotec.2006.11.001
44. Jimtaisong A, Saewan N. Utilization of carboxymethyl chitosan in cosmetics. *Int J Cosmet Sci*. 2014;36(1):12–21. doi:10.1111/ics.12102
45. Chaiwong N, Leelapornpisid P, Jantanasakulwong K, et al. Antioxidant and moisturizing properties of carboxymethyl chitosan with different molecular weights. *Polymers*. 2020;12(7):1445. doi:10.3390/polym12071445
46. Boudier A, Aubert-Pouëssel A, Mebarek N, et al. Development of tripartite polyion micelles for efficient peptide delivery into dendritic cells without altering their plasticity. *J Control Release*. 2011;154(2):156–163. doi:10.1016/j.jconrel.2011.05.016
47. Hu WW, Tsou SL. The effect of alginate on DNA delivery from layer-by-layer assembled films. *Carbohydr Polym*. 2014;101:240–248. doi:10.1016/j.carbpol.2013.09.025
48. Zhang L, Wang J, Ni C, Zhang Y, Shi G. Preparation of polyelectrolyte complex nanoparticles of chitosan and poly(2-acry1amido-2-methylpropanesulfonic acid) for doxorubicin release. *Mater Sci Eng C*. 2016;58:724–729. doi:10.1016/j.msec.2015.09.044
49. Antunes JC, Tavares TD, Teixeira MA, et al. Eugenol-containing essential oils loaded onto chitosan/polyvinyl alcohol blended films and their ability to eradicate *Staphylococcus aureus* or pseudomonas aeruginosa from infected microenvironments. *Pharmaceutics*. 2021;13(2):195. doi:10.3390/pharmaceutics13020195
50. Lall A, Kamdem Tamo A, Doench I, et al. Nanoparticles and colloidal hydrogels of chitosan–caseinate polyelectrolyte complexes for drug-controlled release applications. *IJMS*. 2020;21(16):5602. doi:10.3390/ijms21165602
51. Hamedi H, Moradi S, Hudson SM, Tonelli AE. Chitosan based hydrogels and their applications for drug delivery in wound dressings: a review. *Carbohydr Polym*. 2018;199:445–460. doi:10.1016/j.carbpol.2018.06.114
52. He G, Zheng H, Xiong F. Preparation and swelling behavior of physically crosslinked hydrogels composed of poly(vinyl alcohol) and chitosan. *J Wuhan Univ Technol-Mat Sci Ed*. 2008;23(6):816–820. doi:10.1007/s11595-007-6816-1
53. Wang X, Johnson M, Zhang N, et al. Stimuli-responsive chitosan-based injectable hydrogel for "on-demand" drug release. *Mater Adv*. 2023;4 (23):6439–6448. doi:10.1039/d3ma00430a
54. Lin CX, Yang K, Li PC, et al. Self-healing and injectable chitosan/konjac glucomannan hydrogel with pH response for controlled protein release. *Colloids Surf B*. 2024;242:114089. doi:10.1016/j.colsurfb.2024.114089
55. Sonaje K, Chuang EY, Lin KJ, et al. Opening of epithelial tight junctions and enhancement of paracellular permeation by chitosan: microscopic, ultrastructural, and computed-tomographic observations. *Mol Pharm*. 2012;9(5):1271–1279. doi:10.1021/mp200572t
56. Kumar A, Vimal A, Kumar A. Why Chitosan? From properties to perspective of mucosal drug delivery. *Int J Biol Macromol*. 2016;91:615–622. doi:10.1016/j.ijbiomac.2016.05.054
57. Federer C, Kurpiers M, Bernkop-Schnürch A. Thiolated chitosans: a multi-talented class of polymers for various applications. *Biomacromolecules*. 2021;22(1):24–56. doi:10.1021/acs.biomac.0c00663
58. Jain S, Nuwal K, Mahmood A, et al. Thiolated chitosan as an improved bioadhesive polymer in drug delivery. In: *Chitosan in Drug Delivery*. Elsevier; 2022:247–276. 10.1016/B978-0-12-819336-5.00013-3
59. Langoth N, Kahlbacher H, Schöffmann G, et al. Thiolated CHITOSANS: DESIGN AND IN VIVO EVALUATION OF A MUCOADHESIVE BUCCAL PEPTIDE DRUG DELIVERY SYSTEM. *Pharm Res*. 2006;23(3):573–579. doi:10.1007/s11095-005-9533-5
60. Ahmed S, Ikram S. Chitosan & its derivatives: a review in recent innovations. *Int J Pharm Sci Res*. 2015;6(1):14–30. doi:10.13040/IJPSR.0975-8232.6(1).14-30
61. Canciani B, Semeraro F, Herrera Millar VR, et al. In vitro and in vivo biocompatibility assessment of a thermosensitive injectable chitosan-based hydrogel for musculoskeletal tissue engineering. *IJMS*. 2023;24(13):10446. doi:10.3390/ijms241310446
62. Agnihotri SA, Mallikarjuna NN, Aminabhavi TM. Recent advances on chitosan-based micro- and nanoparticles in drug delivery. *J Control Release*. 2004;100(1):5–28. doi:10.1016/j.jconrel.2004.08.010
63. Ramasamy P, Subhapradha N, Thinesh T, et al. Characterization of bioactive chitosan and sulfated chitosan from Doryteuthis singhalensis (Ortmann, 1891). *Int J Biol Macromol*. 2017;99:682–691. doi:10.1016/j.ijbiomac.2017.03.041
64. Rabea EI, Badawy MET, Stevens CV, Smagghe G, Steurbaut W. Chitosan as antimicrobial agent: applications and mode of action. *Biomacromolecules*. 2003;4(6):1457–1465. doi:10.1021/bm034130m
65. Jung EJ, Youn DK, Lee SH, No HK, Ha JG, Prinyawiwatkul W. Antibacterial activity of chitosans with different degrees of deacetylation and viscosities. *Int J Food Sci Tech*. 2010;45(4):676–682. doi:10.1111/j.1365-2621.2010.02186.x

66. Kamjumphol W, Chareonsudjai P, Chareonsudjai S. Antibacterial activity of chitosan against *Burkholderia pseudomallei*. *MicrobiologyOpen*. 2018;7(1):e00534. doi:10.1002/mbo3.534
67. Kong M, Chen XG, Xing K, Park HJ. Antimicrobial properties of chitosan and mode of action: a state of the art review. *Int J Food Microbiol*. 2010;144(1):51–63. doi:10.1016/j.ijfoodmicro.2010.09.012
68. Li J, Liu Y, Zhao X. Latest research progress on antibacterial properties of chitosan-based nanofibers. *Chem Eng J*. 2025;517:163776. doi:10.1016/j.cej.2025.163776
69. Supernak M, Makurat-Kasprolewicz B, Kaczmarek-Szczepańska B, et al. Chitosan-based membranes as gentamicin carriers for biomedical applications—influence of chitosan molecular weight. *Membranes*. 2023;13(6):542. doi:10.3390/membranes13060542
70. Egorov AR, Kirichuk AA, Rubanik VV, Rubanik VV, Tskhovrebov AG, Kritchenkov AS. Chitosan and Its derivatives: preparation and antibacterial properties. *Materials*. 2023;16(18):6076. doi:10.3390/ma16186076
71. Li W, Zhang H, Wang Z, et al. Non-thermal plasma-induced selective glycosidic cleavage in chitosan produces multifunctional antibacterial wound care biomaterials. *Adv Funct Mater*. 2026;36(33):e19776. doi:10.1002/adfm.202519776
72. Benchamas G, Huang G, Huang S, Huang H. Preparation and biological activities of chitosan oligosaccharides. *Trends Food Sci Technol*. 2021;107:38–44. doi:10.1016/j.tifs.2020.11.027
73. Yilmaz Atay H. Antibacterial activity of chitosan-based systems. In: Jana S, Jana S, editors. *Functional Chitosan*. Springer Singapore; 2019:457–489. doi:10.1007/978-981-15-0263-7_15
74. Xing Y, Xu Q, Li X, et al. Chitosan-based coating with antimicrobial agents: preparation, property, mechanism, and application effectiveness on fruits and vegetables. *Int J Polym Sci*. 2016;2016:1–24. doi:10.1155/2016/4851730
75. Kheirabadi BS, Acheson EM, Deguzman R, et al. Hemostatic efficacy of two advanced dressings in an aortic hemorrhage model in Swine. *J Trauma*. 2005;59(1):25–35. doi:10.1097/01.TA.0000171458.72037.EE
76. Lord MS, Cheng B, McCarthy SJ, Jung M, Whitelock JM. The modulation of platelet adhesion and activation by chitosan through plasma and extracellular matrix proteins. *Biomaterials*. 2011;32(28):6655–6662. doi:10.1016/j.biomaterials.2011.05.062
77. Cao S, Bi Z, Li Q, Zhang S, Singh M, Chen J. Shape memory and antibacterial chitosan-based cryogel with hemostasis and skin wound repair. *Carbohydr Polym*. 2023;305:120545. doi:10.1016/j.carbpol.2023.120545
78. Sun X, Li J, Shao K, et al. A composite sponge based on alkylated chitosan and diatom-biosilica for rapid hemostasis. *Int J Biol Macromol*. 2021;182:2097–2107. doi:10.1016/j.ijbiomac.2021.05.123
79. Sagnella S, Mai-Ngam K. Chitosan based surfactant polymers designed to improve blood compatibility on biomaterials. *Colloids Surf B*. 2005;42(2):147–155. doi:10.1016/j.colsurfb.2004.07.001
80. Hu Z, Zhang DY, Lu ST, Li PW, Li SD. Chitosan-based composite materials for prospective hemostatic applications. *Mar Drugs*. 2018;16 (8):273. doi:10.3390/md16080273
81. Li H, Cheng F, Gao S, et al. Preparation, characterization, antibacterial properties, and hemostatic evaluation of ibuprofen-loaded chitosan/ gelatin composite films. *J Appl Polymer Sci*. 2017;134(42):45441. doi:10.1002/app.45441
82. Chen L, Tianqing L. Interaction behaviors between chitosan and hemoglobin. *Int J Biol Macromol*. 2008;42(5):441–446. doi:10.1016/j. ijbiomac.2008.02.005
83. Huang Z, Zhang D, Tong L, et al. Protonated-chitosan sponge with procoagulation activity for hemostasis in coagulopathy. *Bioact Mater*. 2024;41:174–192. doi:10.1016/j.bioactmat.2024.07.012
84. Liu A, Cui S, Song L, et al. Ultrafast self-gelling, superabsorbent, and adhesive chitosan-based hemostatic powders for rapid hemostasis and wound healing. *Carbohydr Polym*. 2025;355:123362. doi:10.1016/j.carbpol.2025.123362
85. Lan G, Lu B, Wang T, et al. Chitosan/gelatin composite sponge is an absorbable surgical hemostatic agent. *Colloids Surf B*. 2015;136:1026–1034. doi:10.1016/j.colsurfb.2015.10.039
86. Clay JG, Grayson JK, Zierold D. Comparative testing of new hemostatic agents in a swine model of extremity arterial and venous hemorrhage. *Mil Med*. 2010;175(4):280–284. doi:10.7205/MILMED-D-09-00185
87. Morgan MJ, Liu Z. Crosstalk of reactive oxygen species and NF-κB signaling. *Cell Res*. 2011;21(1):103–115. doi:10.1038/cr.2010.178
88. Sies H, Jones DP. Reactive oxygen species (ROS) as pleiotropic physiological signalling agents. *Nat Rev Mol Cell Biol*. 2020;21(7):363–383. doi:10.1038/s41580-020-0230-3
89. Han Q, Shen T, Wang F, Wu P, Chen J. Preventive and therapeutic potential of vitamin C in mental disorders. *Curr Med Sci*. 2018;38(1):1–10. doi:10.1007/s11596-018-1840-2
90. Jridi M, Sellimi S, Lassoued KB, et al. Wound healing activity of cuttlefish gelatin gels and films enriched by henna (Lawsonia inermis) extract. *Colloids Surf A*. 2017;512:71–79. doi:10.1016/j.colsurfa.2016.10.014
91. Koo MA, Hee Hong S, Hee Lee M, et al. Effective stacking and transplantation of stem cell sheets using exogenous ROS-producing film for accelerated wound healing. *Acta Biomater*. 2019;95:418–426. doi:10.1016/j.actbio.2019.01.019
92. Xu Z, Han S, Gu Z, Wu J. Advances and impact of antioxidant hydrogel in chronic wound healing. *Adv Healthcare Mate*. 2020;9(5):1901502. doi:10.1002/adhm.201901502
93. Rajinikanth BS, Rajkumar DSR, K K, Vijayaragavan V. Chitosan-based biomaterial in wound healing: a review. *Cureus*. 2024. doi:10.7759/ cureus.55193
94. Tomida H, Fujii T, Furutani N, et al. Antioxidant properties of some different molecular weight chitosans. *Carbohydr Res*. 2009;344(13):1690–1696. doi:10.1016/j.carres.2009.05.006
95. Rajalakshmi A, Krithiga N, Jayachitra A. Antioxidant activity of the chitosan extracted from shrimp exoskeleton. *Middle East J Sci Res*. 2013;16(10):1446–1451.
96. Xie W, Xu P, Liu Q. Antioxidant activity of water-soluble chitosan derivatives. *Bioorg Med Chem Lett*. 2001;11(13):1699–1701. doi:10.1016/ s0960-894x(01)00285-2
97. Decker EA. Strategies for manipulating the prooxidative/antioxidative balance of foods to maximize oxidative stability. *Trends Food Sci Technol*. 1998;9(6):241–248. doi:10.1016/s0924-2244(98)00045-4
98. Eom TK, Senevirathne M, Kim SK. Synthesis of phenolic acid conjugated chitooligosaccharides and evaluation of their antioxidant activity. *Environ Toxicol Pharmacol*. 2012;34(2):519–527. doi:10.1016/j.etap.2012.05.004

99. Lee SH, Ryu B, Je JY, Kim SK. Diethylaminoethyl chitosan induces apoptosis in HeLa cells via activation of caspase-3 and p53 expression. *Carbohydr Polym*. 2011;84(1):571–578. doi:10.1016/j.carbpol.2010.12.027
100. Lee SH, Senevirathne M, Ahn CB, Kim SK, Je JY. Factors affecting anti-inflammatory effect of chitooligosaccharides in lipopolysaccharides-induced RAW264.7 macrophage cells. *Bioorg Med Chem Lett*. 2009;19(23):6655–6658. doi:10.1016/j.bmcl.2009.10.007
101. Cho YS, Kim SK, Je JY. Chitosan gallate as potential antioxidant biomaterial. *Bioorg Med Chem Lett*. 2011;21(10):3070–3073. doi:10.1016/j.bmcl.2011.03.033
102. Mendis E, Kim MM, Rajapakse N, Kim SK. An in vitro cellular analysis of the radical scavenging efficacy of chitooligosaccharides. *Life Sci*. 2007;80(23):2118–2127. doi:10.1016/j.lfs.2007.03.016
103. Pan H, Yang Q, Huang G, et al. Hypolipidemic effects of chitosan and its derivatives in hyperlipidemic rats induced by a high-fat diet. *Food Nutr Res*. 2016;60(1):31137. doi:10.3402/fnr.v60.31137
104. Wardani G, Nugraha J, Mustafa MR, Kurnijasanti R, Sudjarwo SA. Antioxidative stress and antiapoptosis effect of chitosan nanoparticles to protect cardiac cell damage on streptozotocin-induced diabetic rat. *Oxid Med Cell Longev*. 2022;2022(1). doi:10.1155/2022/3081397
105. Nagamaniammai G, Chithra M, Ganga MU. Study on the effect of prawn (Machrobrachuim rosenbergii) chitosan coating on peeled shallot (Allium ascalonicum). *Curr Res Nutr Food Sci*. 2019;7(3):927–935. doi:10.12944/crnfsj.7.3.31
106. Mao S, Shuai X, Unger F, Simon M, Bi D, Kissel T. The depolymerization of chitosan: effects on physicochemical and biological properties. *Int J Pharm*. 2004;281(1–2):45–54. doi:10.1016/j.ijpharm.2004.05.019
107. Wasikiewicz JM, Yoshii F, Nagasawa N, Wach RA, Mitomo H. Degradation of chitosan and sodium alginate by gamma radiation, sonochemical and ultraviolet methods. *Radiat Phys Chem*. 2005;73(5):287–295. doi:10.1016/j.radphyschem.2004.09.021
108. Chmielewski AG. Chitosan and radiation chemistry. *Radiat Phys Chem*. 2010;79(3):272–275. doi:10.1016/j.radphyschem.2009.11.002
109. Pati S, Chatterji A, Dash BP, et al. Structural characterization and antioxidant potential of chitosan by γ-irradiation from the carapace of horseshoe crab. *Polymers*. 2020;12(10):2361. doi:10.3390/polym12102361
110. Hwang SM, Kim E, Wu J, Kim MH, Lee H, Park WH. Temperature- and pH-induced dual-crosslinked methylcellulose/chitosan-gallol conjugate composite hydrogels with improved mechanical, tissue adhesive, and hemostatic properties. *Int J Biol Macromol*. 2024;277:134098. doi:10.1016/j.ijbiomac.2024.134098
111. Dong Q, Xiong S, Dong X, et al. Light-activated chitosan hydrogel: a bioadhesive platform for emergency hemostasis and bacteria-infected wound management. *Carbohydr Polym*. 2026;372:124557. doi:10.1016/j.carbpol.2025.124557
112. Liu L, Yan A, Zeng J, Geng S, Li X, Huang G. A tri-component hydrogel composed of Bletilla striata polysaccharide, carboxymethyl chitosan and cinnamaldehyde: potent enhancement of diabetic wound healing. *Carbohydr Polym*. 2026;373:124536. doi:10.1016/j.carbpol.2025.124536
113. Nezhad-Mokhtari P, Kashani E, Mazloomi M, et al. Electroactive dopamine-functionalized reduced graphene oxide/alginate hydrogel containing thymol/chitosan nanoparticles for advanced antibacterial and bioadhesive wound dressings. *Carbohydr Polym*. 2026;380:124960. doi:10.1016/j.carbpol.2026.124960
114. Lin H, Wang Z, Li P, et al. Intelligent-responsive hydrogel synergistically mediates immune remodel-antibacterial-angiogenesis cascade for diabetic foot ulcer repair. *Bioact Mater*. 2026;62:508–525. doi:10.1016/j.bioactmat.2026.03.034
115. Lu T, Wang Q, Sun M, et al. Light-driven switchable polyacrylamide/chitosan-based hydrogel dressings for outdoor wound temperature regulation and enhanced skin regeneration. *Carbohydr Polym*. 2026;378:124920. doi:10.1016/j.carbpol.2026.124920
116. Guan R, Su Y, Li S, Yang S, Li X, Wang X. Laponite-reinforced marine bioinspired injectable self-healing adhesive chitosan-based hydrogel for infected wounds. *Carbohydr Polym*. 2026;382:125230. doi:10.1016/j.carbpol.2026.125230
117. Peng S, Wang L, Lu Z, et al. An Injectable conductive multifunctional hydrogel dressing with synergistic antimicrobial, ROS scavenging, and electroactive effects for the combined treatment of chronic diabetic wounds. *SSRN*. 2024. doi:10.2139/ssrn.5042583
118. Xu Y, He F, Hu Z, et al. Non-conductive surfaces electro-fabrication of transparent high-performance layered chitosan-silver-montmorillonite composite hydrogels for infected wound dressing. *Carbohydr Polym*. 2025;369:124306. doi:10.1016/j.carbpol.2025.124306
119. Gong L, Chang L, Chen S, et al. Multifunctional injectable hydrogel with self-supplied H_2S release and bacterial inhibition for the wound healing with enhanced macrophages polarization via interfering with PI3K/Akt pathway. *Biomaterials*. 2025;318:123144. doi:10.1016/j.biomaterials.2025.123144
120. Deng Y, Li P, Peng X, Feng S, Yu X, Zhao Q. Quaternary ammonium chitosan/N-isopropylacrylamide-based Janus hydrogel with asymmetric adhesive, shrinkable, and antimicrobial properties for wound healing. *Int J Biol Macromol*. 2025;327:147416. doi:10.1016/j.ijbiomac.2025.147416
121. Li L, Zhao Z, Gao Y, et al. Dynamic Metal-phenolic coordinated hydrogel for synergistic photothermal/chemodynamic therapy against biofilm-infected wounds and real-time monitoring. *ACS Appl Mater Interfaces*. 2025:acsami.5c17481. doi:10.1021/acsami.5c17481
122. Tan Z, Liu L, Hao L, Zhang J, Dai Y, Yu J. Carboxymethyl chitosan/PVA-based dynamic cross-linked dual network hydrogel loaded with berberine with self-healing, self-adaptive, sustainable release and antibacterial ability for dressing. *Int J Biol Macromol*. 2025;322:146942. doi:10.1016/j.ijbiomac.2025.146942
123. Gao S, Yan T, Ji L, et al. Pathologically responsive Au@Ag nanocomposite spray-coated hydrogel dressing for accelerated healing of infected wounds. *ACS Appl Mater Interfaces*. 2025;17(33):46693–46704. doi:10.1021/acsami.5c10248
124. Zhou D, Li X, Zhu Y, et al. Fungal-derived chitosan-based hydrogels with antimicrobial properties for infectious wound healing. *Carbohydr Polym*. 2025;366:123917. doi:10.1016/j.carbpol.2025.123917
125. Zhang G, Liu Y, Wu J, et al. Chitosan-based double-network hydrogel with synergistic photothermal/nitric oxide therapy for methicillin-resistance *Staphylococcus aureus* infected wound healing. *J Colloid Interface Sci*. 2025;700:138520. doi:10.1016/j.jcis.2025.138520
126. Su H, Jing X, Sun H, Liu Z, Wang D, Meng L. Multifunctional nanocomposite hydrogel dressings with excellent antibacterial and angiogenesis properties for effective treatment of diabetic wounds. *ACS Appl Mater Interfaces*. 2025;17(30):43604–43619. doi:10.1021/acsami.5c08356
127. Lu T, Sun M, Zhou Y, et al. Self-powered chitosan/graphene oxide hydrogel band-aids with bioadhesion for promoting infected wounds healing. *Int J Biol Macromol*. 2024;283:137374. doi:10.1016/j.ijbiomac.2024.137374
128. Zhou R, Huang J, Zhang W, et al. Multifunctional hydrogel based on polyvinyl alcohol/chitosan/metal polyphenols for facilitating acute and infected wound healing. *Mater Today Bio*. 2024;29:101315. doi:10.1016/j.mtbio.2024.101315
129. Wan J, Yin M, Wang F, et al. Natural gelatin / chitosan oligosaccharides / emodin eutectogels with multiple antibacterial effects for accelerated infected wound healing. *Int J Biol Macromol*. 2025;320:145771. doi:10.1016/j.ijbiomac.2025.145771

130. Hu S, Lv J, Yan M, et al. Multifunctional electrospun fiber sponge for hemostasis and infected wound healing. *Small*. 2025;21(23):2409969. doi:10.1002/smll.202409969
131. Jiang T, Chen S, Xu J, et al. Superporous sponge prepared by secondary network compaction with enhanced permeability and mechanical properties for non-compressible hemostasis in pigs. *Nat Commun*. 2024;15(1):5460. doi:10.1038/s41467-024-49578-2
132. Guo H, Ran W, Jin X, et al. Development of pectin/chitosan-based electrospun biomimetic nanofiber membranes loaded with dihydromyricetin inclusion complexes for wound healing application. *Int J Biol Macromol*. 2024;278:134526. doi:10.1016/j.ijbiomac.2024.134526
133. Feng X, Xu H, Bai L, Yang J, Yang W, Hu Y. The polycaprolactone/chitosan (PCL/CS) spun membranes loaded with astragalus polysaccharide by emulsion spinning technology for anti-infective wound dressings. *Int J Biol Macromol*. 2025;329:147615. doi:10.1016/j.ijbiomac.2025.147615
134. Don TM, Tai HC, Chen YC, Huang YC. Preparation of polypyrrole-ulvan nanoparticles and bioactive properties of multifunctional polypyrrole-ulvan/chitosan dressings for enhanced wound healing. *Carbohydr Polym*. 2026;381:125196. doi:10.1016/j.carbpol.2026.125196
135. Yao M, He Q, Tao Y, et al. Chitosan-derived carbon quantum dots with dual ROS scavenging and anti-inflammatory functionalities for accelerated wound repair. *ACS Appl Mater Interfaces*. 2025;17(28):40157–40172. doi:10.1021/acsami.5c07628
136. Erdogan S, Günes SN, Bulbul YE, Eskitoros-Togay ŞM, Dilsiz N. Design of multi-layer electrospun poly(ε-caprolactone)/chitosan nanofiber scaffolds loaded with tigecycline for controlled drug release and antibacterial wound healing. *Int J Biol Macromol*. 2025;322:146955. doi:10.1016/j.ijbiomac.2025.146955
137. Zhang Y, Li X, Chen H, et al. Acetylated yeast mannan endowing biomimetic electrospun nanofibers with hydrophobicity and moisturizing property for accelerated cutaneous defects repair. *Int J Biol Macromol*. 2025;320:145944. doi:10.1016/j.ijbiomac.2025.145944
138. Zhang Q, Wang H, Chen M, Wang L, Che X. Color-changeable and separable PLA/PVP/chitosan tri-layer self-pumping dressing containing astragalus for promoting the healing of infectious burn wound. *Int J Biol Macromol*. 2025;321:146043. doi:10.1016/j.ijbiomac.2025.146043
139. Zhang J, Shi Y, Zhang Y, et al. Antibacterial and proangiogenic hydrogel microneedle patches for wound healing. *Smart Med*. 2025;4(3):e70014. doi:10.1002/smmd.70014
140. Shan M, Wei L, Li Y, et al. An antibacterial and electroactive chitosan-based dressing with dual stimulus-responsive drug delivery for wound healing. *Macromol Rapid Commun*. 2025:e00547. doi:10.1002/marc.202500547
141. Abdulmalik S, Kumbar SG. Scar-reducing ionically conductive chitosan bandage: combining ionic and electrical stimulation for optimal wound healing. *Biomaterials*. 2026;326:123668. doi:10.1016/j.biomaterials.2025.123668
142. Almasoudi SH. Bioengineered chitosan/silk scaffold encapsulated with quercetin nanoparticles accelerates wound healing in a diabetic rat skin defect model. *Tissue Cell*. 2026;98:103119. doi:10.1016/j.tice.2025.103119
143. Chen S, Li C, Teng Y, Wei H, Lu C, Yang H. Photothermal and antimicrobial properties of catechol-chitosan silver nanoparticles/esterified sodium alginate composite hydrogels. *J biomater sci Poly ed*. 2025;1–20. doi:10.1080/09205063.2025.2526292
144. Guo S, Ren Y, Chang R, et al. Injectable self-healing adhesive chitosan hydrogel with antioxidative, antibacterial, and hemostatic activities for rapid hemostasis and skin wound healing. *ACS Appl Mater Interfaces*. 2022;14(30):34455–34469. doi:10.1021/acsami.2c08870
145. Wienk IM, Boom RM, Beerlage MAM, Bulte AMW, Smolders CA, Strathmann H. Recent advances in the formation of phase inversion membranes made from amorphous or semi-crystalline polymers. *J Membr Sci*. 1996;113(2):361–371. doi:10.1016/0376-7388(95)00256-1
146. Strathmann H, Kock K. The formation mechanism of phase inversion membranes. *Desalination*. 1977;21(3):241–255. doi:10.1016/S0011-9164(00)88244-2
147. Bajpai SK, Chand N, Ahuja S, Roy MK. Vapor induced phase inversion technique to prepare chitosan/microcrystalline cellulose composite films: synthesis, characterization and moisture absorption study. *Cellulose*. 2015;22(6):3825–3837. doi:10.1007/s10570-015-0775-z
148. Zirak Hassan Kiadeh S, Ghaee A, Mashak A, Mohammadnejad J. Preparation of chitosan–silica/PCL composite membrane as wound dressing with enhanced cell attachment. *Polym Adv Techs*. 2017;28(11):1396–1408. doi:10.1002/pat.4016
149. Miguel SP, Moreira AF, Correia IJ. Chitosan based-asymmetric membranes for wound healing: a review. *Int J Biol Macromol*. 2019;127:460–475. doi:10.1016/j.ijbiomac.2019.01.072
150. Deville S. Freeze-casting of porous ceramics: a review of current achievements and issues. *Adv Eng Mater*. 2008;10(3):155–169. doi:10.1002/adem.200700270
151. Scotti KL, Dunand DC. Freeze casting – a review of processing, microstructure and properties via the open data repository, FreezeCasting.net. *Pro Mater Sci*. 2018;94:243–305. doi:10.1016/j.pmatsci.2018.01.001
152. Lin X, Feng Y, He Y, Ding S, Liu M. Engineering design of asymmetric halloysite/chitosan/collagen sponge with hydrophobic coating for high-performance hemostasis dressing. *Int J Biol Macromol*. 2023;237:124148. doi:10.1016/j.ijbiomac.2023.124148
153. Ma R, Wang Y, Qi H, et al. Nanocomposite sponges of sodium alginate/graphene oxide/polyvinyl alcohol as potential wound dressing: in vitro and in vivo evaluation. *Composites Part B*. 2019;167:396–405. doi:10.1016/j.compositesb.2019.03.006
154. Wang D, Zhang N, Meng G, He J, Wu F. The effect of form of carboxymethyl-chitosan dressings on biological properties in wound healing. *Colloids Surf B*. 2020;194:111191. doi:10.1016/j.colsurfb.2020.111191
155. Ali Khan Z, Jamil S, Akhtar A, Mustehsan Bashir M, Yar M. Chitosan based hybrid materials used for wound healing applications- A short review. *Int J Polym Mater Polym Biomater*. 2020;69(7):419–436. doi:10.1080/00914037.2019.1575828
156. Iranshahi K, Defraeye T, Rossi RM, Müller UC. Electrohydrodynamics and its applications: recent advances and future perspectives. *Int J Heat Mass Transfer*. 2024;232:125895. doi:10.1016/j.ijheatmasstransfer.2024.125895
157. Ignatova M, Manolova N, Rashkov I. Electrospun antibacterial chitosan-based fibers: electrospun antibacterial chitosan-based fibers. *Macromol Biosci*. 2013;13(7):860–872. doi:10.1002/mabi.201300058
158. Negm NA, Hefni HHH, Abd-Elaal AAA, Badr EA, Abou Kana MTH. Advancement on modification of chitosan biopolymer and its potential applications. *Int J Biol Macromol*. 2020;152:681–702. doi:10.1016/j.ijbiomac.2020.02.196
159. Ziabicki A. *Fundamentals of Fibre Formation: The Science of Fibre Spinning and Drawing*. John Wiley; 1976.
160. Celebioglu A, Saporito AF, Uyar T. Green electrospinning of chitosan/pectin nanofibrous films by the incorporation of cyclodextrin/curcumin inclusion complexes: ph-responsive release and hydrogel features. *ACS Sustainable Chem Eng*. 2022;10(14):4758–4769. doi:10.1021/acssuschemeng.2c00650
161. Zhang T, Xu H, Zhang Y, et al. Fabrication and characterization of double-layer asymmetric dressing through electrostatic spinning and 3D printing for skin wound repair. *Mater Des*. 2022;218:110711. doi:10.1016/j.matdes.2022.110711

162. Liu H, Chen R, Wang P, et al. Electrospun polyvinyl alcohol-chitosan dressing stimulates infected diabetic wound healing with combined reactive oxygen species scavenging and antibacterial abilities. *Carbohydr Polym*. 2023;316:121050. doi:10.1016/j.carbpol.2023.121050
163. Zhao D, Liu J, Liu G, et al. Ascorbyl palmitate/hydroxypropyl-β-cyclodextrin inclusion complex loaded nanofibrous membrane for accelerated diabetic wound healing. *Interdiscip Mater*. 2025;4(1):175–189. doi:10.1002/idm2.12215
164. Shi S, Si Y, Han Y, et al. Recent progress in protective membranes fabricated via electrospinning: advanced materials, biomimetic structures, and functional applications. *Adv Mater*. 2022;34(17):2107938. doi:10.1002/adma.202107938
165. Yang G, Li X, He Y, Ma J, Ni G, Zhou S. From nano to micro to macro: electrospun hierarchically structured polymeric fibers for biomedical applications. *Prog Polym Sci*. 2018;81:80–113. doi:10.1016/j.progpolymsci.2017.12.003
166. Jonidi Shariatzadeh F, Currie S, Logsetty S, Spiwak R, Liu S. Enhancing wound healing and minimizing scarring: a comprehensive review of nanofiber technology in wound dressings. *Pro Mater Sci*. 2025;147:101350. doi:10.1016/j.pmatsci.2024.101350
167. Borbolla-Jiménez FV, Peña-Corona SI, Farah SJ, et al. Films for wound healing fabricated using a solvent casting technique. *Pharmaceutics*. 2023;15(7):1914. doi:10.3390/pharmaceutics15071914
168. Deng L, Kang X, Liu Y, Feng F, Zhang H. Characterization of gelatin/zein films fabricated by electrospinning vs solvent casting. *Food Hydrocoll*. 2018;74:324–332. doi:10.1016/j.foodhyd.2017.08.023
169. Karki S, Kim H, Na SJ, Shin D, Jo K, Lee J. Thin films as an emerging platform for drug delivery. *Asian J Pharm Sci*. 2016;11(5):559–574. doi:10.1016/j.ajps.2016.05.004
170. Pacheco MS, Kano GE, Paulo LDA, Lopes PS, De Moraes MA. Silk fibroin/chitosan/alginate multilayer membranes as a system for controlled drug release in wound healing. *Int J Biol Macromol*. 2020;152:803–811. doi:10.1016/j.ijbiomac.2020.02.140
171. Silva JM, Carvalho JPF, Teixeira MC, et al. Xylan-chitosan based films with deep eutectic solvents for wound healing applications. *Int J Biol Macromol*. 2025;320:145482. doi:10.1016/j.ijbiomac.2025.145482
172. Güneş S, Tıhmınlıoğlu F. Hypericum perforatum incorporated chitosan films as potential bioactive wound dressing material. *Int J Biol Macromol*. 2017;102:933–943. doi:10.1016/j.ijbiomac.2017.04.080
173. Anbukarasu P, Sauvageau D, Elias A. Tuning the properties of polyhydroxybutyrate films using acetic acid via solvent casting. *Sci Rep*. 2015;5(1):17884. doi:10.1038/srep17884
174. Gana FZ, Harek Y, Aissaoui N, Nadjat T, Abbad S, Rouabhi H. Effect of the molar mass of chitosan and film casting solvents on the properties of chitosan films loaded with *Mentha spicata* essential oil for potential application as wound dressing. *J biomater sci Poly ed*. 2024;35(18):2807–2828. doi:10.1080/09205063.2024.2390752
175. Qiao L, Liang Y, Chen J, et al. Antibacterial conductive self-healing hydrogel wound dressing with dual dynamic bonds promotes infected wound healing. *Bioact Mater*. 2023;30:129–141. doi:10.1016/j.bioactmat.2023.07.015
176. Servín De La Mora-López D, Olivera-Castillo L, López-Cervantes J, et al. Bioengineered chitosan–collagen–honey sponges: physicochemical, antibacterial, and in vitro healing properties for enhanced wound healing and infection control. *Polymers*. 2025;17(17):2379. doi:10.3390/polym17172379
177. Xu H, Huang P, Fang H, et al. Multifunctional antimicrobial wound dressing with photothermal promotion based on Bletilla striata polysaccharides and other natural materials. *Int J Biol Macromol*. 2025;327:147278. doi:10.1016/j.ijbiomac.2025.147278
178. Yang L, Zhang X, He W, et al. Preparation of "Five-in-One" chitosan hydrogel for infectious wound repair. *ACS Appl Mater Interfaces*. 2025;17(34):48000–48016. doi:10.1021/acsami.5c10994
179. Mahmoodi M, Mirzababaie SA, Mokhtarzade A, et al. Evaluation of gene expression levels in diabetic rat skin wound healing treated with chitosan/curcumin nanoparticles-loaded sodium alginate/chitosan hydrogels. *Int J Biol Macromol*. 2025;324:147220. doi:10.1016/j.ijbiomac.2025.147220
180. He J, Dong T, Zhou F, et al. Chitosan-based glucose-responsive hydrogel with spatiotemporally controlled bactericidal release for diabetic wound regeneration via multimodal therapy. *Carbohydr Polym*. 2026;373:124446. doi:10.1016/j.carbpol.2025.124446
181. Deng Z, Guo Y, Wang X, et al. Multiple crosslinked, self-healing, and shape-adaptable hydrogel laden with pain-relieving chitosan@borneol nanoparticles for infected burn wound healing. *Theranostics*. 2025;15(4):1439–1455. doi:10.7150/thno.102569
182. Cheng F, Xu L, Dai J, Yi X, He J, Li H. N, O-carboxymethyl chitosan/oxidized cellulose composite sponge containing ε-poly-l-lysine as a potential wound dressing for the prevention and treatment of postoperative adhesion. *Int J Biol Macromol*. 2022;209:2151–2164. doi:10.1016/j.ijbiomac.2022.04.195
183. Huang Y, Yan Z, Chen H, et al. Protamine-loaded quaternized chitosan hydrogel dressing featuring antibacterial and antioxidant properties for promoting postoperative periodontal wound healing. *Int J Biol Macromol*. 2025;330:148259. doi:10.1016/j.ijbiomac.2025.148259
184. Chen G, Yang C, Xu X, et al. Multifunctional hydrogel dressing composed of trichosanthes polysaccharide and carboxymethyl chitosan accelerates cachectic wound healing and reduces scar hyperplasia. *Carbohydr Polym*. 2025;357:123378. doi:10.1016/j.carbpol.2025.123378
185. Herndon DN, ed.. *Total Burn Care*. 4th ed. Saunders Elsevier; 2012.
186. Shu W, Wang Y, Zhang X, Li C, Le H, Chang F. Functional hydrogel dressings for treatment of burn wounds. *Front Bioeng Biotechnol*. 2021;9:788461. doi:10.3389/fbioe.2021.788461
187. Yao Y, Zhang A, Yuan C, Chen X, Liu Y. Recent trends on burn wound care: hydrogel dressings and scaffolds. *Biomater Sci*. 2021;9(13):4523–4540. doi:10.1039/D1BM00411E
188. Ngai D, Schilperoort M, Tabas I. Efferocytosis-induced lactate enables the proliferation of pro-resolving macrophages to mediate tissue repair. *Nat Metab*. 2023;5(12):2206–2219. doi:10.1038/s42255-023-00921-9
189. Tomasso A, Koopmans T, Lijnzaad P, Bartscherer K, Seifert AW. An ERK-dependent molecular switch antagonizes fibrosis and promotes regeneration in spiny mice (*Acomys*). *Sci Adv*. 2023;9(17). doi:10.1126/sciadv.adf2331
190. Xu S, Zhang Y, Dai B, et al. Green-prepared magnesium silicate sprays enhance the repair of burn-skin wound and appendages regeneration in rats and minipigs. *Adv Funct Mater*. 2024;34(9). doi:10.1002/adfm.202307439
191. Uberoi A, McCready-Vangi A, Grice EA. The wound microbiota: microbial mechanisms of impaired wound healing and infection. *Nat Rev Microbiol*. 2024;22(8):507–521. doi:10.1038/s41579-024-01035-z
192. Wu Z, Li M, Liu Q, et al. Engineered multifunctional artificial dermis for infected burn wound healing. *Adv Funct Mater*. 2025;35(8). doi:10.1002/adfm.202415514

193. Rowan MP, Cancio LC, Elster EA, et al. Burn wound healing and treatment: review and advancements. *Crit Care*. 2015;19(1). doi:10.1186/s13054-015-0961-2
194. Noor A, Afzal A, Masood R, et al. Dressings for burn wound: a review. *J Mater Sci*. 2022;57(12):6536–6572. doi:10.1007/s10853-022-07056-4
195. El-Feky GS, Sharaf SS, El Shafei A, Hegazy AA. Using chitosan nanoparticles as drug carriers for the development of a silver sulfadiazine wound dressing. *Carbohydr Polym*. 2017;158:11–19. doi:10.1016/j.carbpol.2016.11.054
196. Massand S, Cheema F, Brown S, Davis WJ, Burkey B, Glat PM. The use of a chitosan dressing with silver in the management of paediatric burn wounds: a pilot study. *J Wound Care*. 2017;26(sup4):S26–S30. doi:10.12968/jowc.2017.26.sup4.s26
197. Saeed SM, Mirzadeh H, Zandi M, Barzin J. Designing and fabrication of curcumin loaded PCL/PVA multi-layer nanofibrous electrospun structures as active wound dressing. *Prog Biomater*. 2017;6(1–2):39–48. doi:10.1007/s40204-017-0062-1
198. Radwan-Pragłowska J, Janus Ł, Piątkowski M, Bogdał D, Matýsek D. Hybrid bilayer PLA/chitosan nanofibrous scaffolds doped with ZnO, Fe3O4, and Au nanoparticles with bioactive properties for skin tissue engineering. *Polymers*. 2020;12(1):159. doi:10.3390/polym12010159
199. Zhu Z, He F, Shao H, et al. Chitosan/alginate nanoparticles with sustained release of esculentoside A for burn wound healing. *ACS Appl Nano Mater*. 2023;6(1):573–587. doi:10.1021/acsanm.2c04714
200. Martyn D, Miyasato G, Lim S, et al. Variation in hospital resource use and cost among surgical procedures using topical absorbable hemostats. *CEOR*. 2015:567. doi:10.2147/ceor.s88698
201. O'Hara LM, Thom KA, Preas MA. Update to the centers for disease control and prevention and the healthcare infection control practices advisory committee guideline for the prevention of surgical site infection (2017): a summary, review, and strategies for implementation. *Am J Infect Control*. 2018;46(6):602–609. doi:10.1016/j.ajic.2018.01.018
202. Schug-Paß C, Sommerer F, Tannapfel A, Lippert H, Köckerling F. Does the additional application of a polylactide film (SurgiWrap) to a lightweight mesh (TiMesh) reduce adhesions after laparoscopic intraperitoneal implantation procedures? Experimental results obtained with the laparoscopic porcine model. *Surg Endosc*. 2008;22(11):2433–2439. doi:10.1007/s00464-008-9876-1
203. Peng X, Xu X, Deng Y, et al. Ultrafast self-gelling and wet adhesive powder for acute hemostasis and wound healing. *Adv Funct Mater*. 2021;31(33). doi:10.1002/adfm.202102583
204. Chang N, Li Y, Zhou M, et al. The hemostatic effect study of Cirsium setosum on regulating α1-ARs via mediating norepinephrine synthesis by enzyme catalysis. *Biomed Pharmacother*. 2017;87:698–704. doi:10.1016/j.biopha.2017.01.022
205. Guo W, Ding X, Zhang H, et al. Recent advances of chitosan-based hydrogels for skin-wound dressings. *Gels*. 2024;10(3):175. doi:10.3390/gels10030175
206. Wang Q, Li Q, Zhu L, Lin C, Chen Q, Chen H. Fabrication of Cu/ZNO-loaded chitosan hydrogel for an effective wound dressing material to advanced wound care and healing efficiency after caesarean section surgery. *Int Wound J*. 2024;21(1). doi:10.1111/iwj.14366
207. Wang CH, Cherng JH, Liu CC, et al. Procoagulant and antimicrobial effects of chitosan in wound healing. *IJMS*. 2021;22(13):7067. doi:10.3390/ijms22137067
208. Geng H, Zhang P, Liu L, et al. Convergent architecting of multifunction-in-one hydrogels as wound dressings for surgical anti-infections. *Mater Today Chem*. 2022;25:100968. doi:10.1016/j.mtchem.2022.100968
209. Nosrati H, Khodaei M, Alizadeh Z, Banitalebi-Dehkordi M. Cationic, anionic and neutral polysaccharides for skin tissue engineering and wound healing applications. *Int J Biol Macromol*. 2021;192:298–322. doi:10.1016/j.ijbiomac.2021.10.013
210. Huang L, Zhu Z, Wu D, et al. Antibacterial poly (ethylene glycol) diacrylate/chitosan hydrogels enhance mechanical adhesiveness and promote skin regeneration. *Carbohydr Polym*. 2019;225:115110. doi:10.1016/j.carbpol.2019.115110
211. Li J, Yu F, Chen G, et al. Moist-retaining, self-recoverable, bioadhesive, and transparent in situ forming hydrogels to accelerate wound healing. *ACS Appl Mater Interfaces*. 2020;12(2):2023–2038. doi:10.1021/acsami.9b17180
212. Wang X, Song R, Johnson M, et al. Chitosan-based hydrogels for infected wound treatment. *Macromol biosci*. 2023;23(9). doi:10.1002/mabi.202300094
213. Yang D, Ho YX, Cowell LM, Jilani I, Foster SJ, Prince LR. A genome-wide screen identifies factors involved in *S. aureus*-induced human neutrophil cell death and pathogenesis. *Front Immunol*. 2019;10. doi:10.3389/fimmu.2019.00045
214. Tavakoli M, Mirhaj M, Varshosaz J, et al. Asymmetric tri-layer sponge-nanofiber wound dressing containing insulin-like growth factor-1 and multi-walled carbon nanotubes for acceleration of full-thickness wound healing. *Biomater Adv*. 2023;151:213468. doi:10.1016/j.bioadv.2023.213468
215. Xia Y, Chen J, Ding J, Zhang J, Chen H. IGF1- and BM-MSC-incorporating collagen-chitosan scaffolds promote wound healing and hair follicle regeneration. *Am J Transl Res*. 2020;12(10):6264–6276.
216. Liang Y, Li Z, Huang Y, Yu R, Guo B. Dual-dynamic-bond cross-linked antibacterial adhesive hydrogel sealants with on-demand removability for post-wound-closure and infected wound healing. *ACS Nano*. 2021;15(4):7078–7093. doi:10.1021/acsnano.1c00204
217. Tan H, Peng Z, Li Q, Xu X, Guo S, Tang T. The use of quaternised chitosan-loaded PMMA to inhibit biofilm formation and downregulate the virulence-associated gene expression of antibiotic-resistant staphylococcus. *Biomaterials*. 2012;33(2):365–377. doi:10.1016/j.biomaterials.2011.09.084
218. Hao Y, Yuan C, Deng J, Zheng W, Ji Y, Zhou Q. Injectable self-healing first-aid tissue adhesives with outstanding hemostatic and antibacterial performances for trauma emergency care. *ACS Appl Mater Interfaces*. 2022;14(14):16006–16017. doi:10.1021/acsami.2c00877
219. Kinney SM, Ortaleza K, Vlahos AE, Sefton MV. Degradable methacrylic acid-based synthetic hydrogel for subcutaneous islet transplantation. *Biomaterials*. 2022;281:121342. doi:10.1016/j.biomaterials.2021.121342
220. Sun H, Saeedi P, Karuranga S, et al. IDF diabetes atlas: global, regional and country-level diabetes prevalence estimates for 2021 and projections for 2045. *Diabetes Res Clin Pract*. 2022;183:109119. doi:10.1016/j.diabres.2021.109119
221. Armstrong DG, Tan TW, Boulton AJM, Bus SA. Diabetic foot ulcers: a review. *JAMA*. 2023;330(1):62. doi:10.1001/jama.2023.10578
222. Armstrong DG, Boulton AJM, Bus SA. Diabetic foot ulcers and their recurrence. *N Engl J Med*. 2017;376(24):2367–2375. doi:10.1056/nejmra1615439
223. Dupré-Crochet S, Erard M, Nüβe O. ROS production in phagocytes: why, when, and where? *J Leukocyte Biol*. 2013;94(4):657–670. doi:10.1189/jlb.1012544
224. Davis FM, Kimball A, Boniakowski A, Gallagher K. Dysfunctional wound healing in diabetic foot ulcers: new crossroads. *Curr Diab Rep*. 2018;18(1). doi:10.1007/s11892-018-0970-z

225. Schreml S, Szeimies RM, Prantl L, Karrer S, Landthaler M, Babilas P. Oxygen in acute and chronic wound healing: oxygen in wound healing. *Br J Dermatol*. 2010;163(2):257–268. doi:10.1111/j.1365-2133.2010.09804.x
226. Chen X, Wang L, Fan S, et al. Puerarin acts on the skeletal muscle to improve insulin sensitivity in diabetic rats involving μ-opioid receptor. *Eur J Pharmacol*. 2018;818:115–123. doi:10.1016/j.ejphar.2017.10.033
227. Chen X, Yu J, Shi J. Management of diabetes mellitus with puerarin, a natural isoflavone from *Pueraria lobata*. *Am J Chin Med*. 2018;46 (08):1771–1789. doi:10.1142/s0192415x18500891
228. Meresman GF, Götte M, Laschke MW. Plants as source of new therapies for endometriosis: a review of preclinical and clinical studies. *Human Reproduction Update*. 2021;27(2):367–392. doi:10.1093/humupd/dmaa039
229. Zeng X, Chen B, Wang L, et al. Chitosan@Puerarin hydrogel for accelerated wound healing in diabetic subjects by miR-29ab1 mediated inflammatory axis suppression. *Bioact Mater*. 2023;19:653–665. doi:10.1016/j.bioactmat.2022.04.032
230. Abri S, Durr H, Barton HA, et al. Chitosan-based multifunctional oxygenating antibiotic hydrogel dressings for managing chronic infection in diabetic wounds. *Biomater Sci*. 2024;12(13):3458–3470. doi:10.1039/d4bm00355a
231. Tsegay F, Elsherif M, Butt H. Smart 3D printed hydrogel skin wound bandages: a review. *Polymers*. 2022;14(5):1012. doi:10.3390/polym14051012
232. Farahani M, Shafiee A. Wound healing: from passive to smart dressings. *Adv Healthcare Mate*. 2021;10(16):2100477. doi:10.1002/adhm.202100477
233. Campos Y, Fuentes G, Almirall A, et al. The incorporation of etanercept into a porous tri-layer scaffold for restoring and repairing cartilage tissue. *Pharmaceutics*. 2022;14(2):282. doi:10.3390/pharmaceutics14020282
234. Doostan M, Doostan M, Mohammadi P, Khoshnevisan K, Maleki H. Wound healing promotion by flaxseed extract-loaded polyvinyl alcohol/chitosan nanofibrous scaffolds. *Int J Biol Macromol*. 2023;228:506–516. doi:10.1016/j.ijbiomac.2022.12.228
235. Maleki H, Doostan M, Khoshnevisan K, Baharifar H, Maleki SA, Fatahi MA. Zingiber officinale and thymus vulgaris extracts co-loaded polyvinyl alcohol and chitosan electrospun nanofibers for tackling infection and wound healing promotion. *Heliyon*. 2024;10(1):e23719. doi:10.1016/j.heliyon.2023.e23719
236. Sun M, Zhang Y, Zhou M. Smart-responsive chitosan dressings: from microenvironmental sensing to multifunctional precision wound healing. *Food Hydrocoll Health*. 2025;8:100243. doi:10.1016/j.fhfh.2025.100243
237. Dang X, Fu Y, Wang X. Versatile Biomass-Based Injectable Photothermal Hydrogel for Integrated Regenerative Wound Healing and Skin Bioelectronics. *Adv Funct Mater*. 2024;34(42):2405745. doi:10.1002/adfm.202405745
238. Dang X, Guo B, Wang X. Biomass-derived conductive hydrogel-based electronic-skin patch for integrated wearable bioelectronics and real-time wound-status monitoring and treatment. *Anal Chem*. 2026;98(10):7561–7579. doi:10.1021/acs.analchem.5c06888
239. Dang X, Tang J, Han S, Wang X, Tao M, Zheng M. Injectable self-healing biomass-based hydrogel bioadhesive integrating skin bioelectronics and regenerative wound healing. *Adv Funct Mater*. 2026;e30332. doi:10.1002/adfm.202530332
240. Hardman D, Thuruthel TG, Iida F. Multimodal information structuring with single-layer soft skins and high-density electrical impedance tomography. *Sci Rob*. 2025;10(103):eadq2303. doi:10.1126/scirobotics.adq2303
241. Naghib SM, Hosseini SN, Beigi A. 3D 4D printing of chitosan-based scaffolds for wound dressing applications. *Carbohydr Polym Technol Appl*. 2024;8:100594. doi:10.1016/j.carpta.2024.100594
242. Chen X, Zhou Y, Zhou S, et al. 3D printing of chitosan hydrogel reinforced with tubular nanoclay for hemostasis and infected wound healing. *Bioact Mater*. 2025;54:404–422. doi:10.1016/j.bioactmat.2025.08.024
243. Huang W, Guo Q, Wu H, Zheng Y, Xiang T, Zhou S. Engineered Exosomes loaded in intrinsic immunomodulatory hydrogels with promoting angiogenesis for programmed therapy of diabetic wounds. *ACS Nano*. 2025;19(14):14467–14483. doi:10.1021/acsnano.5c02896
244. Ma J, Fang Y, Yu H, et al. Recent advances in living algae seeding wound dressing: focusing on diabetic chronic wound healing. *Adv Funct Mater*. 2024;34(2):2308387. doi:10.1002/adfm.202308387